DOCTORAL THESIS

The spatio-temporal pattern of snow cover and its relations to climate change in western aridzone of China

Sun, Bo

Date of Award:
2014

The Spatio-temporal Pattern of Snow Cover and Its Relation to Climatic Change in Western Aridzone of China

SUN Bo

A thesis submitted in partial fulfillment of the requirements
for the degree of

Doctor of Philosophy

Principal Supervisor: Prof. ZHOU Qiming

Hong Kong Baptist University

June 2014

Declaration

I hereby declare that this thesis represents my own work which has been done after registration for the degree of PhD at Hong Kong Baptist University, and has not been previously included in a thesis, dissertation submitted to this or other institution for a degree, diploma or other qualification.

Signature: _____

Date: June 2014

Abstract

Global climatic change as well as its consequences such as extreme weather events and sea-level rising has become a focusing issue in the contemporary world. Alpine snow cover is increasingly regarded as a good and sensitive indicator of climatic change due to the less direct interference by human. In western aridzone of China, majority of mountainous areas are covered by snow in winter seasons. This region is one of the most important seasonal snow cover regions in China and also a typical alpine snow cover region in the mid-high latitudes of the Northern Hemisphere. Being less affected by economic development and human activities in the history, the change of permanent and seasonal snow cover in this region echoes the global climatic and environmental change. In addition, snow melt water, which provides the major water supply in the region, is vital for living beings in the arid and harsh environment. It is therefore necessary to understand the snow cover change during the past decades.

This study aims to investigate the spatio-temporal pattern of snow cover in the western aridzone of China in the past 30 years by using remote sensing technology and to analyze the relationship between the change of snow cover and global climate. The reliability of remote sensing-derived global snow data is firstly examined. Data consistency

and accuracy are assessed against the ground measurements. In order to undertake a down-scale snow depth analysis with other high-resolution environmental data, a method that fuses the low-resolution passive microwave and high-resolution optical snow cover images is proposed. A linear mixture model is adopted in spectral unmixing for modifying snow depth estimates. Time series analysis method is utilized to describe the long-term trend and periodic features. The analysis is applied not only to the whole region but also to the local scale represented by a pixel so that the spatial pattern of the change can be illustrated. Using the result and climatic data, the relationship between snow cover and global/regional climatic change is established.

The results make contribute to the understanding of the impacts of climatic change, at regional level, on the spatio-temporal pattern of snow cover in the western aridzone of China.

Keywords: Snow and ice, alpine snow cover, remote sensing, spatio-temporal pattern, long-term trend, climatic change, western aridzone of China

Acknowledgements

I would like to express my sincere appreciation to Prof. Qiming Zhou, my principal supervisor, for his patient guidance and support during my five-year study in Hong Kong Baptist University (HKBU). He is a mentor not only in my academic career but also in life.

Great thanks go to my co-supervisor Prof. Donggen Wang who led me to the world of statistics. His valuable suggestions inspired me a lot.

I am very grateful to Prof. Xi Chen and Prof. Anming Bao at Xinjiang Institute of Ecology and Geography, Chinese Academy of Sciences (CAS) for their assistance in the field investigation and data collection.

I am most indebted to my classmates at Department of Geography, HKBU (Eve, Bingxia, Helen, Polly, Ray, Winnie, Bobo, Serey, Fenglong, Tao, Richard) and colleagues at Shenzhen Institutes of Advanced Technology, CAS (Ms. Ping Liu, Mr. Shuhong Peng), for their help and continuing friendship. Special thanks to my senior classmate and friend Dr. Jing Qian, for her constant encouragement and assistance.

I appreciate greatly the time, strength and motivational talks from Miss. Yi Liu and Miss. Xue Ao who kept me company almost every day via Internet although they were in hundreds of thousands of miles away. They kept talking to me when I was despaired during the thesis pending period. I will never forget those lucky days.

I would also like to acknowledge the people offering comments and advices throughout the research effort. They are Prof. Jiabing Sun and Prof. Yumin Chen at Wuhan University, Mr. Xuefei Li at Department of Physics and Mr. Xuehu Zhu at Department of Mathematics, HKBU, and the editors and two anonymous reviewers of the journal of *Remote Sensing Letters*.

Extraordinary thanks to many other individuals with whom I have shared such a beautiful life including all my friends in Hong Kong, mainland cities and overseas.

Most importantly, I devote my deepest gratitude to my parents and the whole big family. It is the endless love they gave that braced me up during the most struggling time. Without their support, this work could not have been possible.

Table of Contents

List of Tables

List of Figures

List of Abbreviations

AMSR-E	Advanced Microwave Scanning Radiometer for EOS (Earth Observing System)
ANOVA	Analysis of Variance
ASCII	the American Standard Code for Information Interchange
AVHRR	Advanced Very High Resolution Radiometer
CAS	Chinese Academy of Sciences
CMA	China Meteorological Administration
DEM	Digital Elevation Model
DMSP	Defense Meteorological Satellite Program
EOS	Earth Observing System
ESA	European Space Agency
ENSO	El Niño - Southern Oscillation
ETM+	Enhanced Thematic Mapper Plus
FMI	Finish Meteorological Institute
FT	Fourier Transform
GDP	Gross Domestic Product
GIS	Geographical Information System
HDF	Hierarchical Data Format
ICC	Intra-class Correlation Coefficient
IPCC	the Intergovernmental Panel on Climate Change
LiDAR	Light Detection and Ranging
LSM	Least Square Method

MODIS	Moderate Resolution Imaging Spectroradiometer
MWRI	Microwave Radiation Imager
NAO	North Atlantic Oscillation
NDSI	Normalized Difference Snow Index
NIR	Near-infrared
NOAA	National Oceanic and Atmospheric Administration
NSIDC	National Snow and Ice Data Center (the US)
PCA	Principal Component Analysis
PPI	Pixel Purity Index
RMSE	Root Mean Square Error
RRMSE	Relative Root Mean Square Error
SBX	Statistics Bureau of Xinjiang Uygur Autonomous Region
SBSM	State Bureau of Surveying and Mapping (China)
SCA	Snow-covered Area
SD	Snow Depth
SEM	Standard Error of the Mean
SMMR	Scanning Multichannel Microwave Radiometer
SSM/I	Special Sensor Microwave Imager
SPOT	Système Pour l'Observation de la Terre
SPSS	Statistical Package for the Social Sciences
SRTM	Shuttle Radar Topography Mission
SWE	Snow Water Equivalent
TCI	Terrain Complexity Index
TM	Thematic Mapper

UHI	Urban Heat Island
WAC	Western Aridzone of China

(Intentionally left blank)

Chapter 1 Introduction

Climatic change has become one of the major public concerns and interests in the contemporary world. Although no agreement has been reached on whether we are experiencing a period of global warming, the impact of global climatic change on the regional environment and ecosystem is quite noticeable. To echo climatic change, snow cover has widely been regarded as a sensitive and visible indicator.

The major focus of this study is on the regional impact of global climatic change on the spatio-temporal pattern of snow cover in the aridzone of China. Profited from lower level of urbanization, historical snow cover in western China was less affected by human activities, especially in the mountainous areas. The change in snow cover is considered a better indicator reflecting the changing climate. In another aspect, water resources converted from snowpack are vital for living beings in the arid lands. Therefore, the analysis of the effect of climatic change on the spatio-temporal patterns of snow cover is significant and necessary. In this chapter, study background as well as existing snow cover observation methods are reviewed. Research questions and objectives are then

proposed. Structure of the thesis is presented at the end of this chapter.

1.1 Background

1.1.1 Global climatic change and regional effects

Being a greatly-worried environmental issue, climatic change has generated many concerns all over the world. Especially in recent years, more frequent occurrence of extreme weather events and natural disasters, such as heat waves (Beniston & Diaz, 2004; Luber & McGeehin, 2008), hurricanes and floods (Novotny & Stefan, 2007; Veijalainen *et al.*, 2010) have been often regarded as the consequences of global climatic change.

According to the newly released fifth assessment report of the Intergovernmental Panel on Climate Change (IPCC), a widely accepted viewpoint is that our globe has increasingly become warming in the past decades (IPCC, 2013). Plenty of direct and indirect evidences have been provided to support this inference, *e.g.*, the increasing of global surface temperature (Hansen *et al.*, 2010), polar ice sheet melting, and sea-level rise (Douglas, 1991; Cabanes *et al.*, 2001; Miller & Douglas, 2004). The increasing emission of carbon dioxide (CO_2) due to the industrial and urbanization development are commonly blamed as a major factor that leads to global warming.

Skeptical views exist all the time. Based on historical meteorological

records from world-wide weather stations, the conclusion on rising temperature in the past century is mainly derived from statistical analysis results. Naturally, some scientists suspect the statistics which may contain biases and uncertainties if an unsuitable method were employed (McIntyre & McKitrick, 2005; 2011). Another frequently discussed topic is the location of temperature measurement. Most long-term temperature records are collected from weather stations in large cities. It is argued that population increase and urban heat island (UHI) effect would aggrandize the extent of temperature rise thus creating the bias in the trend analysis.

Setting aside the disagreements on global warming, the regional effect of global climatic change is much more visible. People care more about their local areas. How to cope with climate-induced environmental changes is more of the concern by the local people. According to the previous assessment reports of the IPCC (refer to IPCC, 1995; 2001; 2007; 2013), the proportion of the analyses on regional effects of global climatic change has been continually raised.

1.1.2 Snow cover change in China's aridzone

As an important component of global energy exchange and water cycle, snow has been recognized as a natural and visible indicator for assessing the impact of climatic change. Snow cover on high mountainous regions is always considered as an amplifier of climatic change since the fragile environment and ecosystem are much more sensitive to any environmental

changes (Nogués-Bravo *et al.*, 2007). Given that alpine snow cover change is commonly less affected by urbanization or human activities, it is a more reliable evidence of global climatic change compared to the observations from meteorological stations in populous cities of the world.

The mechanism of snow cover change caused by climate, however, still remains unclear. From the point of view of global warming, two voices in opposite opinions can be widely heard. Scientists discussed that the rising temperature could result in decreasing snow cover in high-altitude regions (Hantel *et al.*, 2012). Arguments were also made that snowfall shall increase on high mountainous regions due to the accelerating ocean-atmosphere circulation as global climate becomes warmer (Black, 2012).

Western aridzone of China (WAC) is a typical region for snow cover at mid-high latitude zones in the north hemisphere. An obvious response to climatic change is the change of water discharge (Wang & Li, 2006; Wang *et al.*, 2010). Increasing water supply has been believed as the consequence of accelerated melting of glaciers on high mountains due to the rising temperature (Shi & Liu, 2000; Chen, 2012). It has been warned that this increasing water flow cannot sustain and its supply will eventually run out if the trend continues (Liu *et al.*, 2006). Apart from melting glaciers, the difference of spatio-temporal distribution of seasonal snow cover also made a contribution to the variation of surface runoff. Observations from both remote sensing and *in situ* data show that inter-

annual variation of snowfall in western China fluctuates during the past decades (Qin *et al.*, 2006). However, the variability of snow cover and its response to climatic change is reported as a complicated issue (Li *et al.*, 2008).

1.1.3 Snow cover observation from the space

Traditionally, monitoring snow cover change for a large region requires long-term and extensive observation data collected from field stations, which requires a high operational cost and intensive labor use. The harsh weather and poor accessibility in the high mountainous regions prevent regular and frequent observations so that *in situ* observations have always been dispersed and rare (Schaffhauser *et al.*, 2008).

With the modern remote sensing technology, it is now possible to obtain the information of large-extent snow cover from the space with greatly improving accuracy at lower cost. Remotely sensed snow cover observation is mainly focused on two aspects, namely snow cover extent and snow depth. Normally, optical images with higher spatial resolution are utilized to detect and monitor the change of snow cover extent, while passive microwave data with the ability of snow depth retrieval are widely utilized to detect and monitor the change of snow depth.

Although many remote sensing techniques have been developed and utilized for snow cover observation, no one is perfect in terms of a regional study. Microwave remote sensing data, commonly characterized by a poor

spatial resolution, is designed and applied to snow cover monitoring at global or country-level scales. When it is applied to a regional study, the bias and uncertainties would be magnified. As to optical remote sensing imagery, there is an inherent weakness in the detection of snow depth. In addition, most optical images with high spatial resolution are limited by the field of view. It is better for monitoring changes in individual glacier and seasonal snow cover at the basin scale. However, those changes can be largely affected by local weather or climatic change, they cannot represent the real situation of snow cover change for a larger region.

1.2 Statement of research questions

In the WAC region, water supply from alpine snow cover is vital for lives and development in the fragile arid ecosystem. The consequences of climatic change can potentially be devastating. Therefore, it is significant to seek the answers to some important questions on the impact of climatic change on snow cover. For a better understanding of the snow cover change in the WAC region, research questions could be raised as follows:

1) Has the snowfall in the aridzone of China changed and become abnormal in the past decades?

2) Has the spatio-temporal distribution of snow cover changed in the past decades?

3) If changes existed, are these changes representing short-term

fluctuations or reflecting a long-term trend?

4) Are these changes related to the regional and global climatic changes? Furthermore, does it reflect the trend of global warming?

1.3 Objectives and significance of this research

Based on the research questions, this study aims to develop an effective methodology for modelling the spatio-temporal pattern of snow cover change over the large area of Xinjiang Uygur Autonomous Region of China; and to analyze the impacts of the corresponding climatic change patterns. The objectives of the study are:

1) To evaluate the reliability of the existing long-term remote sensing snow products and to improve the spatial accuracy;

2) To investigate the spatio-temporal pattern of snow cover during the past decades in terms of snow cover extent and depth;

3) To analyze the relationship between snow cover and climate for assessing the impacts of global and regional climatic changes on alpine snow cover.

The ultimate goal of sustainable development is to achieve the harmony between economic development and natural environment. This research attempts to find, from a macro perspective, the “hard facts” about the impact of human activities on the environment in the past so that some

appropriate counter-measures can be taken. Since the impact of climatic change on snow cover may result in changing snowmelt runoff, which in turn may cause significant change in water supply to the adjacent arid areas, this research will also contribute to the optimum usage of water resources and the establishment of a snowmelt runoff model over the aridzone of China.

1.4 Organization of the thesis

This thesis consists of nine chapters. The overview of each chapter as well as their relevance is addressed as follows.

The first chapter presents the research background. The argument on global climatic change is firstly introduced. The impacts of climatic change on regional snow cover as well as existing snow cover observation techniques are discussed. Followed by the statement of research questions, objectives and the structure of the whole thesis are presented.

The second chapter reviews the related literature and studies on, for example, remote sensing snow observation, long-term change detection and the relationship between snow cover and climate.

Chapter 3 introduces the study area and reviews the previous studies on snow cover change in the study area and related areas. Snow cover change based on two different methods including traditional ground measurement and remote sensing observation are compared and discussed.

After that, a general description of the research framework is presented.

For a long-term observation and monitoring the volume change of snow, passive microware remote sensing data is adopted in this study. **Chapter 4** examines the reliability of the existing remote sensing-based snow depth products over the study area. Using statistical methods, the data consistency of two selected data sets is examined and their accuracies are evaluated based on the ground measurements.

Given that the spatial resolution of passive microwave data is limited, **Chapter 5** presents a data fusion method to improve the spatial resolution of snow depth data using higher-resolution optical-based snow cover extent product.

Chapter 6 describes the spatio-temporal pattern of snow cover change. Time series analysis is applied to the entire region on a pixel-by-pixel basis, so that the regional difference of snow cover change can be expressed. Snow cover parameters including mean and maximum snow depth (SD) and snow-covered area (SCA) are generalized for the analysis.

Chapter 7 analyzes the relationship between snow cover and climate. The impacts of the local/regional climatic change on the spatial distribution of snow cover are discussed. The correlation between regional snow cover change and indicating events caused by climatic change at global scale is also investigated.

Chapter 8 summarizes the major findings of the whole study and

discusses some key issues concerning uncertainties, the validity and limitations of the study.

The last chapter concludes the study and proposes an outlook of this research.

Chapter 2 Theoretical Framework

This chapter clarifies the theoretical framework of this study. Issues and technical challenges on snow cover detection and monitoring using remote sensing technology will be discussed.

2.1 Remotely sensed snow cover observation

Remote sensing technology for large-extent snow cover observation dates back to the 1970s. The earlier observation is based on a series of passive microwave sensors onboard satellite platforms. As the development of remote sensing technology, images retrieved from hyper-spectral and higher spatial resolution sensors, included but not limited to microwave imagery, are utilized for snow cover observation and change detection applications in the past decade. Normally, remote sensing snow observation focuses on two aspects of snow cover, namely snow cover extent and snow depth.

2.1.1 Snow depth detection

Snow depth is an essential parameter for the estimation of snow mass accumulation. Remote sensing snow depth estimation is mainly based on passive microwave, thermal infrared or Light Detection and Ranging (LiDAR) imagery (Prokop, 2008). Among the three techniques, passive

microwave remote sensing is common and has been widely used in large-extent snow cover change studies, because of the better data availability and a successive observation for more than 30 years.

The commonly used passive microwave sensors include Scanning Multichannel Microwave Radiometer (SMMR) onboard the Nimbus-7 satellite, Special Sensor Microwave Imager (SSM/I) onboard the Defense Meteorological Satellite Program (DMSP) series platforms, and Advanced Microwave Scanning Radiometer for the Earth Observing System (EOS) (AMSR-E) onboard the EOS Aqua spacecraft. The major characteristics of those sensors are listed in Table 2.1.

Table 2.1 The major characteristics of passive microwave sensors

Satellite/Sensor	Frequency (GHz)	Number of channels	Spatial resolution (km)	Time period
Nimbus-7/ SMMR	6.6 - 37	5	60	1978 - 1987
DMSP/ SSM/I	19.35 - 85.5	4	25	1987 - present
EOS Aqua/ AMSR-E	6.93 - 89	6	12 - 21	2002 - present

Snow depth estimation from passive microwave remote sensing imagery is based on the Mie scattering theory. Microwaves with longer wavelengths are less affected by the scattering effect. Therefore, snow depth can be detected according to the difference in emissivity between two microwave frequencies (Chang *et al.*, 1987). Figure 2.1 illustrates the principle of snow depth retrieval from passive microwave electro-

magnetic radiation.

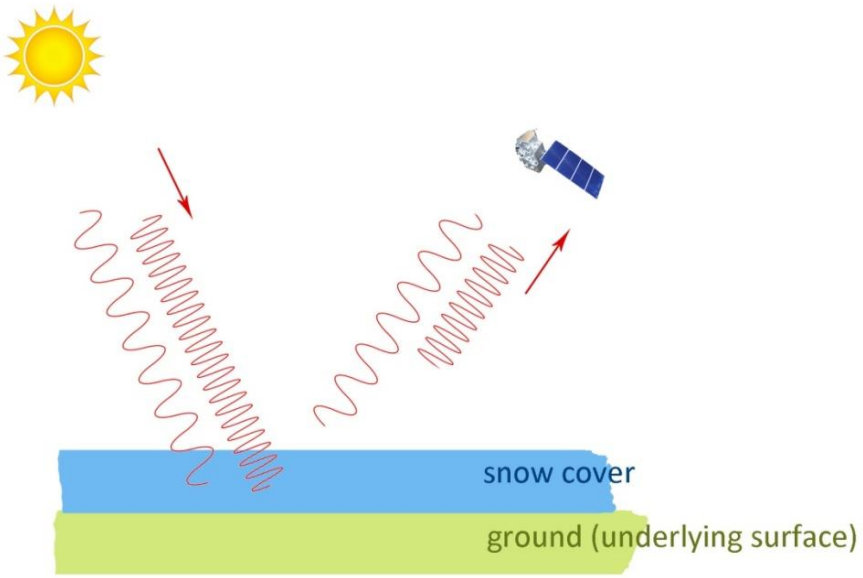

Figure 2.1 Principle of passive microwave snow depth retrieval.

For different platforms and sensors, typically a low-scattering channel in 18/19 GHz and a high-scattering channel in 36/37 GHz are utilized (Walker & Silis, 2002; DeWalle & Rango, 2008). The classical algorithm of snow depth retrieval for global study based on the SMMR data was developed by Chang *et al.* (1987), which is shown as follows (Eq. 2.1).

$$SD = 1.59 \times (T_{18H} - T_{37H}) \quad \text{(Eq. 2.1)}$$

Where, SD denotes snow depth in centimeters (cm); T_{18H} and T_{37H} represent the brightness temperatures in kelvins (K) in passive microwave data at frequencies of 18GHz and 37GHz, respectively, with the horizontal polarization (represented by a subscript "H").

To reduce the errors caused by various snow cover conditions in

different regions, some revised algorithms have been proposed with the assistance of ground measurement data (Li & Che, 2007; Clifford, 2010).

Although passive microwave remote sensing shows effectiveness in detecting snow depth, it should be pointed out that no single and global algorithm would be applicable to all conditions (DeWalle & Rango, 2008). Take China's west as an example, snow depth is usually overestimated by adopting the Chang's algorithm. A possible reason is the larger snow grain size in that region compared with other places in the world (Che & Li, 2004). Apart from snow grain size, some experiments have found that other factors including snow depth, density, wet snow and underlying surface of snow cover also affect the estimation of snow depth significantly.

2.1.2 Snow cover extent detection

(1) Detection from microwave imagery

Obviously, the extent information of snow cover is accompanied with the retrieval of snow depth information. The ground is covered by snow when the snow depth is greater than zero. As to this method, the accuracy of snow cover extent detection is limited by the spatial resolution of microwave imagery which is commonly at a coarse level.

(2) Detection from optical imagery

Optical remote sensing sensors have been widely utilized to detect snow cover extent with higher spatial resolution, such as Thematic Mapper

(TM) and Enhanced Thematic Mapper Plus (ETM+) carried on Landsat series satellites. In order to conduct a long-term and continuous observation, sensors with high repeat frequency (*e.g.*, daily) are more popular, such as Advanced Very High Resolution Radiometer (AVHRR) onboard National Oceanic and Atmospheric Administration (NOAA) series satellites and Moderate Resolution Imaging Spectroradiometer (MODIS) onboard EOS series satellites. The major characteristics of those optical sensors for long-term observations are listed in Table 2.2.

Table 2.2 The major characteristics of optical sensors with frequent snow cover observation

Satellite/Sensor	Spectral range (μm)	Number of channels	Spatial resolution (km)	Time period
NOAA series/ AVHRR	0.58 ~ 12.5	5	1.1	1978 - present
EOS/ MODIS	0.4 ~ 14.4	36	0.5*	2000 - present

* Spatial resolution of 0.5 km for bands 3-7.

To distinguish snow cover from snow-free areas, approaches can be generalized into two broad groups (Rees, 2006). One is based on single band imagery in the visible band, and the other is based on the combination of bands in multi-spectral images.

Since snow has a very high reflectance in the visible band, snow cover can be easily discriminated by setting a threshold of digital value on the single band imagery. The advantage of simplicity for data analysis is

obvious, so are the disadvantages. The determination of the threshold value is often a subjective matter and heavily relies on the local experience. A threshold set in one region often cannot be applied to another. In addition, the single-band approach suffers from the confusion caused by cloud cover which typically presents similar spectral reflectance in the visible band (see Figure 2.2).

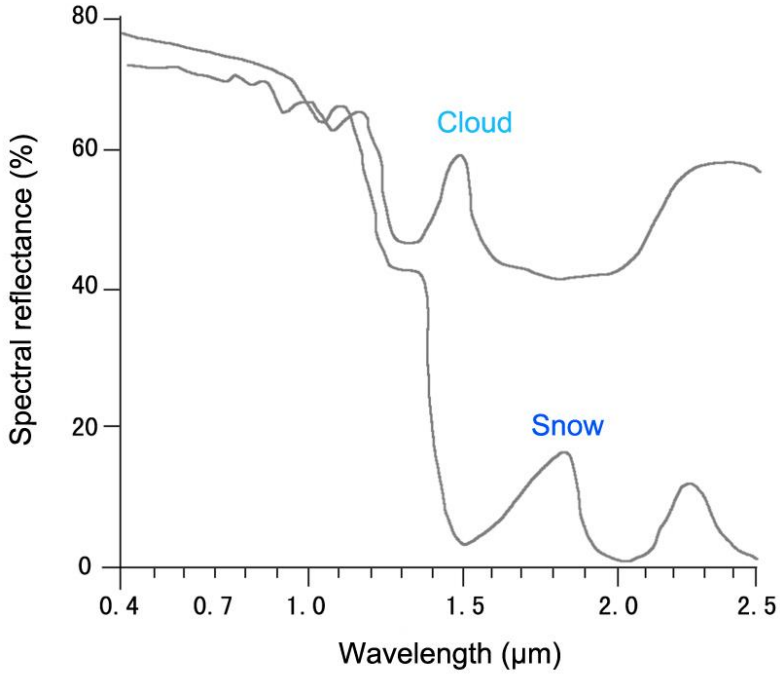

Figure 2.2 Spectral reflectance curves of snow and cloud (retrieved from CMA, 2007).

An alternative approach adopts a so-called normalized difference snow index (NDSI). The detection of snow cover is based on a normalized ratio of visible band to near infrared band (Hall *et al.*, 1995). A threshold, which varies in different seasons, is then utilized to separate snow cover from the background (Rees, 2006). This method not only takes the advantage of the spectral differences of snow versus non-snow and clouds,

but also reduces the influence of atmospheric effects and viewing geometry (Salomonson & Appel, 2004). The NDSI is expressed as Equation 2.2.

$$NDSI = \frac{R_v - R_s}{R_v + R_s} \quad \text{(Eq. 2.2)}$$

Where, R_v denotes the reflectance on a visible band and R_s represents the reflectance on a near-infrared (NIR) band.

Since numerous hyper-spectral sensors like MODIS have been launched into the space, better data sources have been provided for snow cover observation. Taking MODIS imagery as an example, the snow-mapping algorithm uses bands 4 (0.545-0.565 μm) and 6 (1.628 – 1.652 μm) to calculate the NDSI (Hall *et al.*, 2002). Accordingly, a time series of global snow cover extent product with cloud removed, to some extent, has been issued.

2.2 Mixed pixel problem in snow cover observation

Remote sensing sensors used for large-extent snow cover observation at regional or continental scales normally have very coarse spatial resolutions. Issues and problems caused by mixed pixel are common in many applications.

In remote sensing, a mixed pixel means a pixel (the minimum resolved unit of an image) measuring the average radiance over portions when it includes more than one land cover type or feature on the ground.

Theoretically, mixed pixel problem cannot be avoided since not a single sensor is sensitive to all ground features. Thus, depending on the spatial resolution of the sensor and the spatial structure of the ground, a digital image comprises a range of "pure" and "mixed" pixels (Lillesand *et al.*, 2008). The mixed pixels present a difficulty of image classification since their spectral characteristics are not representative of any single land cover type.

Spectral mixture analysis is commonly adopted to solve the mixed pixel problem. There are two assumptions for spectral mixture, the linear and non-linear. At a very coarse resolution level, Singer and McCord (1979) indicated that the observed spectral response on a mixed pixel can be considered as a linear combination of the signatures of the component cover types, which are often referred to as "endmembers" (Ichoku & Karnieli, 1996).

$$R_b = \sum_{k=1}^{n} f_k R_{bk} + \varepsilon_b \qquad \text{(Eq. 2.3)}$$

Where, R_b is the reflectance in band b; k is the number of endmembers; f_k equals the fraction of the endmember k; R_{bk} equals the reflectance contributed by the endmember k; in in band b; ε_b is the residuals. For a constrained unmixture solution; f_k is subject to the following restrictions: $\sum_{k=1}^{n} f_k = 1$ and f_k = [0, 1].

Endmembers can be determined by Principal Component Analysis (PCA) and Pixel Purity Index (PPI) from image itself when a spectral

library is not available (Lu *et al.*, 2003). According to Equation 2.3, the determination of the proportions of the areas corresponding to endmembers at the sub-pixel level is critical for linear spectral unmixing, although it is always difficult to obtain their spatial distributions (Ichoku & Karnieli, 1996). Multi-resolution data fusion is a frequently used method for retrieving the sub-pixel information. Besides, statistical methods like Least Square Method (LSM) can be used for the decomposition of the proportion information. As for passive microwave mixture, Bellerby *et al.* (1998) proposed a method to separate uncontaminated land and sea brightness temperature on mixed pixels using 8-adjacent pixels. However, this method may be inappropriate for snow cover detection, since the spectral mixture of snow and non-snow cover can be mosaicked and it is difficult to find a clear border between them as the border between land and sea.

2.3 Long-term change detection and time series analysis

Multi-temporal change detection techniques are commonly used for detecting and analyzing the process of a long-term change. Snow cover information retrieved from long-term and continuous remote sensing observations presents a time series data. To understand the dynamic patterns of snow cover change during the past decades, time series analysis can be applied.

2.3.1 Multi-temporal change detection

Change detection is the process of identifying differences in the state of an object or phenomenon by observing it at different times (Singh, 1989). The objectives of change detection can be generalized into the following aspects: (1) if a change happened; (2) what is the change's destination; and (3) how is the change process (Zhou *et al.*, 2007). In general, digital change detection methods can be divided into two broad groups, namely bi-temporal change detection and temporal change trajectory analysis (Coppin *et al.*, 2004). The former measures the change of ground features based on two epochs, while the latter is based on a time-series data. Since it is agreed that description of ground feature change is a complicated process (Gong *et al.*, 2008), temporal change trajectory analysis is better for understanding the change dynamics.

However, most of existing change detection methods are based on bi-temporal change detection, such as image differencing and image ratioing. Seldom cares for temporal trajectory analysis (Gong *et al.*, 2008). At present, there are three thoughts for analyzing change trajectory. One is based on the comparison of paired imagery. For this approach, temporal trajectory analysis is decomposed into bi-temporal change detection. Another approach is based on models like generalized linear model (*e.g.*, Morisette *et al.*, 1999), Markov random field model (*e.g.*, Kasetkasem & Varshney, 2002), and support vector machines (*e.g.*, Nemmour & Chibani, 2006). The other is based on time series analysis (*e.g.*, Li *et al.*, 2013). As

the demands of understanding change process have been increasing, temporal trajectory analysis for change detection should be got more focuses.

2.3.2 Time series data and their characteristics

A time series is a sequence of observations typically with a uniform time interval. An example of time series is the daily closing stock prices. In the natural world, there are many cases of time series such as daily average temperatures, monthly river discharge, annual rainfall amounts and the daily snow depth. Time series analysis is concerned with identifying the nature of the phenomenon and making a forecast by extracting the patterns of a time series (Cryer & Chan, 2008).

A time series can be decomposed into four patterns which listed as follows. Normally, one or a combination of those patterns is considered when describing a time series:

(1) Trend,

(2) Periodicity,

(3) Seasonality, and

(4) Random noise

As a natural phenomenon, snow cover time series show a seasonal pattern with a 12-month interval. Excluding the analyses of seasonality and random noise, the trend and the periodicity patterns are always

focused in long-term snow cover change studies. Trend pattern means the general tendency of snow cover change in area or depth. Periodicity pattern indicates the fluctuation features at a large time scale, *e.g.*, the inter-annual fluctuation of snow cover (Ke & Li, 1998).

2.4 The relation between snow cover and climatic changes

Climate is dynamic and could be affected by many factors (Bengtsson, 1999). It is therefore called a "system" which consists of atmospheric, land and oceanic components. Climate modelling is based on a mathematical representation of the climate (WMO, 2014). Normally, climate models are relevant to the concept of the scale. Spatially, we have global, regional and local climates (also known as microclimate). At the time scales, we have million-year-level, thousand-year-level, century-level and present climate models.

This study is focused on regional snow cover and its relationship to the climatic change, thus the regional and local climates are both considered as the factors that affect the change of snow cover and its spatio-temporal distribution.

2.5 Summary of this chapter

This chapter has reviewed and discussed the related technologies and analytical methods that will be involved in the study, including remote sensing snow detection, data fusion for spectral mixture analysis, remote

sensing change detection methods, time series analysis and climatic model analysis.

From the existing studies, remote sensing snow detection has an obvious advantage for large-scale snow cover change studies. Weakness and unsolved problems also exist. The reliability of global snow data in the regional study is unclear. As for change detection method, a long-term and temporal trajectory analysis is expected. The analysis should be conducted under the appropriate temporal and spatial scales.

(Intentionally left blank)

Chapter 3 Study Area, Data and Methodology

Comprising the major part of China's aridzone, Xinjiang Uygur Autonomous Region of China is chosen as the study area for investigating regional snow cover change. Using the modern techniques, snow cover change can be monitored by both ground measurement and remotely sensed imagery. Remote sensing technology providing a large extent observation compared with ground measurement is adopted for studying snow cover change. Data including remote sensing imagery and reference data used in this study will be introduced in this chapter.

From previous studies over the study area, most remote sensing applications are concentrated on the changes of individual glaciers in local basins or regional snow cover during a short period of time. For the former case, conclusions on climatic change could be largely affected by local weather conditions. For the latter one, the lack of a long-term observation restricts the discussion on the responses to global climatic change, which somehow should be a long-term trend. To overcome the weakness of the previous studies, a long-term observation based on remote sensing technology highlights this study. The overview of the general method will be

presented at the end of this chapter.

3.1 Introduction to the study area

This study is conducted in Xinjiang Uygur Autonomous Region of China. Xinjiang is located in the northwest of China (Figure 3.1). The geographical extent ranges from 73°40 Ɛ to 96°23 Ɛ and from 34°25 Ɲ to 49°10 Ɲ (SBX, 2012). It covers an area of over 1.66 million square kilometers and takes up approximately one sixth of China's total area (SBX, 2012).

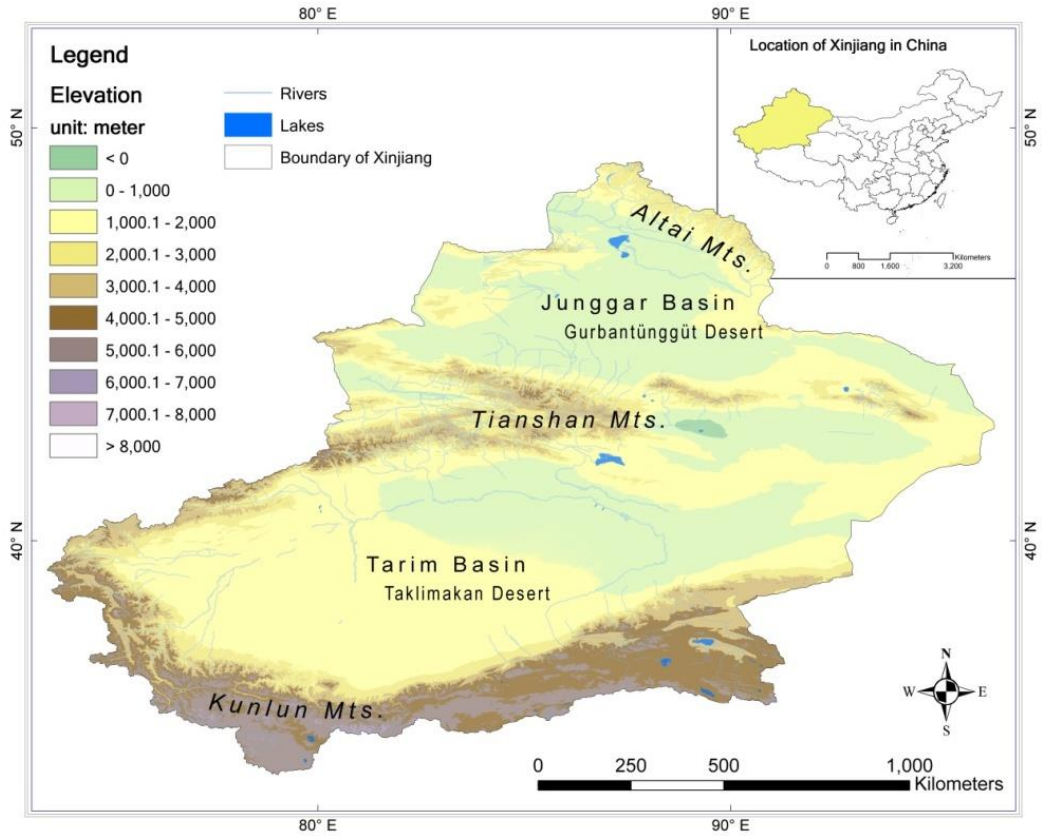

Figure 3.1 Location map of the study area and the topographic characteristics.

The topography of the region characterizes as three parallel mountain ranges with two basins lying between them. The three great mountain ranges include the Altai Mountains, the Tianshan Mountains and the Kunlun Mountains. In the middle of the three, the Tianshan Mountains extending from west to east divide the study area into two parts: North and South Xinjiang. The two largest deserts in China – the Taklimakan and Gurbantünggüt, located in the Tarim and Junggar Basins, respectively, are bounded by the great mountain ranges. The elevation ranges from -154 m at Aydingkol Lake (refer to SBSM, 2008) to 8611 m at *K2*, the peak of Qogir (refer to Chen, 2010). This forms a complex terrain with various types of underlying surfaces.

Situated in the hinterland of the Eurasian continent, Xinjiang has a typical continental climate with the average annual precipitation of 157.4 mm (Chen, 2012). The average annual temperature of Xinjiang is around 10.0 °C (Li, 1991). Because of its large territory, the distribution of precipitation and temperature shows a large variance with different longitudes, altitudes, terrains and underlying surfaces. Average annual precipitation can reach to 255 mm in the north, while this figure is only 106 mm in the south (Li, 1991). The Taklimakan Desert is regarded as the one of the most extreme arid region in the world.

Regardless its low annual precipitation, Xinjiang is rich in snow precipitation in the winter. It is regarded as one of the most important snow cover regions in China (Li, 1988). Similar to the rainfall, the spatial

distribution of snowfall is uneven. As the high mountains block the water vapor, the snow cover is mainly located in the north and some parts in the Kunlun Mountains. This can be visualized from a satellite image (Figure 3.2). The vertical zonation of snow cover is also obvious. Li (1991) described snow cover conditions in different altitude categories by taking the Tianshan Mountains as an example (Table 3.1).

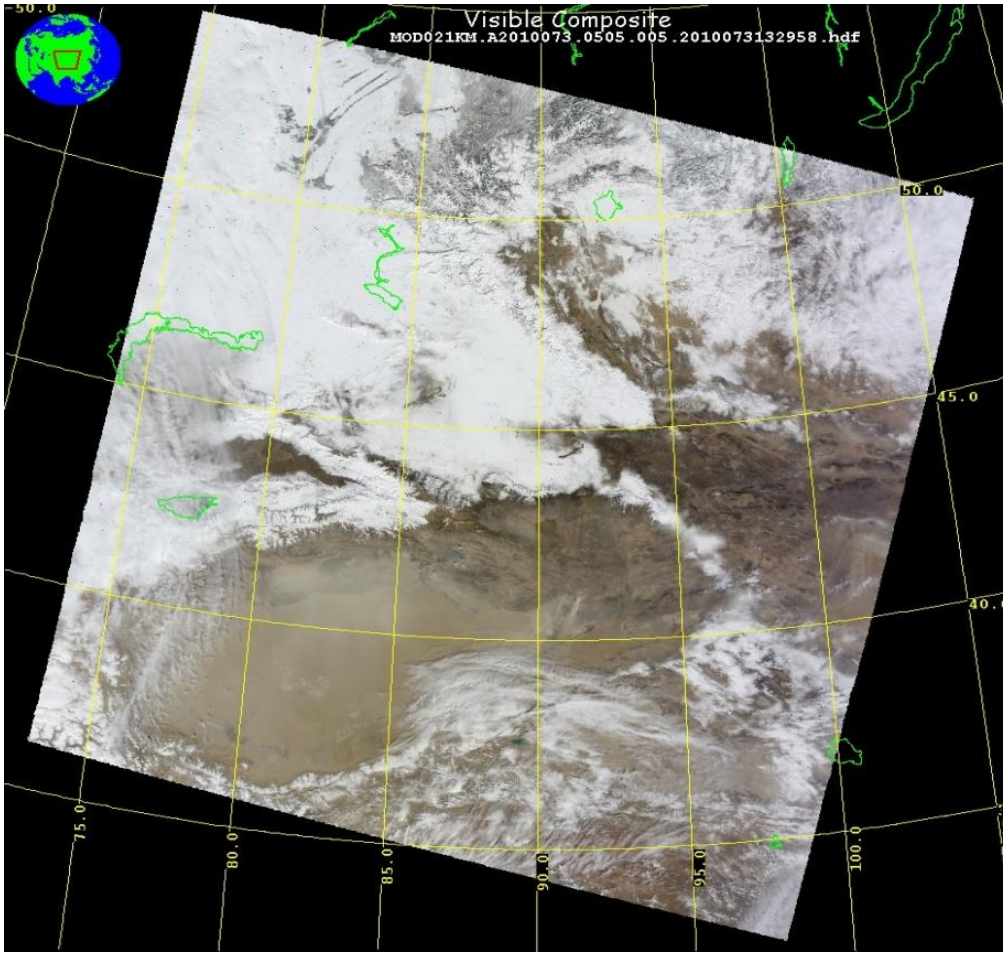

Figure 3.2 Snow cover distribution in Xinjiang from MODIS image on March 14th, 2010, pure white color represents the snow cover but the floccule is cloud.

Table 3.1 Vertical zonation of snow cover in the north slope of the Tianshan Mountains (retrieved from Li, 1991, pp.122)

Altitude (m)	Snow cover duration (day)	Maximum snow depth (cm)
1500	140-150	50
2000	170-180	80
2500	200-220	80
3000	240-270	100
3500	300-320	100

Note: Data for other altitude categories are not available.

The snowmelt water from alpine glaciers and seasonal snow cover provides the major water supply in the form of surface runoff. Most runoff is through rivers such as the Tarim River, which is the longest inland river in China and the second longest in the world. Oases along the rivers and at fringe of alluvial fans along the front-range of the mountains are the most important habitats. Xinjiang has a large population of more than 21.8 million according to the sixth census in 2010; and its gross domestic product (GDP) reached to 543.747 billion yuan in 2010 (SBX, 2012). Thus, snow cover being the potential water supply is extremely important for people living and industrial development in Xinjiang.

3.2 Review of previous studies

Previous studies on snow cover change in Xinjiang and related regions are based mainly on two data sources, namely ground measurements and remotely sensed imagery. Snow cover change from historical literature

and documents will not be discussed in this thesis.

3.2.1 Snow cover change from ground observation

Ground-based snow observation, including the measurements from field investigation and weather stations, provides a consistent and continuous record which is better for long-term studies. Station snow cover data in Xinjiang dates back to the 1960s when the majority of weather stations were established. The stations, located in towns and cities, are mainly distributed in the piedmont areas or basins. The better data availability from greater number of weather stations makes the Tianshan Mountains a popular region for snow cover studies.

According to Qiu and Sun (1992), the distribution of snow cover in the Tianshan Mountains is not uniform. Snow cover in the western part is much deeper than that in the eastern part, and maximum snow depth on the north slope of the Tianshan Mountains is larger than that on the south. Based on 45-year records of 17 stations, Yang *et al.* (2007) indicated that the maximum snow depth in the Tianshan Mountains had increased with a rate of 1.15 cm per ten years during the period of 1959-2003, while no obvious change of snow cover duration was observed. To illustrate the regional differences, Wang *et al.* (2010) analyzed the long-term trend of snow depth for each weather station. Their result is mapped in the following Figure 3.3.

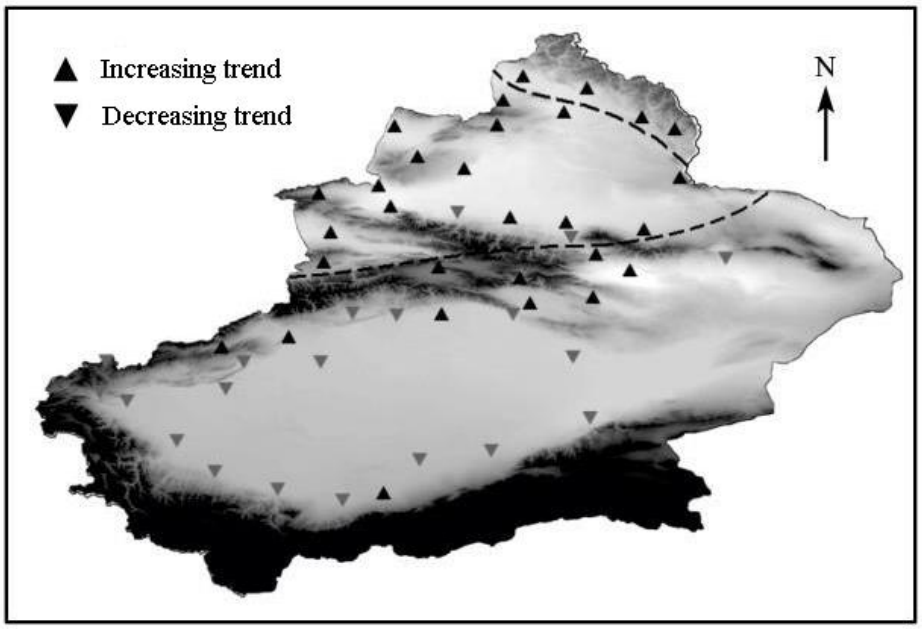

Figure 3.3 The trend of snow depth change in weather stations over Xinjiang during 1961-1999 (retrieved from Wang *et al.*, 2010).

Given that snow cover in towns and cities could be affected by human activities, scientists also focused on selected glaciers and snow observation stations in high mountains. During the past half century, remarkable changes occurred on most glaciers in Xinjiang such as Ürümqi Glacier No.1 (Li *et al.*, 2007; Lan *et al.*, 2007) and glaciers in the Tarim Basin (Ma *et al.*, 2010; Gao *et al.*, 2010). Especially in the last 15 years of the 20th century, the glacier retreat accelerated (Lan *et al.*, 2007). Based on the historical records from Tianshan Snow-cover & Avalanche Research Station (43°16´N, 84°24´E, 1776 m), snowfall, measured by snow depth and cover duration, around the station has increased (Zhang & Wei, 2001; Xu & Wei, 2004; Gao *et al.*, 2005; Shi *et al.*, 2009), with a large fluctuation of annual maximum snow depth (Shi *et al.*, 2009).

3.2.2 Snow cover change detected by remote sensing observation

Remote sensing based snow observation in China dates back to the early 1990s. Two types of remotely sensed data are commonly used, namely passive microwave and optical imagery. Analyses on snow depth and volume change are mainly based on the passive microwave data, while analyses on snow extent change mainly rely on the latter type that has relatively a higher spatial resolution.

The premier data set utilized for evaluating large-scale snow cover change is based on passive microwave imagery. It provides the capability of snow depth detection as well as snow water equivalent. Chang *et al.* (1987) proposed a global algorithm for snow depth retrieval based on the difference of brightness temperatures between two microwave frequencies. On the basis of this algorithm, the modified algorithms have been developed to match the snow features in western China and to fit for other passive microwave sensors (*e.g.*, Chang *et al.*, 1992; Li, 1999; Che *et al.*, 2008; Sun *et al.*, 2007, 2010). The major algorithms applied to Xinjiang are summarized in Table 3.2.

Based on passive microwave data, the snow cover in Xinjiang is not a pervasive feature that shows a uniform coverage in space (Li, 1993). In contrast to the southern region, North Xinjiang is a “stable snow cover region” with snow cover duration of greater than 60 days in a hydrological year (Che & Li, 2005; Zhang *et al.*, 2008). Regional differences in snow

depth illustrate that snow cover is mainly concentrated in low and high mountainous areas, rather than basins or plateaus (Cao *et al.*, 1994; Li *et al.*, 2010). According to statistical analysis, the snow storage in the whole North Xinjiang has shown, but not significantly, an increasing trend during the past decades (Li *et al.*, 2010). In the meantime, large seasonal and inter-annual fluctuations can be observed (Qin *et al.*, 2006; Che *et al.*, 2008; Dai *et al.*, 2010). Some findings based on passive microwave data show a consistent result with ground measurement data. For instance, snow depth reaches to a maximum in February or March and the ablation period starts in the last 10 days of March (Che *et al.*, 2008).

Optical imagery offers an option for monitoring snow cover change by detecting snow extent change. Considering the characteristic of higher spatial resolution, this kind of data gives more details of snow cover and is usually employed for studies in a basin scale. Li *et al.* (2004) investigated eight glaciers in the Tianshan Mountains using three Landsat and Système Pour l'Observation de la Terre (SPOT) images in different eras (*i.e.*, 1977, 1986 and 2000) and concluded that seven of them had retreated with a rate of 10-15 meter per year since 1986. Based on a time series of MODIS snow cover data from 2001 to 2008, Mu *et al.* (2010) observed that the area of snow cover decreased in the Khash River Basin, west of the Tianshan Mountains. However, according to Dou *et al.* (2010), the area of snow cover in the whole Tianshan region had generally increased during the similar period from 2000 to 2006, and the decreasing

trend was only found in the regions with elevation above 4000 m because of the retreating glaciers. Apart from the large differences in spatial extent, snow cover also distributed unevenly in time. The percentage of snow cover in Xinjiang ranged from 10% to 40% among the study years (Liu *et al.*, 2003).

Some efforts have also been made on snow depth retrieval from higher-resolution optical imagery (*e.g.*, Liang *et al.*, 2004; Liu *et al.*, 2006; Fu *et al.*, 2007). The snow depth retrieval algorithms are based on statistical regression model. Due to the lack of a physical basis, the applicability of the optical images to snow depth detection has been severely questioned.

Table 3.2 Snow depth retrieval algorithms adopted in Xinjiang by using passive microwave data

Proposers	Algorithm	Descriptions
Chang *et al.* (1987)	$SD = 1.59 \times (T_{18H} - T_{37H})$	Global algorithm under the assumptions of snow density of 0.3 g/cm^3 and snow grain size of 0.3 mm; applied to SMMR data.
Chang *et al.* (1992)	$SD = 2.0 \times (T_{18H} - T_{37H}) - 8$	Modified Chang's algorithm for western China; applied to SMMR data.
Cao *et al.* (1993)	$SD = 1.59 \times (T_{18H} - T_{37H}) - x$, When x equals to 8 for plateau; equals to 6 for high mountains; equals to 4 for rolling hills; equals to 0 for the other situation.	Modified Chang's algorithm for western China; applied to SMMR data
Li (1999)	$SD = 2.0 \times (T_{18H} - T_{37H}) - 8$, for the plateau; $SD = 2.0 \times (T_{18H} - T_{37H}) - 6$, for high mountains; $SD = 1.59 \times (T_{18H} - T_{37H}) - 3$, for low mountains, rolling hills and basins.	Regional algorithm for northwest China; applied to SMMR data
Sun *et al.* (2006)	$SD = - 6.489 + 0.493 \times sf \times (T_{19V} - T_{37H}) + 0.869 \times (T_{37V} - T_{37H}) - 0.18 \times (T_{89V} - T_{89H})$	Regional algorithm for Xinjiang, applied to AMSR-E data.

(To be continued on next page)

(Continued)

Sun *et al.* (2007)	$SD = -8.475 + 0.895 \times (T_{19V} - T_{37H}) + 0.345 \times (T_{89V} - T_{89H})$	Regional algorithm for Xinjiang, applied to FY-3 MWRI data.
Che *et al.* (2008)	Formula 1: $SD = 0.78 \times (T_{18H} - T_{37H}) / (1 - f)$ Formula 2: $SD = 0.66 \times (T_{18H} - T_{37H}) / (1 - f)$	Algorithm for China; formula 1 for SMMR data from 1978 - 1987; formula 2 for SSM/I data from 1987 - 2006.*

Where, SD means snow depth in centimeters (cm); T with subscripts (*e.g.*, T_{18H}, T_{37V}) represent the brightness temperatures (K) in passive microwave data at different frequencies (*e.g.*, 18GHz and 37GHz) with the horizontal (H) or vertical (V) polarization; f means the forest area fraction; sf means daily snow fraction retrieved from MODIS daily snow product.

* After 2010, SSM/I and AMSR-E data were calibrated to SMMR data and the uniform formula 1 was used later on, this can be referred to Che (2011).

Comparing with the ground measurement, the space-borne observations tend to overestimate snow cover. This has been reported by numerous studies on mean winter snow volume (Cao & Li, 1993), snow cover duration (Che & Li, 2005) and snow-covered area (Liang *et al.*, 2008). A reasonable explanation for the "overestimation" of snow volume is that ground-measured snow depth represents the situation of snow cover at weather stations in piedmont or basins, while satellite- derived data represents the entire region including high mountains with heavy snow (Cao & Li, 1993). However, this cannot explain all. A pixel in a snow-cover image is characterized by the general situation in the area covered by it. For a passive microwave image, with a very coarse resolution of 25x25 km, a pixel covers an area of 625 km^2. It is therefore almost impossible to find a pixel which is fully covered by snow.

3.2.3 Discussion on the relationship between climatic change and regional snow cover in the study area

The relationship between climatic change and alpine snow cover in the aridzone of China has been investigated for many years. According to Shi *et al.* (2003), the regional climate in northwestern China which was characterized as warm-dry since the end of the little ice age mutated to warm-wet in the hydrological year of 1986/1987. The average precipitation in Xinjiang including snowfall has increased by 22% in North Xinjiang and 33% in South Xinjiang since then. As for permanent

snow cover, the effect of change in temperature is much more noticeable (Zhang *et al.*, 2007). Temperature rising especially in summer seasons explains the accelerated retreat of alpine glaciers since 1980s (Li *et al.*, 2007; Wang *et al.*, 2008). On the other hand, average winter temperature in Xinjiang is far below 0 °C (*i.e.*, -4.3 °C, according to Li, 2001). Temperature, observed with a rising rate of less than 0.4 °C per ten years in Xinjiang during the last half century (Xu, 1997; Li, 2001; Shi *et al.*, 2009), is not the major factor affecting snow cover accumulation in winter but vapor is. Warm-wet climate that brings more vapor caused the increasing seasonal snow cover in the past three decades (Li, 2001; Zhang & Wei, 2001; Gao *et al.*, 2005).

At a larger scale, snowfall in Xinjiang is dominated by the westerly circulation in the Northern Hemisphere. Affected by the global climatic system, snow cover representing the accumulation of snowfalls has a synchronous relation with the most important signs of global climatic fluctuations. The relationship was reported that snow mass in Xinjiang is related to the El Niño - Southern Oscillation (ENSO) events in the Pacific Ocean with a correlation coefficient of 0.63 (Li, 1989) and to the North Atlantic Oscillation (NAO) events with similar cycles of fluctuations like 2 or 6-7 years (Yang *et al.*, 2007). However, the physical mechanism of the relationship between snow cover and the atmospheric circulation still remains unclear (Li, 1993).

3.3 Data used in the study

This study aims to analyze the long-term change of snow cover using remote sensing images. Therefore, passive microwave data which offers a continuous snow cover observation for more than 30 years is employed. It provides the capability of extracting snow extent as well as snow depth information. Reference data include snow cover extent products derived from optical remote sensing and ground-based snow depth measurements. Other ancillary data include topography and land cover maps. To analyze the impact of climate on snow cover, climatic data are also acquired from local and regional weather stations.

3.3.1 Passive microwave snow depth data

Snow depth data sets retrieved from passive microwave sensors dated back to the late 1970s are acquired including the GlobSnow Snow Water Equivalent (SWE) product (version 1.3, "the GlobSnow product" for short afterward) and Long-term Snow Depth Dataset of China (updated to 2010, "the WestDC product" for short afterward). The former is issued by Finish Meteorological Institute (FMI) as a part of the GlobSnow project supported by European Space Agency (ESA). The latter is issued by Environmental and Ecological Science Data Center for West China (WestDC). This kind of data is free-of-charge and can be downloaded from Internet.

3.3.2 Optical snow extent data

Snow cover extent product with a higher spatial resolution is utilized to improve the spatial resolution of snow depth data sets. The MODIS data with shorter repeat cycle is selected for matching the time interval of snow depth data. In the study, the 8-day composite product with spatial resolution of 0.05 degree (MOD10C2) is adopted to minimize the effect of cloud. This kind of data is free for change and can be collected from National Snow and Ice Data Center (NSIDC) of the United States.

3.3.3 Ground reference data

Daily ground snow depth measurements collected from standard weather stations and a snow observation station in the Tianshan Mountains are utilized as ground reference for accuracy assessment. The temporal coverage of the ground data covers the period from 1980 to 2011. The location and elevation information as well as observation periods for those stations are shown in Appendix I.

3.3.4 Climatic data

Local and regional climatic conditions are considered as the factors of snow cover change in the China's west. To represent the local weather condition, station meteorological records including surface air temperature and precipitation are used. To represent the regional climatic condition, a time series of radioactivity data over eastern and western parts of China are utilized.

3.3.5 Other ancillary data

- Grid digital elevation model (DEM): DEM data with 90 meters resolution (Shuttle Radar Topography Mission (SRTM) DEM v4.1) is utilized for analyzing the topographical effects on snow cover change.
- Land cover map: land cover maps based on remote sensing image classification and field investigation are utilized for minimizing the impact of underlying surface of snow cover on snow cover detection.

3.4 Research design and methodology

The issue of remote sensing data quality is first dealt with. Given the poor spatial resolution, the long-term snow depth data set is fused with optical snow cover extent products so as to improve the spatial resolution. Time series analysis is then employed to evaluate the long-term trend of snow cover change. The analysis is applied to the whole study region and to each pixel as well so that spatio-temporal pattern of snow cover can be illustrated. Statistical correlation analysis is adopted in the investigation on the relationship between the changes of snow cover and climate. Both local (weather condition) and continental climate are considered as the factors that cause the change. The local climate is represented by climatic parameters such as temperature and precipitation, while the continental climate is represented by generalized atmosphere-ocean interaction and

solar radiometry indices. The impacts of climatic change on snowfalls and the spatial distribution of snow cover are then analyzed.

Figure 3.4 shows the research procedures and the adopted snow cover data in each step. The major analysis methods are illustrated in Table 3.5. Details and analytical results will be presented in the following chapters.

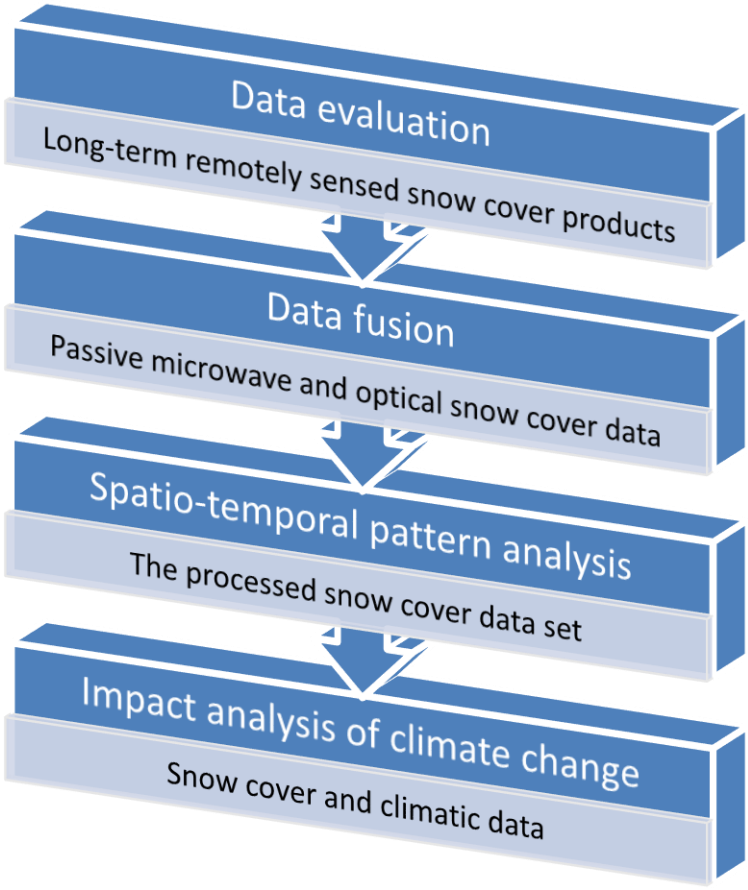

Figure 3.4 Research procedures and snow cover data used in each step.

Table 3.3 Major analysis methods in the study

Procedures	Analysis methods	Descriptions /Adopted indices
Data evaluation	Consistency test & accuracy assessment	Intra-class correlation coefficient (ICC) & root mean square error (RMSE)
Data fusion	Spectral mixture analysis	Linear spectral unmixing (linear mixture model)
Spatio-temporal analysis	Time series analysis	long-term trend & seasonality (cycle or seasonal variations)
Impact analysis of climatic change	Correlation analysis & regression analysis	Correlation coefficient (Pearson's *r*) & regression models

Note: ICC is utilized to evaluate the consistency of two remote sensing snow depth data sets, while RMSE is utilized to assess their accuracies based on ground truth data.

3.5 Summary of this chapter

Being a typical arid area in the mid-high latitude region of the Northern Hemisphere, Xinjiang of China is chosen as the study area because snow cover in high mountains of this region is very sensitive to global climatic change, and snowmelt water plays a vital role for lives. This chapter has introduced the geographical characteristics of the study area and reviewed the relevant studies of snow cover change in that region. From the previous studies, the limitations of the existing snow observation methods for a long-term study are generalized: (1) the accuracy of passive microwave based snow depth estimate is low due to the very coarse spatial resolution;

(2) optical remote sensing fails to detect snow depth although it has a higher spatial resolution. In addition, the existing studies on snow cover and global climatic change is restricted by local snow cover. A study at the regional scale is needed.

The data used in this study and general methodology are presented. This study aims to establish the spatio-temporal pattern of snow cover in the western aridzone of China, so that the impact of climatic change can be analyzed, not only on the total amount but also the spatial distribution of snow cover. Data processing and analysis methods are generally introduced including data assimilation and statistical analyses.

Chapter 4 Evaluation of Remotely Sensed Snow Cover Observation[1]

Passive microwave remote sensing technology can provide large-extent and all-weather observations of snow cover for more than 30 years. However, due to the limitation of technology, the spatial resolution of this kind of data is very low. Given the spatial heterogeneity of snow physical parameters, the snow depth products derived from passive microwave sensors cannot guarantee a high accuracy for all over the world.

This chapter attempts to evaluate the reliability of long-term snow cover data sets retrieved from remote sensing images for regional study. For the study area, two products provide long-term full coverage including GlobSnow and WestDC. Given that both of them are originated from the same data source, the consistency of the two products is first evaluated. Using the ground measurement

[1] Some of the contents of this chapter have been published in journal, which can be referred to: Zhou, Q., & Sun, B. (2013). Reliability of long-term snow depth data sets from remote sensing over the western arid zone of China. *Remote Sensing Letters*, 4(11), 1039-1048.

data, the accuracies of these products are also assessed at different temporal scales. Moreover, seasonal and topographical effects are also examined so as to test if they are significant factors affecting data accuracy.

4.1 Introduction

Among various parameters of snow cover, snow depth is considered vital, particularly for estimating the snow accumulation by snow volume. The accurate and reliable snow depth data are highly desirable not only for estimating the snowmelt runoff but also for evaluating the impacts of changing snow cover on the fragile ecosystem.

Passive microwave remote sensing technology provides a long-term and continuous observation of snow cover at global scale for more than 30 years. This technology has shown its capability of providing a large-extent and continuous observation of snow depth at all-weather conditions (Chang *et al.*, 1987). Based on this technology, some long-term global snow depth data sets have been produced and released. To build an empirical model for snowmelt runoff estimation, these long-term time series data sets are needed. However, the microwave based snow cover products are known to suffer from a number of issues due to the coarse spatial resolution. In regard to a regional study, lower accuracy and lack of ground validation data have hampered the applications in the past.

For covering the study area, two products are readily available

including the GlobSnow and the WestDC products (refer to §3.3.1). With a coarse spatial resolution (*e.g.*, 25 km), these products aim to support studies at the global or international scales. The applicability of the products, however, has been questioned for local applications due to the uncertainties caused by physical and validation limits. The physical parameters of snow cover such as density and grain size might vary at different places. Errors caused by spatial heterogeneity of snow are difficult to avoid. Research works also pointed out that diverse underlying surface of snow cover, complex topography and wet snow would reduce the accuracy of snow depth detection (Chang *et al.*, 1991; Dong *et al.*, 2005). For validation, the limited availability of ground observation data make the calibration of the snow depth estimation results very weak by using only few weather stations and short period of time (Chang *et al.*, 2005; Pulliainen, 2006; Che *et al.*, 2008; Luojus *et al.*, 2010).

Because of the above uncertainties, it is necessary to evaluate the reliability of the two remote sensing products for the study area. Accuracies of selected available snow depth data sets are assessed based on multiple years of ground measurements from available weather stations. In order to verify seasonal and locational effects on the data reliability, the impacts of wet snow and geographical location are also investigated in this chapter.

4.2 Two long-term snow depth products

The GlobSnow product and the WestDC product are both originated from the same source of space-borne passive microwave sensors, *i.e.*, Scanning Multichannel Microwave Radiometer (SMMR) onboard Nimbus-7, Special Sensor Microwave Imager (SSM/I) onboard the Defense Meteorological Satellite Program (DMSP) series platforms, and Advanced Microwave Scanning Radiometer for the Earth Observing System (EOS) (AMSR-E) onboard EOS Aqua (refer to §2.1).

Snow depth estimates of the GlobSnow product were derived by using an algorithm based on a semi-empirical snow emission model which combines brightness temperature difference between vertically polarized channels of 19 GHz and 37 GHz and ground observation data (Pulliainen, 2006). The depth values were then converted to SWE values by assuming a constant snow density of 0.24 g/cm^3 regardless of location and season (Takala *et al.*, 2011). Compared to independent ground reference data over the Russia, the accuracy of the product was reported with a RMSE of 43.2 mm for Eurasia and about 30 mm to 40 mm for restricted analysis to SWE values below 150 mm (Luojus *et al.*, 2010; Takala *et al.*, 2011).

Snow depth estimates of the WestDC product were derived by using a modified Chang's algorithm (Chang *et al.*, 1987) to adapt into the environment in China (Che *et al.*, 2008). Two channels with the same frequencies (*i.e.*, 19 GHz and 37 GHz) but in a different polarization were

employed for snow depth retrieval after distinguishing snow cover from rainfall, cold desert and frozen ground (Che *et al.*, 2008). Based on the records from limited meteorological stations in 1983/1984 and 1993, the accuracy of the product was evaluated in general with a standard deviation of 6 cm but the actual value varied according to the sensors (Che *et al.*, 2008).

The general properties of the two selected products are listed in the following Table 4.1.

Table 4.1 The general properties of the snow depth products under the investigation

	The GlobSnow product	**The WestDC product**
Measurement	snow water equivalent (mm)	snow depth (cm)
Coverage	north hemisphere (above latitude 35°N)	China (60°E - 140°E, 15°N - 55°N)
Period	November 1979 – December 2010	November 1978 – December 2010
Data intervals	daily, weekly, monthly (average and maximum)	daily
Projection	Equal-Area Scalable Earth Grid (EASE-Grid) - north hemisphere	Latitude-longitude
Data format*	HDF4	ASCII

Note: Due to some physical reasons, a mountain mask is utilized, which means not all mountain areas are included in the GlobSnow products.

* HDF4 is the first version of hierarchical data format (HDF), ASCII, abbreviated from the American Standard Code for Information Interchange, is the most common data format in computers.

4.3 Evaluation methods

The evaluation of remote sensing snow depth products is based on the analysis of point data. Pairs of snow depth estimates from the two remote sensing products were sampled according to the locations of weather stations. Accordingly, ground measurements for the sampling sites were collected as ground reference data. Statistical methods such as intra-class correlation coefficient (ICC) and root mean square error (RMSE) were adopted for evaluating data reliability including consistency and accuracy. In order to present the differences of data reliability in respect to time and space, the sample data were categorized and analyzed by season and geographical parameters such as latitude, altitude and terrain complexity.

4.3.1 Data sampling method

Remote sensing long-term snow depth data sets, including the GlobSnow and the WestDC products, were evaluated. Given that some mountainous regions were excluded in the GlobSnow product, no test data was chosen from the missing regions so as to keep the results of accuracy assessment comparable. Test data sets were collected for 35 sampling sites (see Figure 4.1). The locations of the samples were defined based on two criteria: (1) there was a ground observation station where the historical ground measurement could be acquired; (2) snow depth estimates from both of the remote sensing products were available. To match the time series of the two products, the data acquired in the period of 1979-2010 were

utilized. Considering seasonal effect on data reliability, the whole snow season covering the falling and melting periods should be taken into account. In this study, therefore, the time series from November to April of the next year were used.

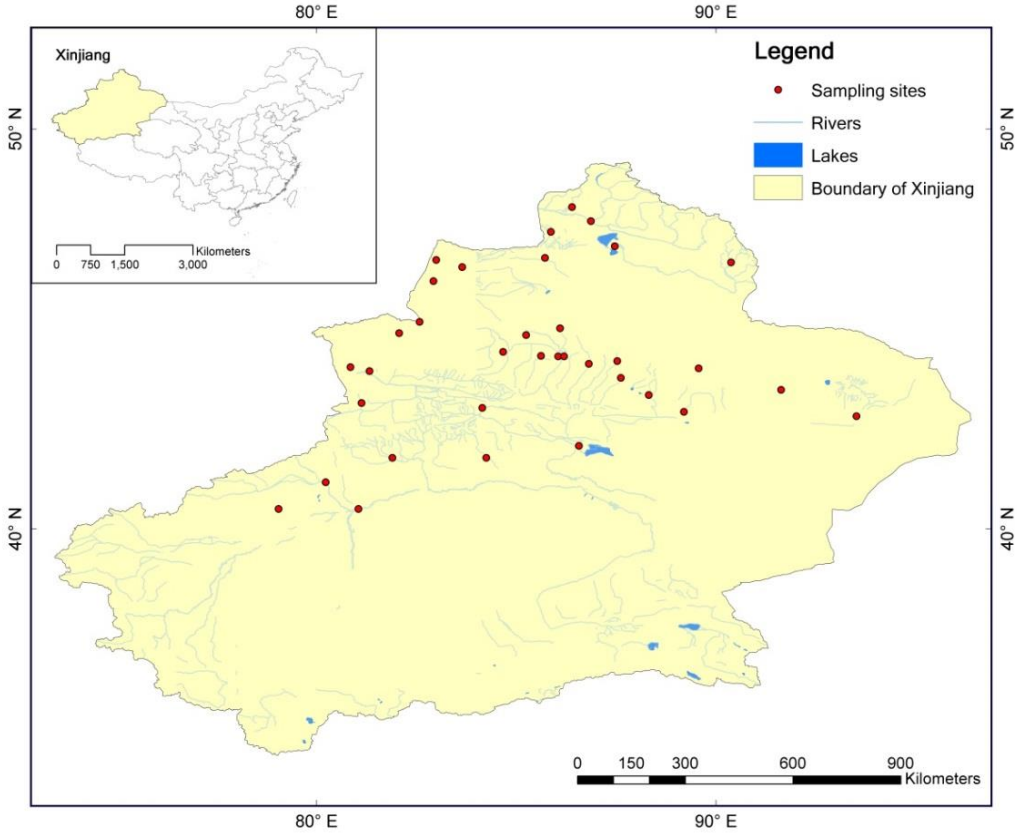

Figure 4.1 Location of sampling sites for data validation.

Ground measurements at the 35 sampling sites were acquired for data validation. For an individual assessment, none of them were involved in the creation of the two selected products. To assess the two products in different eras, three-year data for each decade were utilized, namely, 1983-1986, 1992-1995 and 2002-2005.

4.3.2 Data generalization and processing

For assessing time scale effects, the WestDC weekly and monthly data sets were derived. A 7-day moving average was applied to the WestDC daily data to generalize weekly data, in the same way that the GlobSnow weekly data were produced. The WestDC monthly data were calculated using the mean and maximum values of the generalized weekly data within a month.

Because the GlobSnow product provides the measurement of SWE rather than snow depth, to make the two data sets comparable, equation 4.1 was applied for converting the SWE values back to snow depth estimates (SD, cm), with the fixed snow density (0.24 g/cm^3) as adopted in the derivation of SWE estimates (Takala *et al.*; 2011).

$$\mathrm{SD} = (\mathrm{SWE}) \times 0.1 \times \frac{\rho_{\mathrm{water}}}{\rho_{\mathrm{snow}}} \qquad \text{(Eq. 4.1)}$$

Where, SWE represents SWE estimate in millimeters, ρ_{water} and ρ_{snow} stand for the densities of water and snow, respectively.

Daily ground measurement data was generalized to weekly and monthly data so as to match the temporal resolution of the test data sets.

4.3.3 Terrain analysis and topographic categories

A digital elevation model (DEM) with 90-meter spatial resolution (SRTM DEM v4.1) was utilized for the analysis of topographical effects.

A terrain complexity index (TCI), which measures the variation of

elevations within an area, was derived based on the DEM data. There are many different suggestions on the analytic unit for analyzing the terrain complexity in Xinjiang's high mountainous areas such as the Tianshan Mountains (Zhao *et al.*, 2009) and the Altai Mountains (Tang *et al.*, 2006). According to Wang and L ü (2009), the optimal analytic unit of TCI for the whole Xinjiang is 2.56 km^2. In this study, the standard deviation of altitude was used for measuring relief amplitude in an area with the radius of 10 grid cells (approx. 2.54 km^2). To match the spatial resolution of remote sensing products (*i.e.*, 25 km), the mean TCI in the coarse pixel was calculated. Considering that the accuracy of the SRTM DEM data is about ±10 m (refer to Farr *et al.*, 2007), the sampling sites were classified into two terrain complexity classes, *i.e.*, TCI < 10 m or TCI ≥ 10 m.

4.3.4 Consistency test

Intra-class Correlation Coefficient (ICC) was employed to assess the conformity of the two remote sensing products. For repeated measurements on the same sample group, it indicates how alike the results given by different observers are (Shrout & Fleiss, 1979; McGraw & Wong, 1996). Different from Pearson correlation coefficient (r) which demands independent variables, the application of ICCs does not need the assumption of independence (Bland & Altman, 1990). Given that the two products originated from the same data source and pairs of samples can be treated as two measurements on the same group of targets, the ICC is more

suitable for this case.

The ICC is conceptualized as the ratio of between-group variance to the total variance. The calculation is defined by several forms (Shrout & Fleiss 1979; McGraw & Wong 1996). How to choose an appropriate ICC model is based on three decisions: (1) which variance model should be adopted: one-way, two-way random or two-way fixed; (2) are you interested in absolute agreement or just the consistent ratings without the same actual scores? (3) whether you plan to rely on a single judge or a combination of several judges? (Shrout & Fleiss, 1979; Norušis, 2012). In this study, the ICC(C, 1) model defined by equation 4.2 (McGraw & Wong, 1996) was employed, since the analytical results need to be applied to the whole study region beyond the samples.

$$\hat{\rho}_{\mathrm{ICC(C,1)}} = \frac{\mathrm{M_R} - \mathrm{M_E}}{\mathrm{M_R} + (k-1)\mathrm{M_E}} \qquad \text{(Eq. 4.2)}$$

Where, $\hat{\rho}_{\mathrm{ICC(C,1)}}$represents the ICC value calculated under the ICC(C, 1) model, $\mathrm{M_R}$ = mean square for pairs of estimates; $\mathrm{M_E}$ = residual mean square; k = the number of observations. In this study, two observations were made on a single case, so that k = 2.

The range of the ICC is [0, 1]. A greater ICC represents better data consistency. According to Landis and Koch (1977), ICC > 0.4 is acceptable; ICC = 0.6 is the threshold for excellent consistency; and ICC > 0.8 shows a perfect consistency. In this study, to minimize the bias caused by non-snow cover measurements, we excluded the cases with paired

remote sensing estimates being equal to zero from the ICC computation.

4.3.5 Assessment of data accuracies

Root Mean Square Error (RMSE) is a measure of the differences between values predicted and the values actually. The RMSE was calculated to assess the accuracies of remote sensing products by using the following equation 4.3.

$$\mathrm{RMSE} = \sqrt{\frac{\sum_{i=1}^{n}\left(D_i' - D_i\right)^2}{n}} \qquad \text{(Eq. 4.3)}$$

Where D_i and D_i' denote ground measurement and remote sensing estimate, respectively for the *i*th sample, n is the number of samples (sample size).

Relative RMSE (RRMSE) was calculated through dividing the RMSE by ground measurement to show the relative errors for different categories for the analyses of seasonal and spatial position effects.

4.3.6 Analyses of seasonal and topographical effects

Daily data sets from 1979 to 2010 were utilized for analyzing the seasonal and locational effects. The ICC and RMSE by month were calculated to indicate the seasonal effect on data reliability. Accuracy assessment indices (*i.e.*, RMSE, RRMSE) by site were calculated and then grouped based on latitude, altitude and terrain complexity classes to show their differences in space. Analysis of Variance (ANOVA) was employed to test whether data accuracy statistically varied by location and geographical features. All statistical analyses were performed by using

Statistical Package for the Social Sciences (SPSS) software (version 16, SPSS Inc.).

4.4 Accuracy assessment result

4.4.1 Consistency of two products and overall accuracies

Figure 4.2 shows some examples of raw data. From these figures, disagreements are shown between two long-term snow depth data sets as well as ground data. Table 4.2 shows the results of consistency test and accuracy assessment at different time scales. The daily data shows a moderate consistency (ICC = 0.438) while the generalized weekly and monthly data are clearly more consistent. Both monthly average and maximum present an excellent consistency (ICC > 0.6). The data validation result also shows that the generalized data yield a better accuracy with lower RMSE, except for monthly maximum.

(a)

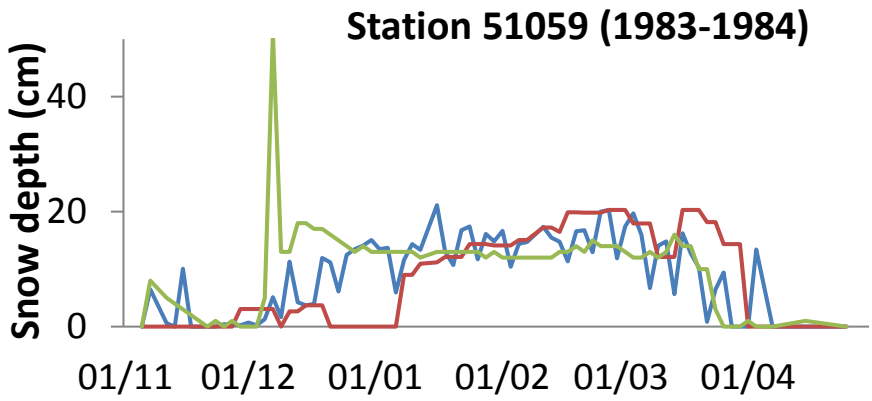

(b)

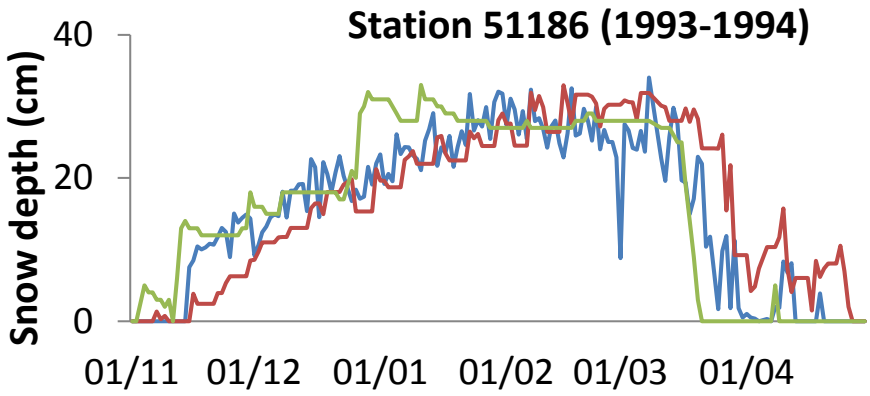

(c)

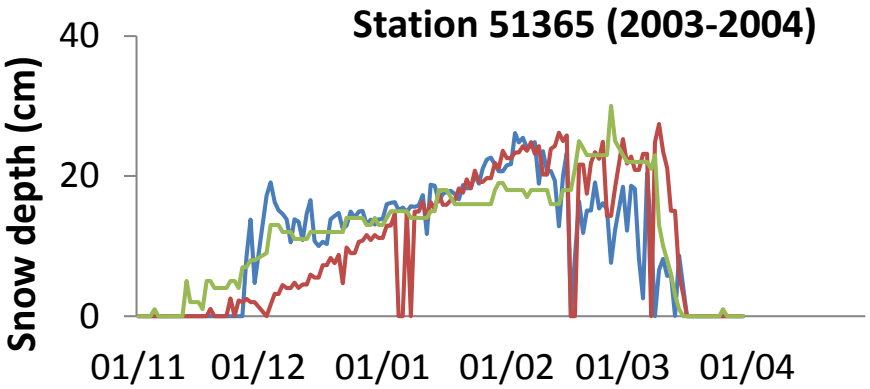

Figure 4.2 Examples of raw snow depth data, blue, red and green curves represent the GlobSnow estimates, the WestDC estimates and ground measurement of snow depth respectively.

Table 4.2 Data consistency and accuracy assessments for the two remote sensing products under different temporal resolutions

		Daily	Weekly	Monthly (ave.)	Monthly (max.)
Consistency test	Sample size	94342	128371	5243	5305
	ICC*	0.438	0.569	0.622	0.620
Accuracy assessment	Sample size	28960	37697	1250	1250
	RMSE (1) (cm)	9.54	8.02	7.23	10.27
	RMSE (2) (cm)	8.23	7.43	6.56	8.56

Note: RMSE (1) is for the GlobSnow product, RMSE (2) is for the WestDC

product.

*p < 0.05, ICCs for single measures are adopted to match the form of ICC(C, 1).

4.4.2 Seasonal effect on data reliability

Table 4.3 shows the variation of data consistency and accuracy for different months. Since samples with the value of zero are excluded in consistency test, sample size of each month implies the number of snow accumulation days. Accordingly, March is regarded as the last month of stable snow accumulation period while April is the start of snow melting period. The impact of snow melting on the reliability of remote sensing snow depth detection is obvious as the test data in March has shown a much better consistency than that in April.

Table 4.3 Data consistency and accuracy assessment by month

		NOV	DEC	JAN	FEB	MAR	APR
Consistency test	Sample size	6953	17925	23902	21897	17969	5696
	ICC*	0.165	0.249	0.353	0.407	0.425	0.037
Accuracy assessment	Sample size	5022	5680	5825	5049	5183	2156
	RMSE (1) (cm)	4.04	8.51	11.63	12.94	9.74	2.34
	RMSE (2) (cm)	3.79	7.71	8.14	10.07	10.87	4.09

Note: RMSE (1) is for the GlobSnow product, RMSE (2) is for the WestDC product.

*p < 0.05, ICCs for single measures are adopted.

By compared to ground measurement data, Figure 4.3 illustrates absolute errors (*i.e.*, RMSE) and relative errors (*i.e.*, RRMSE) as well for different months. From November to April, the RMSE varies from more than 13 cm to around 2 cm, while the RRMSE shows that the reliability of remote sensing estimates becomes very low in April compared with the ground measurements.

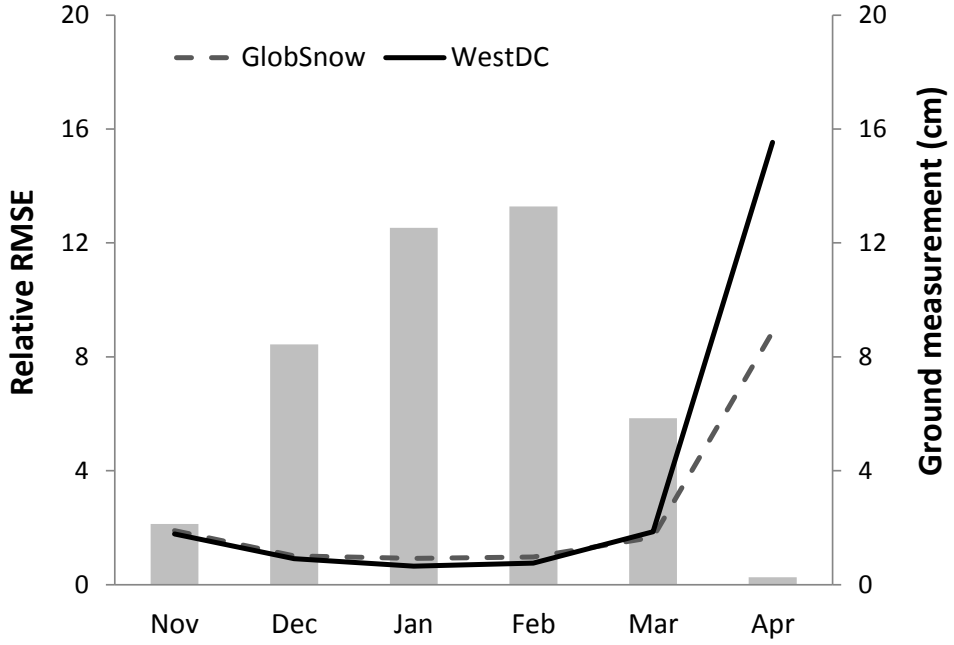

Figure 4.3 Relative RMSE of daily snow depth data sets for different months.

4.4.3 Spatial position effects on data reliability

According to the ANOVA results (Table 4.4), the altitude and terrain complexity are not statistically significant factors that affect data accuracy at a 95% confidence level. The latitude, however, is significant.

Table 4.4 The *p*-values in ANOVA tests by different locational factors

	Latitude	Altitude	Terrain complexity
the GlobSnow product	0.025	0.892	0.076
the WestDC product	0.000*	0.071	0.623

* It means $p < 0.001$ in SPSS software.

Table 4.5 shows the mean RMSE of each latitude zone category with standard error of the mean based on daily data. Compared to the ground measurement data, Figure 4.4 also shows relative errors for different latitude zones. The results suggest that data in high latitude regions yield a higher RMSE and the difference is more obvious in the WestDC than the GlobSnow product. Taking the ground reference data into account, the relative errors are similar for both the two data sets except for the region of 42 °N below.

Table 4.5 Mean RMSE by latitude zone category with standard error of the mean

	GlobSnow daily product		WestDC daily product	
Latitude zone	RMSE	SEM	RMSE	SEM
< 42 °N	6.81	1.65	2.13	0.63
42 °N - 44 °N	8.19	0.86	5.02	1.49
44 °N - 46 °N	7.63	0.52	8.39	0.54
> 46 °N	10.85	1.00	9.61	0.94

Note: RMSE means root mean square error; SEM means standard error of the mean; results are reported in centimeters.

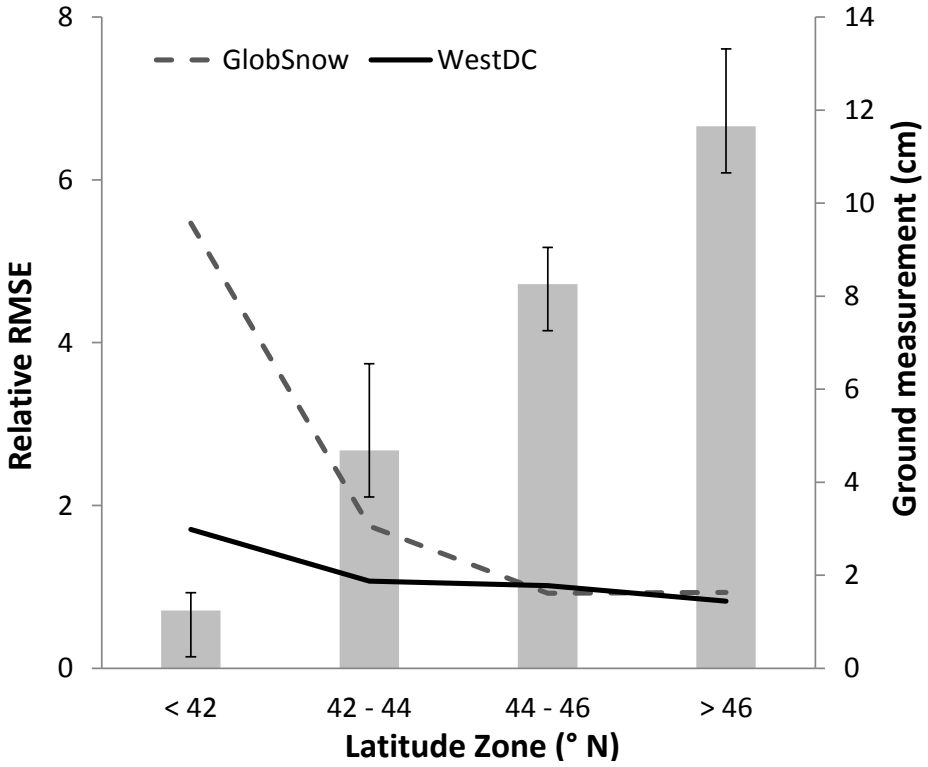

Figure 4.4 Relative RMSE associated with monthly average of ground data for different latitude zones.

4.5 Analysis and discussion

4.5.1 Data reliability over the study area

Although originated from the same data source, remote sensing snow depth products do not correlate well. Furthermore, their accuracies are not high for the study area, which can be justified by the RMSE results. Some reasons for the low accuracy in our test might be: (1) that the snow depth retrieval algorithms designed for global or country-level scales need to be further calibrated for the study area; (2) that the snow depth detected in the snow melting period gives low data reliability; and (3) that the spatial heterogeneity due to the coarse spatial resolution increases the uncertainty

of the snow depth estimates. Comparatively, the WestDC product provides a better accuracy of snow depth estimate than the GlobSnow product, regardless of analytic temporal scales.

The seasonal effect is proven significant for data reliability. Since the snow depth retrieval algorithms normally assume dry snow, the quality of snow depth products is deteriorated during the snow melting period. For instance, our tests show that the ICC rapidly falls down to the unacceptable level in April, and the relative error in April is also much lower than that in other months.

Scatter plot can be used to get a quick impression of data consistency between two data sets. Dots in scatter plot should fall on the reference line of $y = x$ if two data sets measure the same values. When dots are concentrated lower than that line, the estimation of y method tends to be larger than that of x method, and *vice versa*. Taking the WestDC product as an example, a scatter plot (Figure 4.5) is presented to show the correlation between remote sensing estimates and ground measurements. Figures 4.4(a) and (b) show the correlations in January (representing the snow accumulation period) and in April (representing the snow melting period), respectively. Comparing these two figures, it is suggested that the agreements between remote sensing estimates and ground measurements varied greatly with the season, as the January data has shown a much closer agreement than that of April.

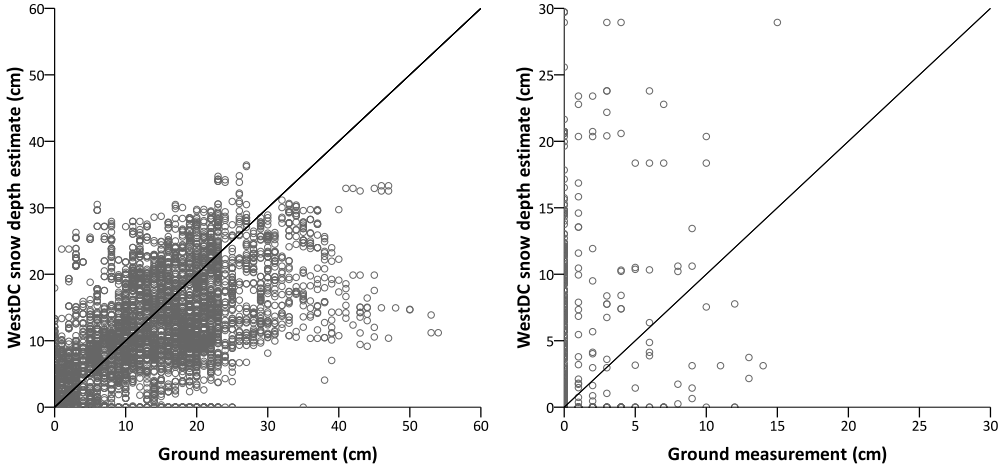

(*a*) (*b*)

Figure 4.5 The scatter plots of the WestDC estimates against ground measurements: (a) in January, and (b) in April.

According to statistical analysis, the accuracy of remote sensing snow depth estimate is also highly related to latitude zone. The absolute errors increase from low to high latitude regions. However, the relative errors remain unchanged except for the region of 42 ° N below. This implies that the absolute error increases as the thickness of snowpack increases within a certain range. Given that average snow depth in the region of 42 °N below is lower than 1 cm, the large relative error confirms that passive microware is less reliable in detecting the depth of thin snow (Tait & Armstrong, 1996; Armstrong & Brodzik, 2002).

4.5.2 ICC limitations

The ICC provides a quantitative means to reflecting the extent to which snow depth estimates given by two methods tend to be alike. Since this index is based on the comparison between group variance and total

variance, it should be pointed out that ICC has its limitation. This kind of coefficient depends on the range of observed values. For example, ICC is not suitable for evaluating the consistency of data sets whose ranges are smaller and homogeneous.

4.5.3 Some inconsistency with other studies

It is noted that the errors of the GlobSnow product reported in the study are less than in the documentary (Takala *et al.*, 2011). A reason is that the accuracy varies at different regions. Besides, Chang *et al.* (2005) indicated that more sites used in accuracy assessment would yield a better result. It should be pointed out that possible "value jumps" in the GlobSnow products indicated by Hancock *et al.*, (2013) may also cause uncertainties.

4.6 Summary of this chapter

It is important to understand the reliability and applicability of remote sensing snow depth data sets for snow cover studies in terms of snow volume change. In this study, two readily available long-term products were compared and evaluated for the western aridzone of China. The results indicate that these two products do not correlate well for the study area, and their accuracies compared to the corresponding ground measurements are rather low. Comparatively the WestDC product shows a better accuracy than the GlobSnow product. Seasonal factor and latitude have statistically significant effects on data reliability.

The results from this study suggest: (1) that during the snow melting period remote sensing snow depth estimates become less trustworthy; and (2) that the data quality is appeared better at lower latitude than at higher latitude regions, excluding the measurements of thin snow. From the point of view of multi-temporal analysis, this study also suggests that generalized data at a coarser time scale can improve the data consistency and accuracy. It is therefore concluded that a more generalized temporal scale should be employed for a long-term time series analysis based on these existing remote sensing snow depth data sets. Further studies will aim to improve the data reliability by calibrating the remote sensing snow depth estimates with other reference data, such as higher-resolution optical snow cover imagery and terrain parameters derived from digital elevation models.

(Intentionally left blank)

Chapter 5 Fusion of Snow Cover Extent and Depth Data

According to the pervious study of Chapter 4, the accuracies of long-term remote sensing snow products are very low for regional studies. To improve the spatial resolution of this kind of data, an image fusion method will be proposed in the present chapter. A linear spectral mixture model is adopted to handle the mixed pixel problem in passive microwave data for getting more accurate snow depth estimates. The proposed method takes the advantages of higher spatial resolution offered by optical sensors and the ability of snow depth detection by passive microwave sensors.

5.1 Introduction

5.1.1 Remote sensing image fusion: a review

Data fusion combines data from multiple sources with the purposes of improving the potential values and interpretation performances or producing a high-quality visible representation of the source data (Zhang, 2010). As for remote sensing data, higher spectral resolution in a normal case means lower spatial resolution due to some physical reasons and the limitation of technology. It is not surprising that an ideal “super sensor”

does not exist (Lillesand *et al.*, 2008). Remote sensing data fusion techniques are therefore developed to integrate spatial and spectral information acquired from different sensors mounted on satellites, aircraft and ground platforms to produce more comprehensive and detailed information of the earth observation.

Remote sensing data fusion techniques can be classified into three different levels according to the stage at which the fusion takes place: the pixel, the feature and the decision levels (Pohl & van Genderen, 1998). At pixel level, image fusion means fusion at the lowest processing level referring to the merge of measured physical parameters. Feature-level fusion combines the detection and extraction of objects from different data sources. Decision-level fusion combines the results from multiple algorithms to yield a final decision (Pohl & van Genderen, 1998). A combination of the three levels is often applied in practical operations (Zhang, 2010).

5.1.2 Data fusion of snow cover observations

With the development of remote sensing technology, a large amount of high spatial resolution images and products are now available. Among current snow cover products, the MODIS product is widely used in regional snow cover studies for the advantages of comparatively high spatial resolution and mature classification algorithm (Dozier & Painter, 2004; Wang & Che, 2012). However, the optical remote sensing based

product is severely affected by cloud cover, especially for the daily product (Hall & Riggs, 2007; Wang *et al.*, 2008).

Fusion methods of multi-source data have been proposed for the removal of cloud in optical snow cover products. Generally, two fusion schemes are widely adopted. One is based on the combination of two paired snow cover extent products such as Terra (AM-1) and Aqua (PM-1) MODIS products (*e.g.*, Wang & Xie, 2009). A multi-day combination is used to reduce the cloud coverage. The other is based on the fusion of passive microwave and optical snow cover products (*e.g.*, Liang *et al.*, 2008; Gao *et al.*, 2010; Wang & Che, 2011). It takes both the advantages of high spatial resolution of optical sensors and cloud penetration of passive microwave sensors.

5.1.3 Objectives

From the existing studies, data fusion is focused on the improvement of snow cover extent detection rather than the accuracy of snow depth estimation. Although many efforts have been undertaken to produce a relative accurate snow depth product from passive microwave remote sensing data, the low spatial resolution of microwave imagery limits the further improvement. Estimation of snow depth or snow water equivalent is probably affected by mixed pixel problem especially in mountainous areas with complex topography.

In order to improve the accuracy of long-term remote sensing snow

depth data from the perspective of its spatial resolution, this study aims to develop a fusion method of integrating snow cover extent and depth products. Apart from the improvement of spatial resolution, snow depth estimates will be calibrated with high-resolution snow cover extent information.

5.2 Problem formulation

A pixel of snow depth product such as the WestDC product covers a large area of 625 km^2 (25 km ×25 km). Due to the spatial heterogeneity of snow, snow cover is not evenly distributed in a pixel. The estimated snow depth value represents an overall situation of snow cover in such a large area.

The case of "pure" snow covered pixel is a minority. The overwhelming majority of snow-covered pixels in the snow depth product are the mixture of snow and non-snow covers in a finer spatial resolution. Figure 5.1 shows a case of mixed pixel problem in snow depth product. Right figure represents a snow-covered pixel with lower spatial resolution of 0.25 degree. Covering the same area, left figure shows more details detected from a finer-resolution optical imagery such as MODIS snow cover extent product. Given that the spatial resolution of MODIS data is 0.05 degree, a pixel in the WestDC product can be divided into twenty-five sub-pixels using the pixel size of the MODIS product.

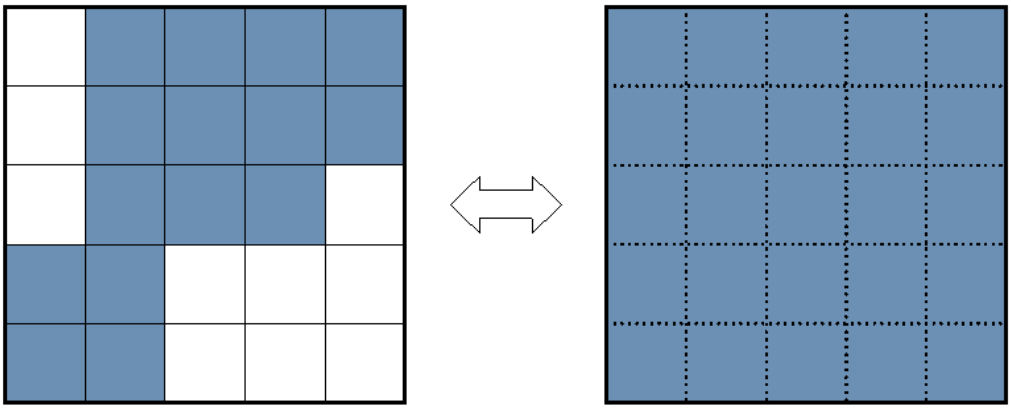

Figure 5.1 Example of mixed pixel problem in snow depth data, blue cell means the sub-pixel covered with snow and blank cell means a snow-free sub-pixel.

The retrieval of snow depth is based on passive microwave brightness temperature, which is more commonly known as the microwave energy or signal received by sensors. For the case shown in Figure 5.1, the value of brightness temperature in a coarse pixel (right figure) represents the emission of microwave from both snow and snow-free areas (left figure). It is normally considered as a linear combination of different endmembers (Liang, 2004), which can be represented by the following equation.

$$Tb = \sum \lambda_i Tb_i + \varepsilon \qquad \text{(Eq. 5.1)}$$

Where, Tb denotes the brightness temperature of a given pixel;

Tb_i denotes the partial brightness temperature contributed by component *i*;

λ_i is the proportion of component *i* in that mixed pixel, and in this formula $\sum \lambda_i = 1$;

ε means the residuals.

Definition of "pure" pixels of the endmemebers is the key to spectral

linear unmixing. A commonly adopted solution is to fine pure pixels for each endmember from the original image. However, it is almost impossible to find pure pixels in passive microwave images due to the coarse resolution. To simplify the analysis, two cover types, namely snow cover and non-snow cover are considered in the study. Accordingly, Equation 5.1 can be simply expressed as:

$$Tb = \lambda_{snow} Tb_{snow} + \lambda_{others} Tb_{others} \quad \text{(Eq. 5.2)}$$

Where, Tb denotes the brightness temperature of a given pixel;

Tb_{snow} and Tb_{others} denote the brightness temperatures contributed by snow cover and non-snow cover, respectively;

λ_{snow} and λ_{others} represent the proportions of snow cover and non-snow cover in that mixed pixel, respectively; here $\lambda_{snow} + \lambda_{others} = 1$.

5.3 Fusion scheme

Since the spectrum mixture is a large-scale phenomenon regarding the passive microwave pixel, a linear unmixing method would be appropriate and adopted for settling the mixed pixel problem. Considering a mixed pixel in snow depth data, signal received by sensor consists of different components as Equation 5.1 shows. Signal from the part of snow cover in that pixel should be separated so as to retrieve more accurate estimate of snow depth. This separation can be realized according to the proportion information of snow cover in a mixed pixel provided by high-resolution snow cover extent data. Combining the modified snow depth estimates

with high-resolution snow cover extent data, the fused data offering more accurate snow depth estimates with a higher spatial resolution. Figure 5.2 shows the process of the proposed fusion method.

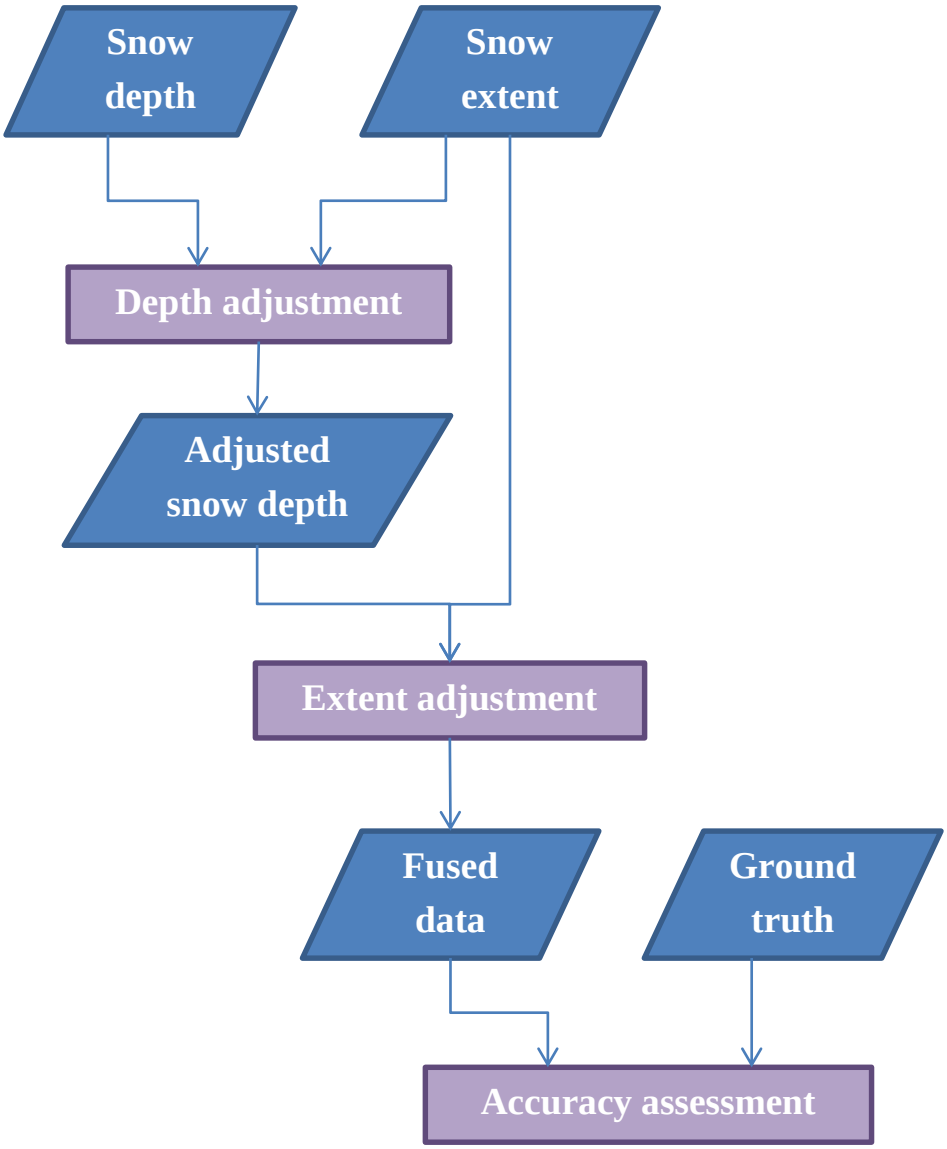

Figure 5.2 Flowchart of data fusion.

Snow depth estimates of the WestDC product are retrieved from passive microwave data based on the Che's algorithm (refer to Che *et al.*, 2008). According to Equation 5.2, snow depth estimates can be adjusted

by the following Equation 5.3.

$$SD' = \frac{SD - 0.78 \times (1 - \lambda_{snow})(Tb_{19H,others} - Tb_{36H,others})}{\lambda_{snow}} \quad \text{(Eq. 5.3)}$$

Where, SD' and SD represent the adjusted and the original snow depth estimate of the WestDC data respectively;

λ_{snow} is the proportions of snow cover in a mixed pixel;

$Tb_{19H,others}$ and $Tb_{36H,others}$ denote the brightness temperatures of the other components in 19 GHz and 36 GHz channels with horizontal polarization respectively.

5.4 Experiment of data fusion

5.4.1 Data and data processing

Remote sensing snow cover products: Two products namely MODIS snow cover extent (Hall *et al.*, 2006) and the WestDC snow depth product (Che *et al.*, 2011) were used in data fusion. These two data sets have high temporal resolutions (*e.g.*, one-day repeat cycle) but low spatial resolutions (*e.g.*, 0.5 km, which is around 0.05 degree for the MODIS data, 25 km, which is around 0.25 degree for the WestDC data). Because it is difficult to distinguish heavy cloud from snow cover in optical imagery, an 8-day MODIS composite (MOD10C2) was adopted so that the effect of cloud cover can be minimized. To maintain the consistency of snow cover condition for the two data sets, the WestDC weekly product was

employed. The same commencement date of the two composites was chosen as the observation time. In this experiment, snow cover products of January 1st, 2008 were used for the implement of data fusion. The paired products were projected to the same coordinate system so that they can be well matched in overlaying analysis. Table 5.1 shows the characteristics of the two data sets. It should be noted that the paired products were cropped to match the study area.

Table 5.1 Characteristics of the fusion data

Data name	Platform/Sensor	Coverage	Spatial resolution	Time interval	Projection
MOD10C2	EOS Terra/ MODIS	Global	0.05 deg.	8 days	Latitude-longitude
The WestDC weekly	EOS Aqua/ AMSR-E	China	0.25 deg.	Weekly	Latitude-longitude

Passive microwave brightness temperature data: Passive microwave brightness temperature data acquired at the same observed date was collected to calculate the partial brightness temperature of non-snow cover components in a mixed pixel.

Ground measurement data: To evaluate the data fusion result, ground-based snow depth measurements from 40 weather stations including a snow observation station (*i.e.*, the Tianshan Station) were sampled as the ground reference. Those sampling sites are mainly distributed in the north Xinjiang where heavy snow is observed. To match the temporal resolution

of the remote sensing images, a 10-day composite by maximum value was adopted.

Other ancillary data: A DEM with 90 m resolution was utilized for analyzing the topographical effects. Terrain complexity index was generalized based on the DEM to measure the variation of elevations within an area. Sampling sites were categorized in either one of two terrain complexity classes, TCI < 10 and TCI ≥ 10. The classification of terrain features can be referred to §4.2.3.

5.4.2 Data fusion and validation method

In the fusion operation, snow depth estimates from the WestDC product were firstly calibrated based on Equation 5.3. In the equation, two critical parameters need to be determined or calculated before calibrating snow depth estimate, namely snow cover proportion (*i.e.*, the part of λ_{snow} in Equation 5.3, named as "Part A" afterward) and the brightness temperature difference between two microwave frequencies of non-snow cover (*i.e.*, the part of $\left(Tb_{19H,others} - Tb_{36H,others}\right)$ in Equation 5.3, named as "Part B" afterward).

As for the Part A, the MODIS product provides the proportion of snow cover for each pixel. Thus, to get the snow cover proportion of a WestDC pixel, 25 snow cover proportion values given by the MODIS product were averaged as the proportion of snow cover for the corresponding WestDC pixel.

As for the Part B, since it is difficult to get the actual brightness temperature difference for all the other land cover types by pixel, a general mean value of the difference for all snow-free pixels within the whole study region was employed as an estimate. In the study, a snow-cover mask generated from the WestDC product was applied to the passive microwave brightness temperature data for getting the snow-free pixels.

Figure 5.3 illustrates the fusion operation by pixel.

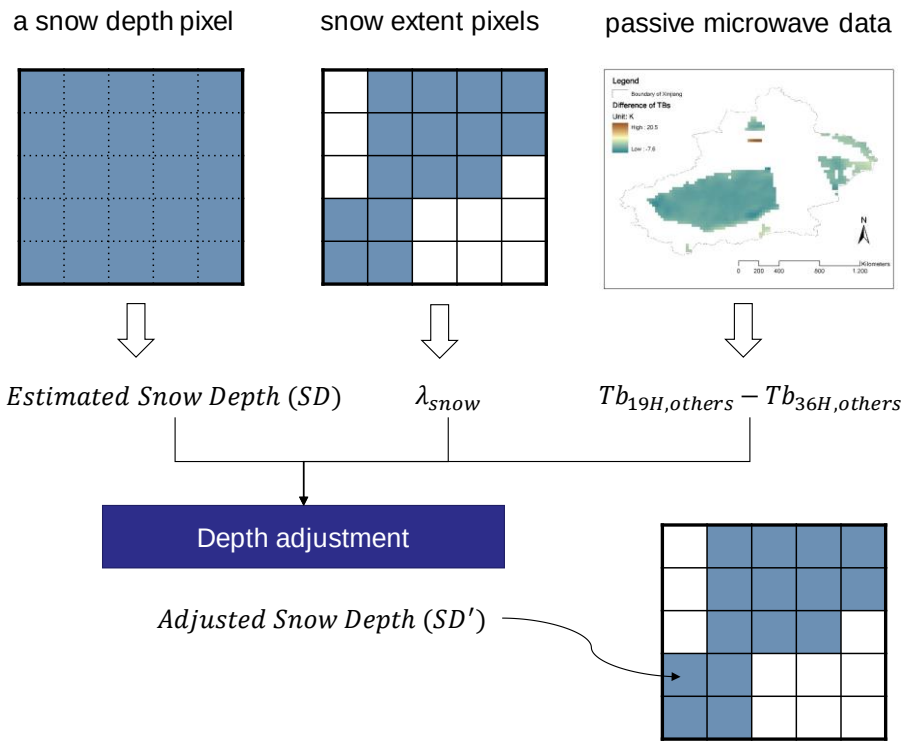

Figure 5.3 Data fusion operation.

10-day ground observation composites of the 40 sampling sites were adopted as ground truth data. RMSE analysis, comparing the estimates against the ground measurements, was employed to evaluate the overall accuracy of the fused data. In order to analyze geographical effects on data

accuracy, all samples were grouped by altitude and TCI. The ANOVA test was employed to examine whether data accuracy statistically varied by altitude and topographical features.

5.4.3 Fusion result and accuracy assessment

According to the experimental passive microwave data, the brightness temperature difference between two microwave frequencies of non-snow cover is -2.67 K. Based on this figure and snow cover proportion of every coarse pixel, all snow depth estimates were modified and then fused with fine-resolution snow cover extent product. Figure 5.4 illustrates the original snow depth product and the fusion result. Compared to the original snow depth product, the fused data with a higher spatial resolution show more details of snow cover from a spatial aspect, especially in the boundary between broad snow and non-snow covered regions.

From the correlation analysis result, snow depth estimates from the fused data agree well with that from the WestDC product (r = 0.95). However, compared to the ground reference data, the accuracy is not high with the RMSE of 5.62 cm. Figure 5.5 shows snow depth estimates from the fused data against ground measurement data. According to the ANOVA test, terrain complexity and altitude fail to be the statistically significant factors (p = 0.298 and p = 0.628, respectively) that affect the accuracy of the fusion result.

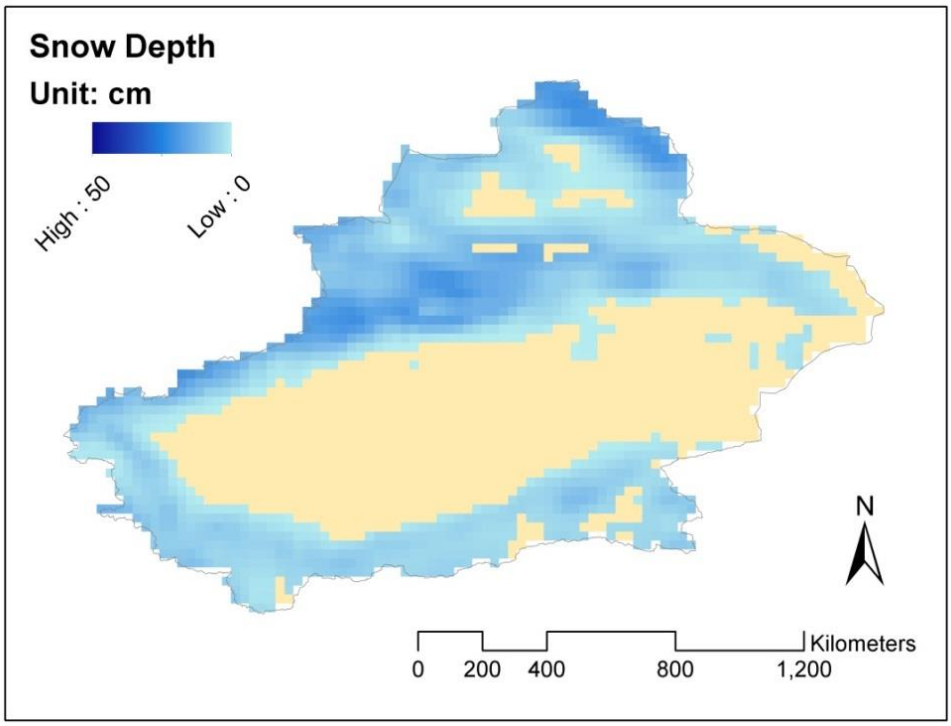

(a)

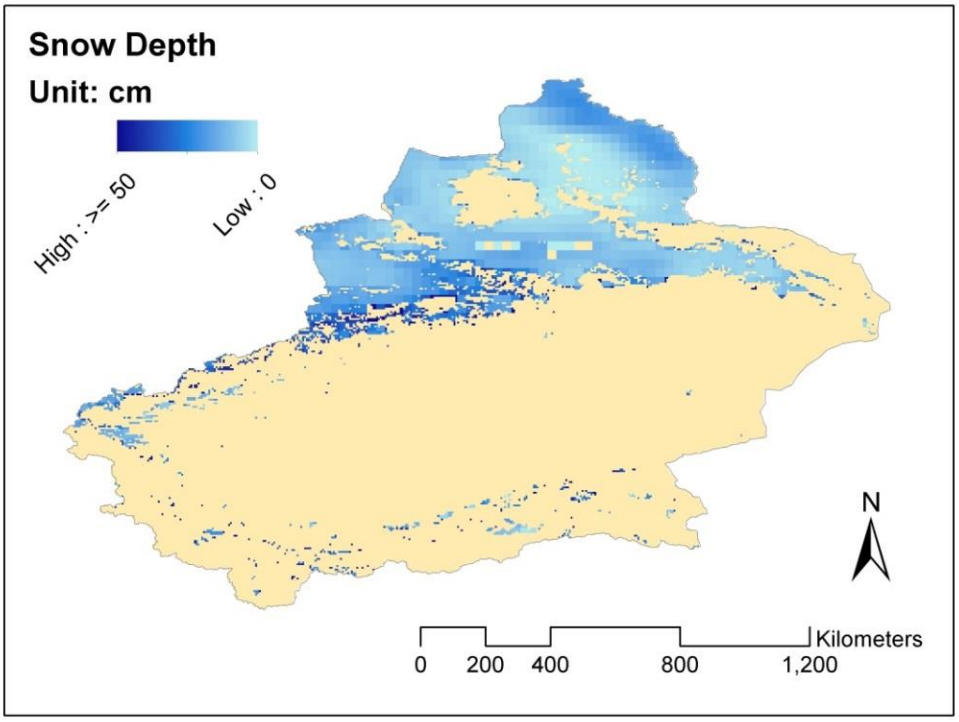

(b)

Figure 5.4 Snow depth estimates from Che's algorithm (a) and the proposed fusion method (b).

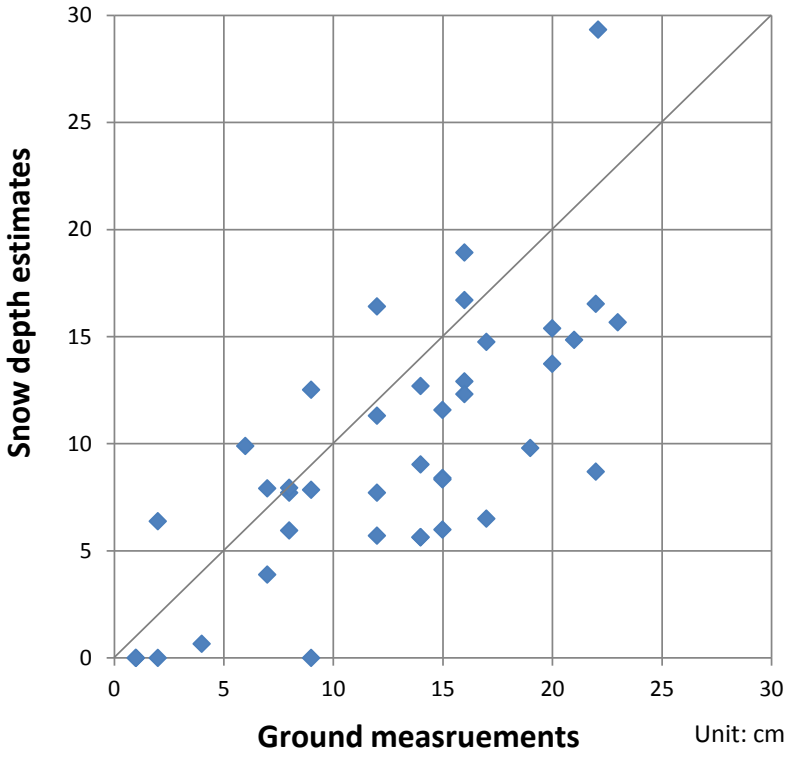

Figure 5.5 Adjusted snow depth estimates against ground truth.

5.5 Analysis and discussion

5.5.1 Fusion effect in visualization

In the original snow depth data, an even thickness of snow cover is assumed for every snow-coved pixel. When dissolving the coarse pixel into finer ones, the fused data gives more details of snow cover extent at sub-pixel level. As for MODIS snow cover extent product, a pixel with snow-covered area larger than 50% is demarcated as a snow-cover pixel. Less than 50% is regarded as non-snow cover pixel. This may explain the appearance of the “saw tooth” shape at the fringes of some snow cover regions.

Another reason for the sudden change in space of snow depth estimate is due to the thin layer of snow which is reported to be difficult to detect from optical remote sensing imagery. Thus, when taking the optical snow cover extent product as a reference, thin snow on the fringe areas of Taklimakan desert and the Kunlun Mountains would not be displayed in the fused data. Meanwhile, uncertainties can also come from the original snow depth data. Che *et al.* (2008) pointed out that it is difficult to distinguish thin snow from the frozen land using passive microwave data. The large area in the Kunlun Mountains displayed as a snow-covered region in the WestDC data may not actually be covered by snow.

5.5.2 Limitations of the fusion

To determine the exact brightness temperature contributed by snow cover is the key to get an accurate estimate of snow depth. Great efforts should be made to remove the part contributed by non-snow cover types. Although this part can be retrieved by measuring the brightness temperature of the underlying surface in the following summer or melting season, a change may happen in the underlying surface due to seasonal changes. In addition, the statuses of satellite and sensor as well as the atmosphere at the moment of data acquisition would also be different. Therefore, it is better to find "pure" pixels for non-snow cover types in the original passive microwave data. In this study, it is difficult to find such a

"pure" pixel in this study due to the coarse spatial resolution. A pixel covering a huge area contains various land cover types. As an alternative way, the mean value of brightness temperatures given by non-snow cover types was adopted. For this reason, a bias in snow depth estimate may be created.

According to the pervious chapter (Chapter 4), the accuracy of remotely sensed long-term snow depth products have low data accuracies with RMSEs ranging from 6.6 cm to 8.2 cm at different time intervals. Although the accuracy level of snow depth estimates was not significantly improved for the fused data, the precision of snow mass estimation will nevertheless benefit from the finer spatial resolution of the fused imagery.

5.6 Summary of this chapter

This chapter demonstrates an image fusion method that combines optical snow cover extent with microwave snow depth products for improving the spatial resolution of snow depth product and data accuracy. MODIS 8-day composite snow cover extent product was utilized to identify the proportions of snow and non-snow cover components for each pixel. Snow depth estimates were calibrated and then merged to the high-resolution snow cover extent product. Compared with ground measurements from 40 weather stations, the fused product shows a similar data accuracy as the original product. This suggests that the fusion algorithm is valid and the practical method has proven to be effective to

enhance the spatial resolution of snow depth product.

Physical methods for obtaining brightness temperature difference between two microwave frequencies of the other land cover types should be further developed so as to better calibrate the snow depth estimates.

(Intentionally left blank)

Chapter 6 Spatio-temporal Pattern of Snow Cover

Ground measurement data from meteorological stations is commonly utilized in snow cover change studies. However, ground meteorological stations are normally disperse and unevenly distributed. It is difficult to perceive the regional difference in a large area. Remote sensing imagery is therefore employed to monitor snow cover change in continuous space and time.

Given a long time series of snow cover data, time series analysis method is adopted for characterizing the long-term change in this chapter. For better understanding the spatio-temporal pattern of snow cover change, the change analysis is conducted under two spatial scales, namely, the regional and pixel-level scales. Snow cover parameters generalized from snow depth data set are utilized for the analysis including mean and maximum snow depth (SD) and snow-covered area (SCA). Due to the difficulty of collecting all the original microwave imagery for getting a fused data set, snow depth product with spatial resolution of 25 km level will be utilized so as to keep a unified spatial scale in the analysis.

6.1 Introduction

6.1.1 Long-term observation of snow cover

Traditional *in situ* observation provides a reliable and long-term time series of snow cover data. For a large region, not all areas can be observed due to the limited number of ground stations. Ground measurements from weather stations are normally dispersed and uneven distributed. In high mountainous areas, where permanent and seasonal snow cover would be most probably located, the ground measurements is rare, due to the difficulty of getting access to, especially in winter seasons (Schaffhauser *et al.*, 2008).

Comparing with ground measurement data, remotely sensed data offers the possibility of observation with a large perspective from the space (Li, 1999), including the observation of alpine snow cover (Jonas *et al.*, 2009; Durand *et al.*, 2009). Among various sensors, a series of passive microwave sensors enables a long-term and continuous archive of snow cover observation. Table 6.1 lists the main features of long-term snow cover observation approaches.

Table 6.1 Comparison of long-term snow cover observations

	In situ observation	Remote sensing
Measurements	snow depth, snow density, snow pressure	Snow-covered area, snow depth
Data reliability	Very high	High
Duration	> 50 years	> 30 years
Frequency	Daily	Daily*
Continuous in time	Yes	Yes
Continuous in space	No	Yes

* Passive microwave daily observation is available since 1987, before that, the observation was based on two-day interval.

6.1.2 Expression of multi-dimensional snow cover information

Study on snow cover change constitutes a multi-dimensional analysis featured by the measurements of snow depth in geographical location (spatial dimension) and time (temporal dimension). Since traditional *in situ* observation data are dispersed in space, spatial interpolation and resampling techniques are commonly adopted. Like most applications of spatial interpolation, the accuracy of interpolated data relays on the number and distribution of sample points. When only very few ground stations is available, the spatial interpolation results can only yield a low accuracy.

Remote sensing imagery naturally provides spatially continuous "observed" rather than "estimated" data. Figure 6.1 illustrates the multi-dimensional information of snow cover retrieved from remote sensing

images. As for each grid cell (pixel), it contains a time series data.

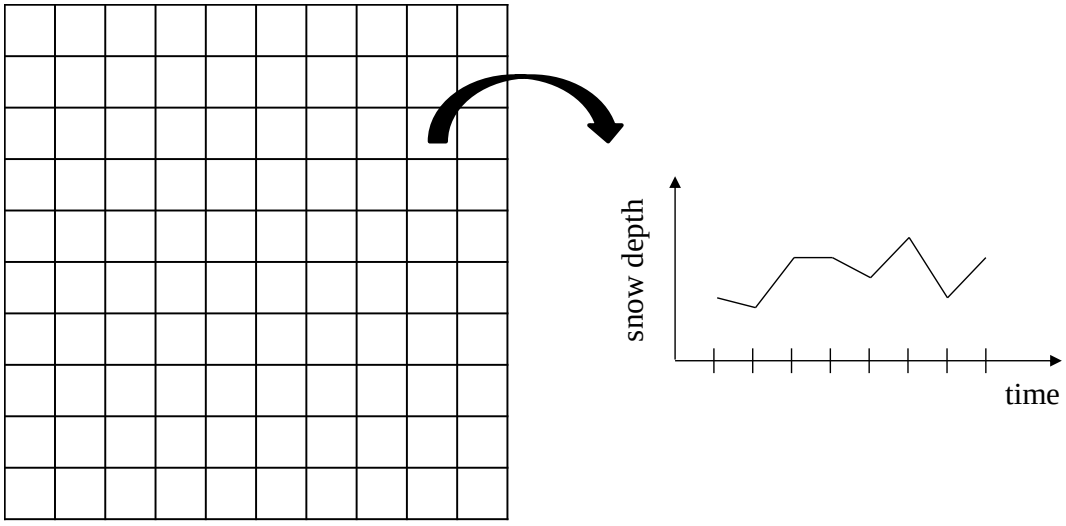

Figure 6.1 Spatio-temporal expression of multi-dimensional snow cover information.

6.1.3 Objectives

This study attempts to model and visualize the spatio-temporal pattern of long-term snow cover change using remote sensing technology. According to the results from Chapter 4, the WestDC snow depth data sets are employed for the change analysis for its better estimation on snow depth. The analysis is undertaken based on two spatial scales - the regional-level and pixel-based analyses.

6.2 Time series analysis of snow cover data

Given a long time series of snow cover data, time series analysis was adopted for snow cover change detection. The periodicity and the trend of the snow cover time series were examined.

6.2.1 Preprocessing of time series snow cover data

Moving average method is useful in time series analysis for smoothing the effect of irregular fluctuation of data and making the change trend clear. In this study, a 7-day moving average was applied to the original daily data to generate a new daily data set[2]. Since multi-day accumulation of snow cover is meaningful, the average of snow depth values in the previous six days and the present day was calculated and regarded as the moving average snow depth on the present day (Equation 6.1). The calculation process is shown in Figure 6.2.

$$\bar{y}_i = \frac{1}{7}\sum_{j=1}^{7} y_{i-j+1} \qquad \text{(Eq. 6.1)}$$

Where, y_i is the snow depth at time i; $\bar{y}_i$ is the averaged snow depth at time i.

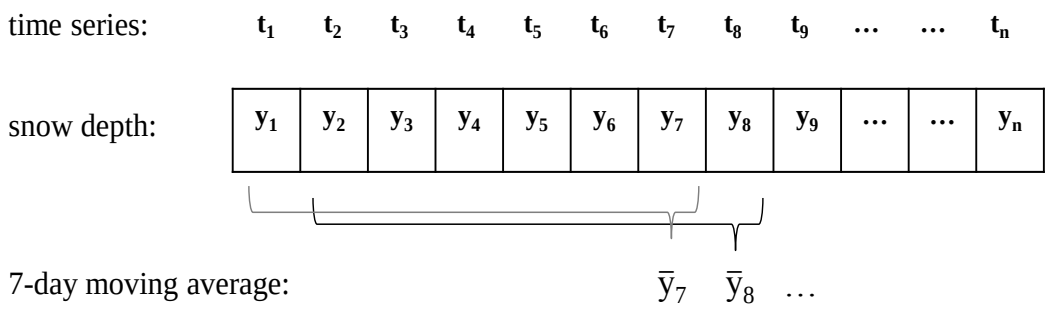

Figure 6.2 A 7-day moving average method adopted in the processing of the original daily data.

[2] In Chapter 4, the generalized data set with the same average process was called weekly data so as to match the naming of the other product. The data with one-day interval is in essence daily data.

There is no doubt that a 12-month seasonal periodic pattern exists in the snow cover data. In order to minimize the impact of periodic pattern on the trend of change, the snow depth data are organized with a 12-month interval. Accordingly, monthly and yearly data were generalized based on the moving-averaged data, including the mean and maximum snow depth in a month and in a hydrological year, respectively. In this study, the period from November to April of the next year was considered as the snow season in the study area.

6.2.2 Periodicity analysis

By transforming data to the frequency domain, spectral analysis techniques are utilized for perceiving the periodicity of time series data. Based on the Fourier analysis (or Fourier Transform, FT), time series data can be transformed into complex numbers in the form of a + bi, where a and b are the real and imaginary parts of a complex number, respectively; i is the imaginary unit ($i^2 = -1$).

Accordingly, the spectral density of a time frequency that can be calculated as:

$$P(f) = \frac{1}{N} |\mathrm{F}(f)|^2 = \frac{1}{N} (a^2 + b^2) \qquad \text{(Eq. 6.2)}$$

The corresponding frequency (f) of the largest spectral density ($P(f)$) implies the periodicity (T) of the time series data by the equation of $T = 1 / f$.

6.2.3 Trend analysis

Change trend, which means the increasing or decreasing in snow cover over a long time period, is a major concern of this study. The rate of change is often utilized to describe a long-term trend (Dou *et al.*, 2010). Assuming that snow depth over time could be expressed by a linear equation as Equation 6.3, the change rate is defined by the slope of b. Positive value means an increasing trend, while negative value means decreasing.

$$y = a + bx \qquad \text{(Eq. 6.3)}$$

where y = snow depth; x means time series = 1, 2, …, n.

According to the historical data, the slope of b can be estimated based on the principle of least square method (LSM) expressed by Equation 6.4.

$$b = \frac{\sum(x_i-\bar{x})(y_i-\bar{y})}{\sum(x_i-\bar{x})^2} = \frac{n\times\sum x_i y_i - \sum x_i \sum y_i}{n\times\sum {x_i}^2 - (\sum x_i)^2} \qquad \text{(Eq. 6.4)}$$

Where, x means time series; x_i denotes the ith observation; y_i denotes the observed snow depth at time i; $\bar{x}$ and $\bar{y}$ represent the means of x and y respectively; n is the total number of samples.

6.3 Regional-level analysis of snow cover change

Monthly snow cover time series was used for the regional-level analysis of the entire Xinjiang. Three snow cover parameters were generalized and utilized including monthly mean and maximum snow depth (SD) and

maximum snow-covered area (SCA). The first two parameters are calculated by the average or the maximum of snow depth values in a month. For monthly maximum SCA, it means that once a pixel was covered by snow within a month, even though it might melt afterward, this area should be counted in. Figure 6.3 shows the fluctuations of the three parameters during the 32-year study period.

Monthly data was utilized for analyzing the periodicity of snow cover change. The spectral density for each snow parameter was calculated in MATLAB® software (refer to Appendix III). The results are shown in Figure 6.4. Transferred from the frequency, an obvious 12-month periodicity can be observed.

Generalized from the monthly data, seasonal mean SD, maximum SD and maximum SCA were utilized for analyzing the long-term trends. The results are illustrated in Figure 6.5. From the results, snow cover of Xinjiang has a very slight change in general.

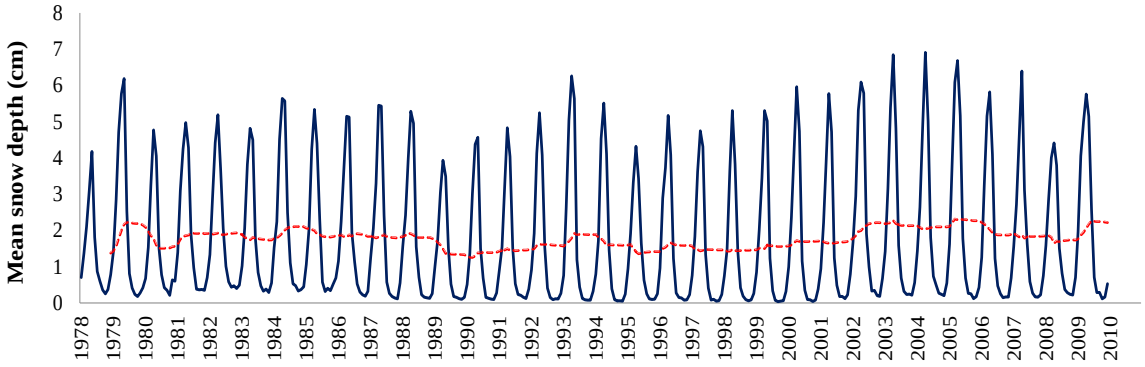

(a)

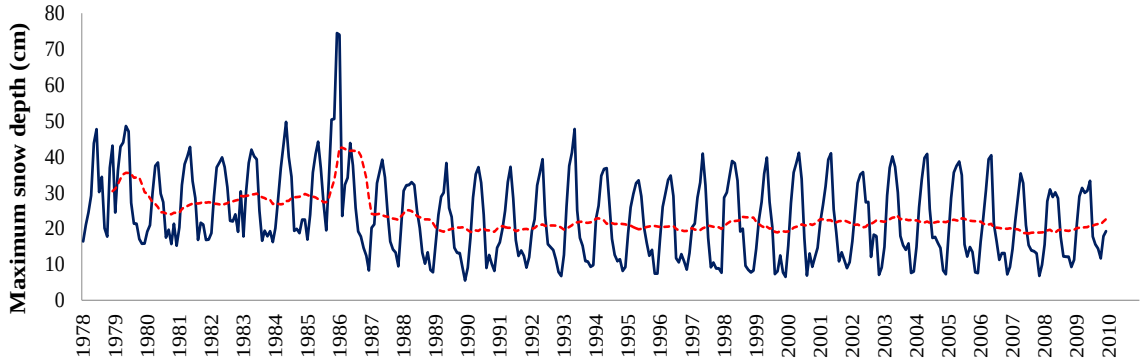

(b)

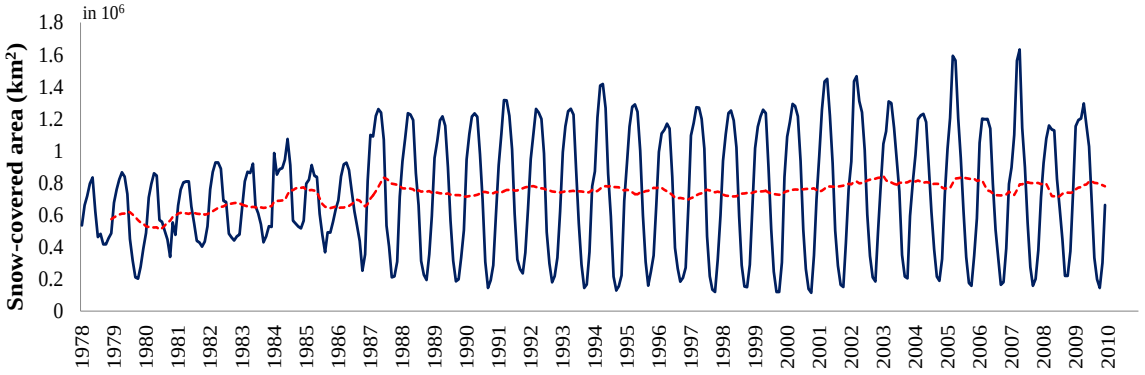

(c)

Figure 6.3 Variation of snow cover in Xinjiang by (a) monthly mean snow depth, (b) monthly maximum snow depth and (c) maximum snow-covered area in a month, red curve shows a 12-month moving average.

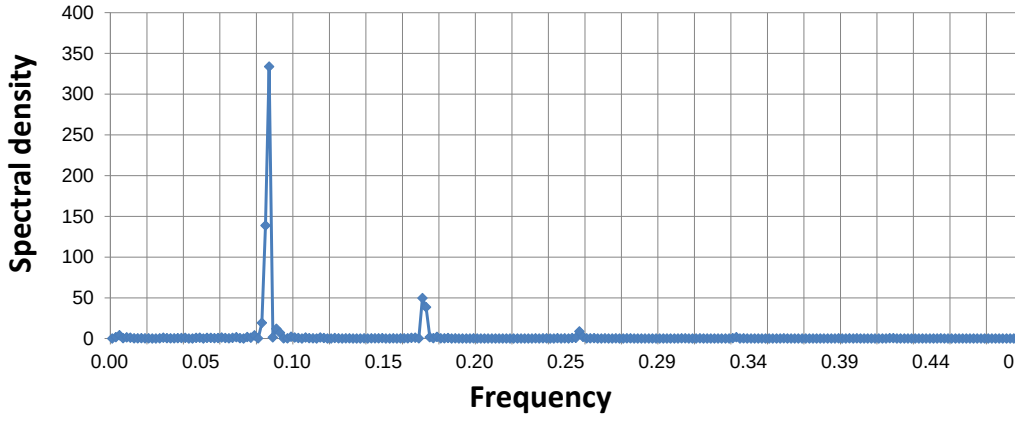

(a)

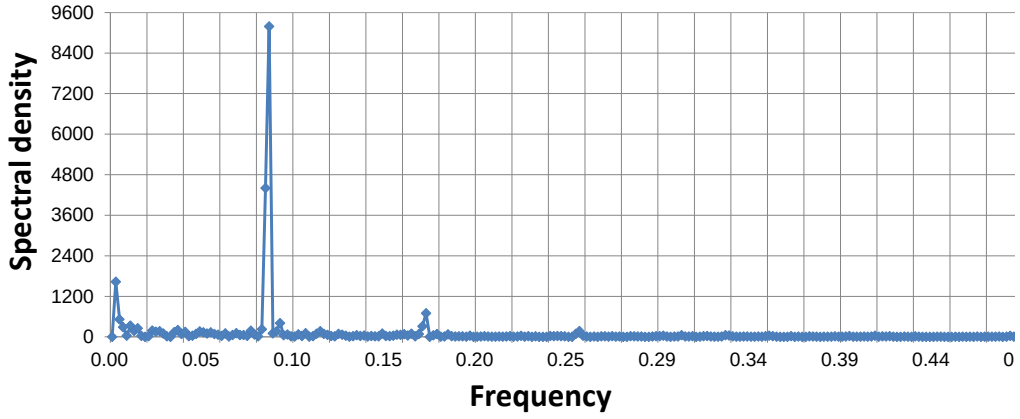

(b)

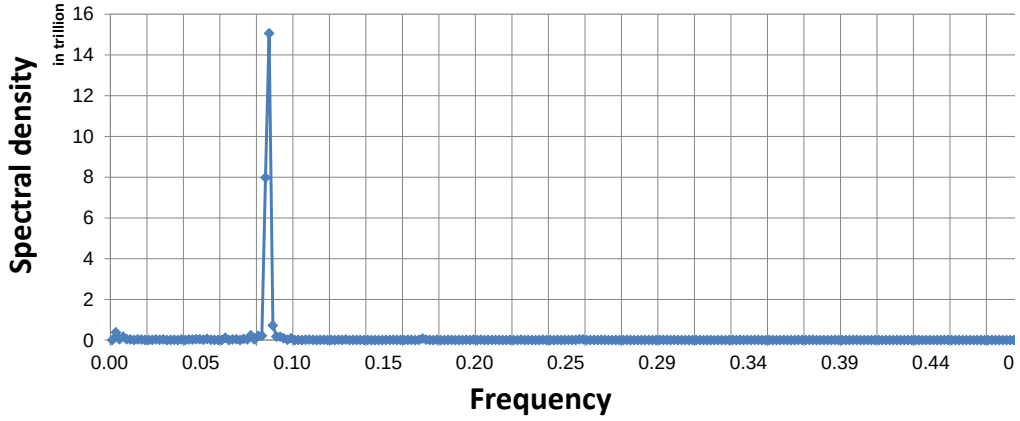

(c)

Figure 6.4 Spectral analysis for time series of (a) monthly mean SD, (b) monthly maximum SD and (c) monthly maximum SCA.

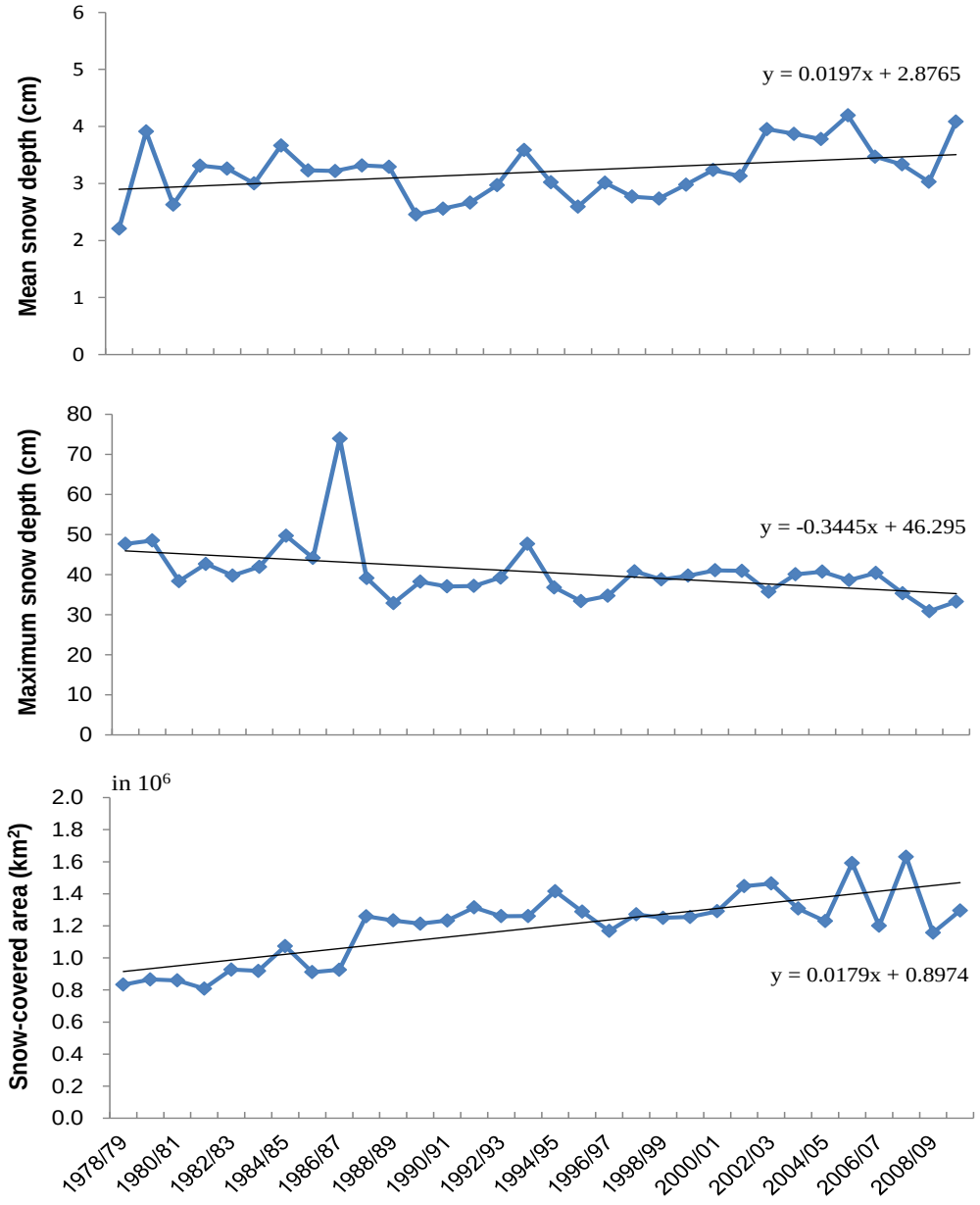

Figure 6.5 Change trends of snow cover in Xinjiang by seasonal mean snow depth, maximum snow depth and maximum snow-covered area from 1978 to 2010.

6.4 Spatio-temporal analysis of snow cover change

To represent the regional variation of snow depth change, time-series trend analysis was conducted at a pixel-by-pixel level. Snow depth data with a 12-month interval was utilized so as to remove the seasonal periodic

pattern and make the change trend more obvious. Trend analysis results were then imported into Geographical Information System (GIS) (ArcGIS 10.0, ESRI© Inc.). In the following figures, blue color stands for an increasing trend, while red color stands for a decrease in snow depth.

6.4.1 Change trend of annual snow cover

Figures 6.6(a) and (b) display the change trends of mean and maximum snow depth in snow seasons during the 32-year study period. Seasonal mean and maximum snow depth were calculated by the mean and the maximum of snow depth during a snow season (*i.e.*, from November to April of the next year) respectively. It is noted that the maximum snow depth in winter also represents the maximum of the whole hydrological year.

From the results, snow depth in snow seasons including mean and maximum depth has decreased in high mountainous areas such as the Altai and the Tianshan Mountain ranges. The increase of mean snow depth mainly distribute in the fringes of the two basins, river valley and mountain pass in the west. The maximum snow depth increased in some piedmont areas in the North.

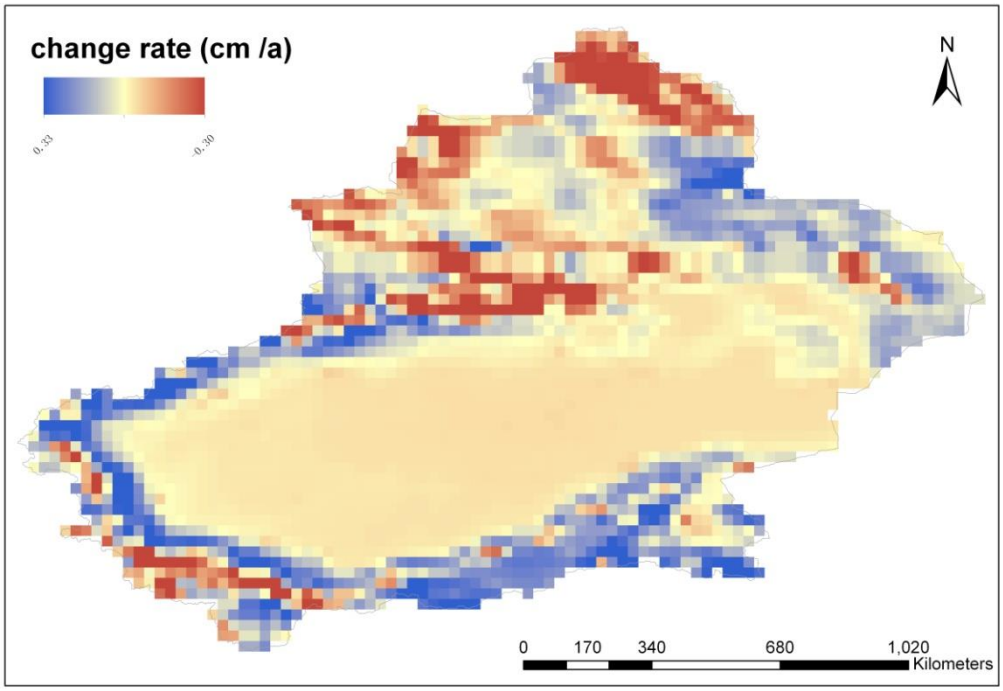

(a)

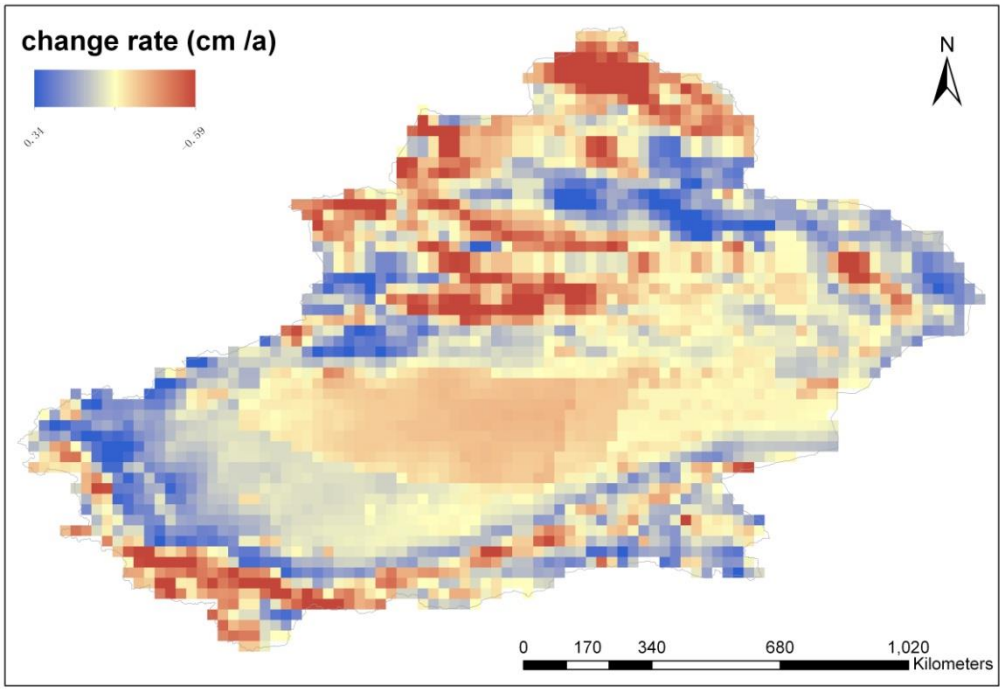

(b)

Figure 6.6 The spatial pattern of snow cover change from 1978-2010 by (a) mean snow depth and (b) maximum snow depth in snow seasons.

6.4.2 Seasonal alteration of snow cover

In order to reveal the seasonal alterations of snow cover, the trend of snow depth change was analyzed on monthly basis (Figures 6.7(a)-(k)).

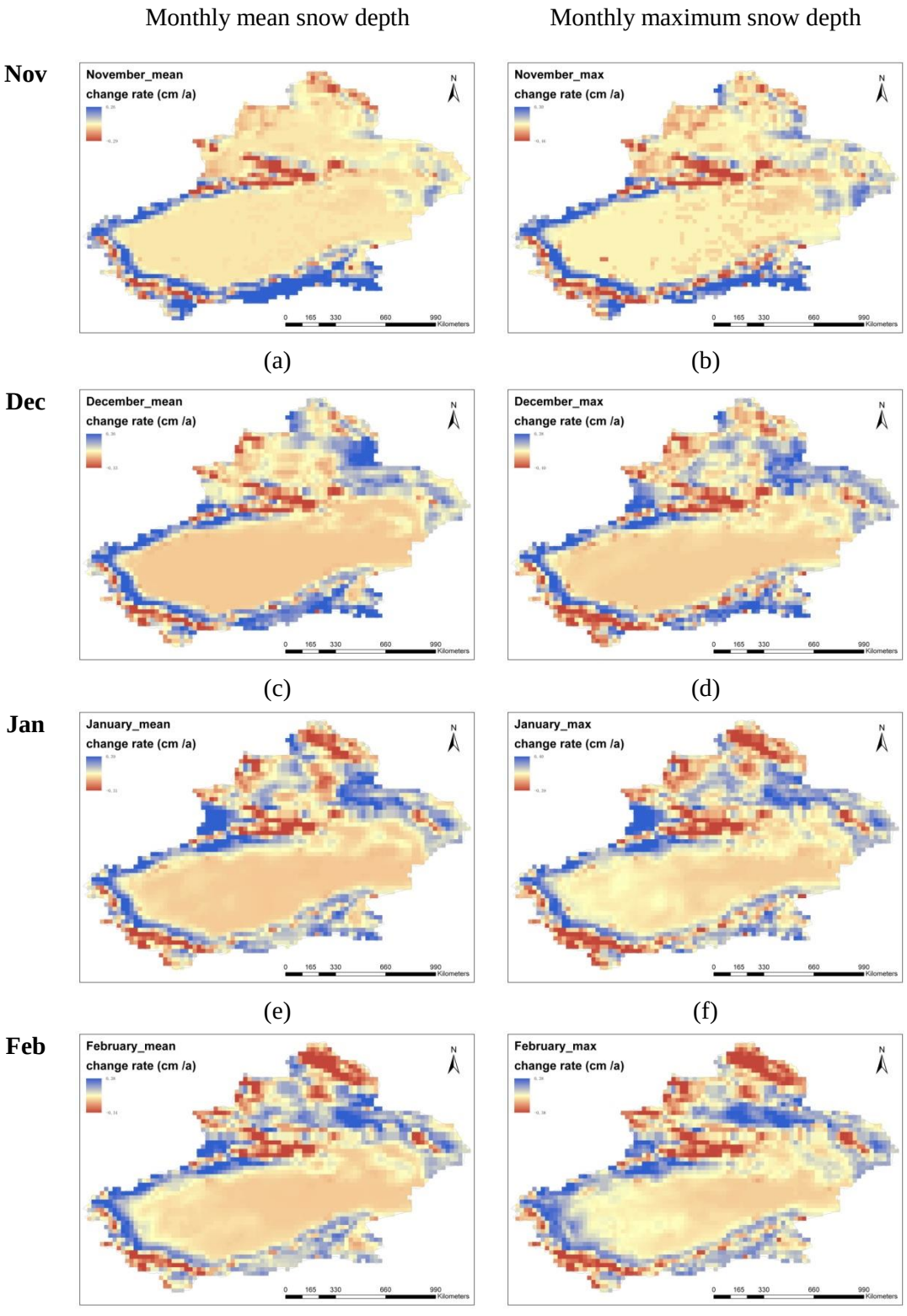

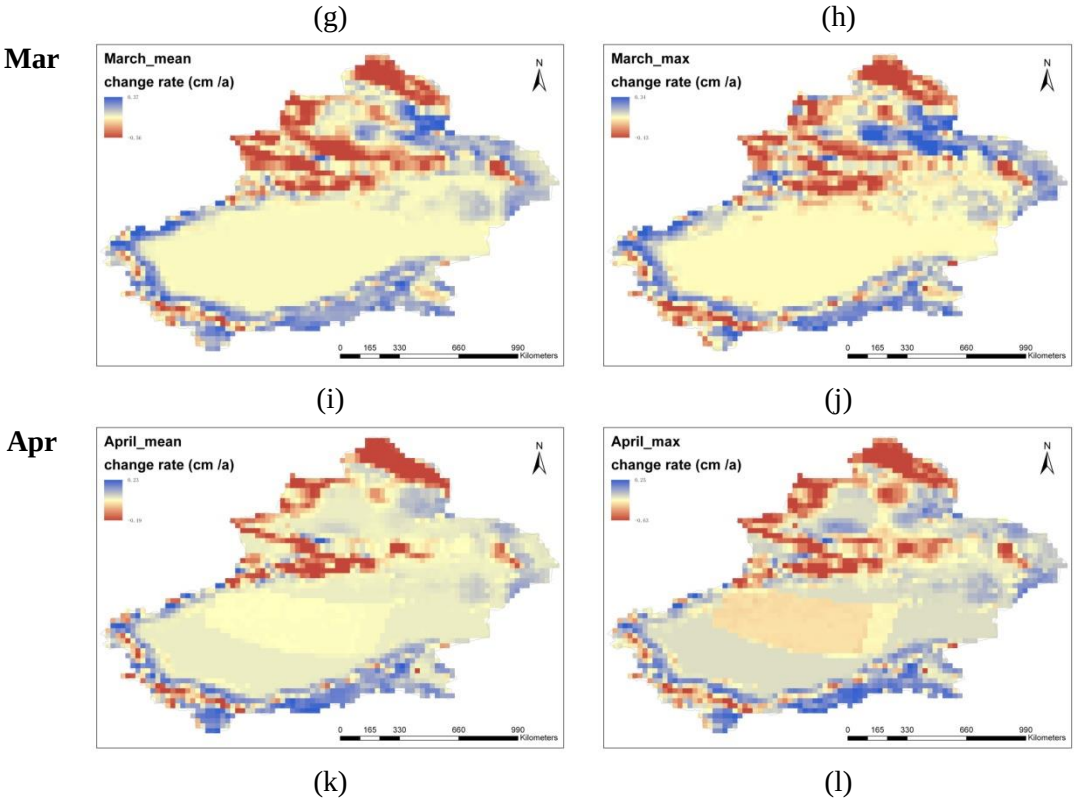

Figure 6.7 Snow cover change in different seasons, figures in left column show the change trends of monthly mean snow depth, and figures in right column show the change trends of monthly maximum snow depth.

Winter snow dominates the majority of snow cover in the whole year. Therefore, snow cover change based on monthly snow depth data in winter seasons (*i.e.*, from January to March) shows a similar spatial pattern as those of seasonal or annual data. In springs (*i.e.*, April in this study), almost all of alpine snow covered regions show a decreasing trend when snow began to melt, particularly in the North.

6.5 Analysis and discussion

6.5.1 Spatio-temporal pattern of snow cover in Xinjiang

From the regional-level analysis, Xinjiang has not experienced a significant change in snow cover in the past three decades. Meanwhile, inter-annual and inner-annual fluctuations exist (Figure 6.3(a)). Maximum snow depth had an abrupt drop after the hydrological year of 1986/1987 (Figure 6.3(b)). At the same time, the abrupt change was also noticeable in snow cover extent. Since the hydrological year of 1986/1987, snow-covered area has a trend of expansion in winter seasons but show a shrinking trend in summer seasons (Figure 6.3(c)). The inner-annual analysis shows that the decreasing snow cover mainly occurs in springs, especially for the high mountain ranges. In winters, both increasing and decreasing trends can be observed. In terms of temporal distribution during a year, snow cover is dominantly observed in winter. Therefore, winter snow cover shows almost the same change pattern as the all-year-round analysis.

The spatial pattern of the decreasing snow cover can be observed in high mountainous regions, *e.g.*, the Altai and the Tianshan Mountains. The increasing snow cover is mainly distributed in the piedmont areas and fringes of the two great basins (Figure 6.6(a)). Because snowfalls seldom occurred in the Taklimakan desert, no change of snow cover is observed there. The snow cover shows a similar spatial pattern as that of the

maximum snow depth (Figure 6.6(b)).

6.5.2 A possible reason about the change pattern

Climatic shift plays an important role in regional snow cover change. Shi *et al.* (2003) indicated that the regional climate in China's northwest has mutated from warm-dry to warm-wet since the hydrological year of 1986/1987. The abrupt changes in maximum snow depth and snow-covered area in this study are probably due to this reason.

On the basis of the climate shift theory, the water vapor transmitted to the upper space of Xinjiang would increase. Because high mountain ranges block water vapor, the transfer of water vapor in winters is mainly from the mountain pass in the west, and forms snowfalls in the first place. Therefore, the increase of snow cover occurs in that region.

Considering the temperature factor, the warming climate is not a favorable factor for snow cover maintaining. Temperature rising in spring and summer will result in the decrease of snow cover especially for the glaciers in high mountains.

6.6 Summary of this chapter

A time series analysis method was adopted for analyzing the long-term trend of snow cover change. The analysis was conducted in two spatial scales including the regional and pixel-by-pixel scales, so that the spatio-temporal pattern of snow cover can be well represented. Apart from

modelling the spatial pattern of the change, the temporal pattern of snow cover change was also analyzed.

Results show no obvious change of snow depth in Xinjiang during the past three decades. However, spatial disparity exists for different regions and at different time periods. Snow cover tends to become less in high altitude regions, while it likely increases in the piedmont areas and mountain passes. In the temporal aspect, the snow cover in springs showed a significant decreasing trend, while it does not show a significant change in the year.

From the analysis in this chapter, one suggestion is that the change of the spatio-temporal pattern is the local/regional response to the climatic change in China's northwest since the hydrological year of 1986/1987. The details of the impact of such climatic change on snow cover will be discussed in the next chapter.

Chapter 7 The Relation between Snow Cover and Climatic Changes

The impact of climatic change on the spatio-temporal pattern of snow cover in Xinjiang will be evaluated based on two climate models in two spatial scales, namely the regional and continental models. According to the regional climate model, the spatial pattern of snow cover changed in response to the change of local weather conditions. Meteorological records from weather stations over Xinjiang are utilized to analyze the impact of local weather conditions on snow cover distribution in the study area. Statistical methods such as correlation analysis are employed. The regional snow cover is affected by the continental climate. Thus, the relationship between the regional snow cover and climatic factors which cause the continental climatic change is modeled based on a regression analysis.

7.1 Introduction

Climate-induced snow cover change is investigated from two aspects: (1) the change of regional climate and (2) the change of climate at a larger spatial scale (*e.g.*, continental or global). For example, temperature change

caused by the regional climatic change affects the accumulation and maintenance of snow cover, while the variation of water vapor in the upper atmosphere caused by continental or global climatic change may cause the change of the total snowfall amount in a region.

This study aims to establish the relationship between the regional snow cover and continental climate. The impact of regional climatic change on the spatio-temporal pattern of snow cover will be investigated.

7.2 Factors of Xinjiang's climate

Generally, the climate of Xinjiang depends on the following factors such as solar radiation, atmospheric circulation and geographical facts (Li, 1991).

Solar radiation: The Latitude is the controlling factor of the direct solar radiation on the ground. Other factors include cloud cover and patency of atmosphere. The solar radiation is the driving force of atmospheric circulations at larger spatial scales.

Compared with the same latitude zones, the total solar radiation of Xinjiang is less than the norm of the Eurasian continent, but greater than that of China's East. This is largely due to the cloud cover in the region, which is greater than the average in the Eurasian continent but much less than that in China's East.

Atmospheric circulation: Atmospheric circulation is the large-scale

movement of air mass on Earth. Including the ocean-atmosphere interaction, it is an important part in climate systems that regional heat balance and water vapor transfer depend on. The change of atmospheric circulation like the ENSO event is always regarded as an indicator of global climatic change.

The Westerlies play a significant role in the precipitation in Xinjiang, where the air currents carrying plenty of water vapor are blocked by high mountain ranges.

Geographical facts: Xinjiang locates in the hinterland of the Eurasian continent and is far away from the nearest coastline. The Tibetan Plateau in the south has blocked the Southwest Monsoons from the Indian Ocean. Therefore, water vapor from the ocean can seldom reach to this area. This forms an extreme arid area in the World.

Regarding the topographical features, the climatic conditions are affected by the high mountain ranges. The Tianshan Mountains extended from west to east blocks air currents within the study area. Thus, two different types of climate have formed in the North and South.

Given that the geographical facts can be considered no-change in the time scale of this study, the first two factors are regarded as the reasons behind the change of climatic conditions.

7.3 Data and analytical methods

7.3.1 Snow cover data

Snow cover at pixel-level scale is utilized for analyzing the relation between snow cover and regional climate. Monthly snow depth data from 1978 to 2010 are employed, including monthly mean and maximum snow depth (SD).

Snow cover at regional scale is utilized for analyzing the relationship between snow cover and continental climate. The generalized data of snow cover in snow seasons from the hydrological year of 1978/1979 to 2009/2010 are employed, including seasonal mean and maximum snow depth (SD) and maximum snow-covered area (SCA).

Both pixel-level and regional-level data are retrieved based on the analyses in Chapter 6.

7.3.2 Climatic data

Climatic parameters such as the temperature and precipitation reflect the climatic conditions in a region. In this study, annual and monthly climatic data from 18 local meteorological stations (Figure 7.1) during the period of 1978-2010 are utilized for the impact analysis of regional climatic change. Climatic parameters are selected including temperature, precipitation, humidity, air pressure and wind speed, as shown in Table7.1.

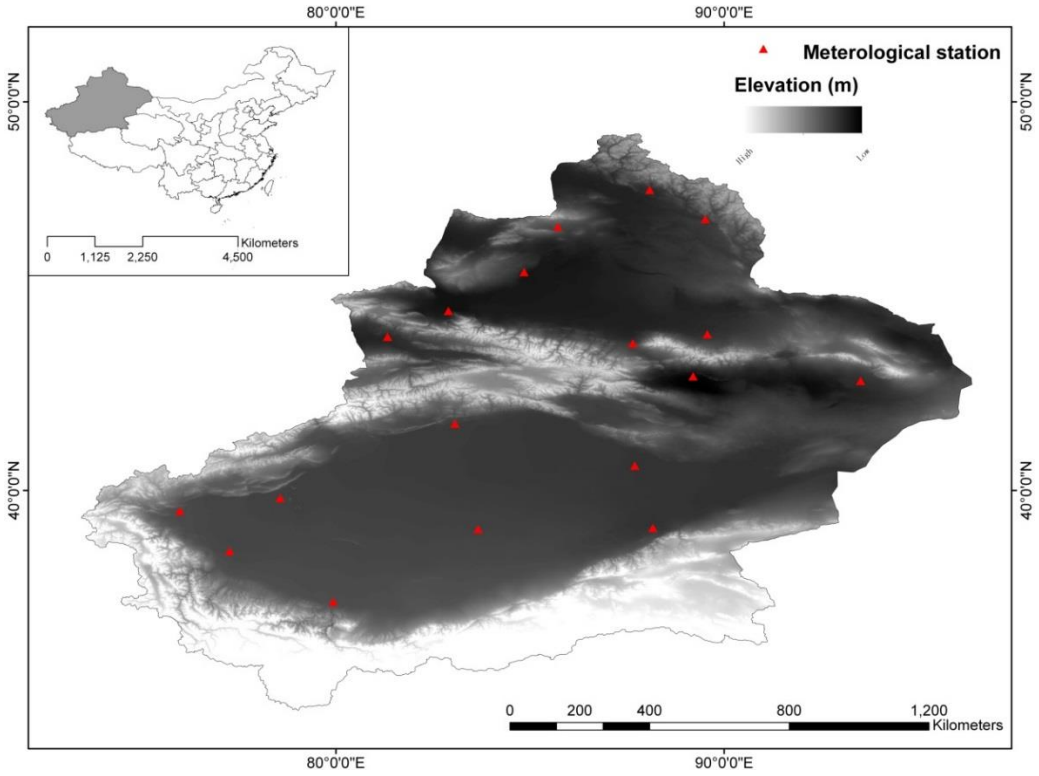

Figure 7.1 Distribution of local meteorological stations.

Table 7.1 Monthly climatic parameters adopted in this study

Climatic parameter	*Unit*	*Descriptions*
Mean temperature	°C	Monthly average of temperatures
Maximum temperature	°C	Monthly average of daily maximum temperatures
Precipitation	mm	Total amount of precipitation within a month
Mean relative humidity	%	Monthly average of relative humidity
Mean air pressure	h Pa	Monthly average of air pressure
Mean wind speed	m/s	Monthly average of wind speed

In this study, the change of incident solar radiation is considered an important factor that may have an impact on the change of regional and global climate. Thus the incident solar radiation measurement in China is used as an indicator of the continental climatic change. The annual incident solar radiation data from 10 ground stations over the nation during the same study period of 1978-2010 are utilized for analyzing the impact of continental climatic change. The distribution of the 10 solar radiation observation stations is illustrated in Figure 7.2.

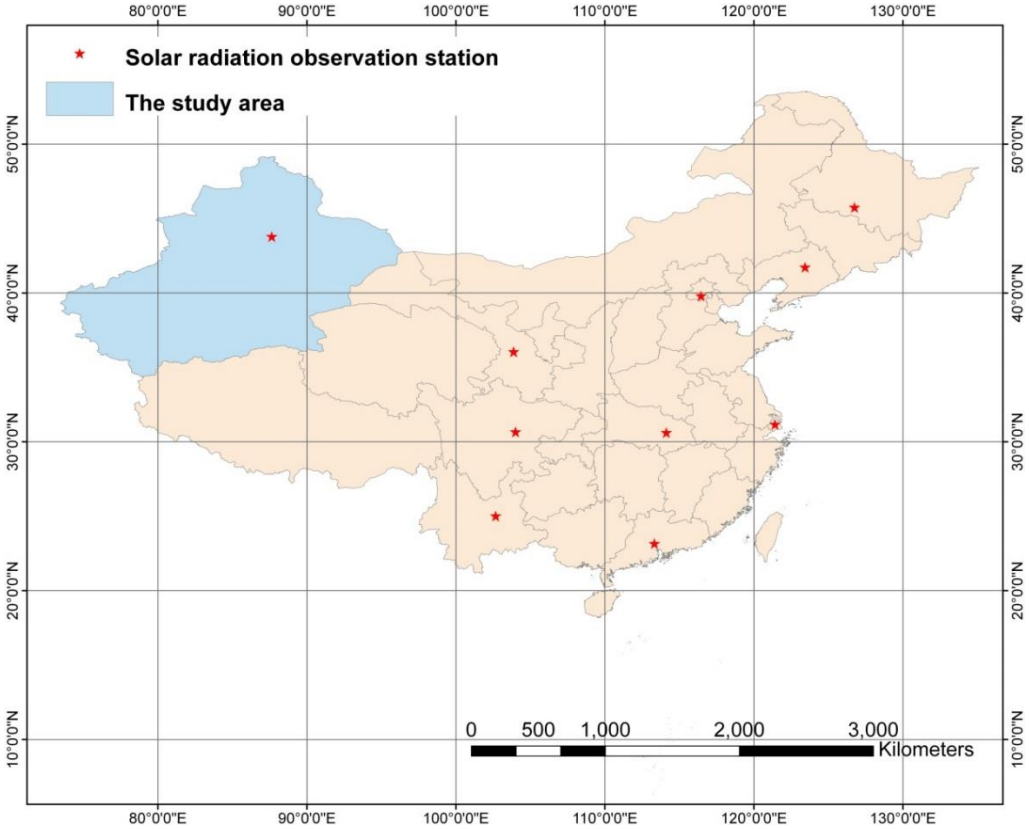

Figure 7.2 Distribution of solar radiation observation stations in China.

7.3.3 Data processing

For the solar radiation data, a national mean value is generated for each year. In addition, to discriminate between western and eastern parts of

China, the 10 stations are divided into two sub-regions using the longitude of 100 ° E as a dividing line. For each sub-region, the regional mean of solar radiation is calculated.

7.3.4 Analytical methods

To investigate the relationship between the snow cover of Xinjiang and the regional and continental climates, statistical analysis methods such as correlation analysis and regression analysis are applied.

7.4 The relation to regional climatic factors

Table 7.2 shows the correlations between the snow cover and climatic parameters at the regional scale.

Table 7.2 The Pearson's correlation (*r*) between snow cover and regional climatic parameters ($p < 0.05$)

	T_{mean}	T_{max}	P	RH	AP	WS
Mean SD	-0.46	-0.44	0.04	0.43	0.10	-0.13
Maximum SD	-0.47	-0.46	0.07	0.46	0.12	-0.10

Note: T_{mean}, T_{max}, P, RH, AP, WS stand for mean air temperature, maximum air temperature, precipitation, relative humidity, air pressure, wind speed, respectively.

According to Pearson correlation analysis, snow depth, regardless of maximum or mean depth, has a negative relationship with air temperature but a positive one with humidity. In other words, higher temperature or

less humidity would result in thinner snow cover, and *vice versa*. Besides these two parameters, the relations to the other climatic parameters are not obvious ($r < 0.2$).

Table 7.3 Change trends of snow depth and climatic parameters for the local meteorological stations

Station ID	Mean SD	Max. SD	Mean Temp.	Max. Temp.	Humid
51076	-0.160	-0.274	0.016	0.038	0.005
51087	-0.062	-0.073	0.055	0.041	-0.020
51156	0.046	-0.006	0.037	0.031	0.029
51243	0.011	-0.013	0.024	0.018	0.081
51334	0.022	-0.073	0.046	0.041	-0.042
51379	0.027	-0.008	0.018	0.034	0.000
51431	0.001	-0.087	0.047	0.049	-0.082
51463	0.021	0.031	0.057	0.039	-0.093
51573	0.017	-0.026	0.061	0.053	-0.152
51644	0.029	0.094	-0.007	0.022	0.268
51709	0.023	0.190	0.054	0.037	-0.197
51716	0.003	0.041	0.028	0.023	0.074
51747	0.000	-0.034	-0.047	-0.056	0.511
51765	-0.002	-0.046	0.004	-0.022	-0.258
51777	-0.004	-0.007	-0.035	-0.097	0.633
51811	0.013	0.157	-0.002	-0.024	-0.347
51828	0.005	0.052	-0.175	-0.088	0.276
52203	0.043	0.114	0.009	0.042	-0.714

Note: Maximum temperature (Max. Temp.) is the annual mean of monthly maximum temperature for different stations.

Since temperature and humid are relevant to snow cover change, the trends of snow depth change and climatic change represented by temperature and humid by stations are shown in Table 7.3.

7.5 The relation to continental climatic factors

Figure 7.3 compares the inter-annual fluctuations of snow cover and solar radiation from 1978 to 2010. The correlations between snow cover parameters and solar radiation at different regions are listed in Table 7.4.

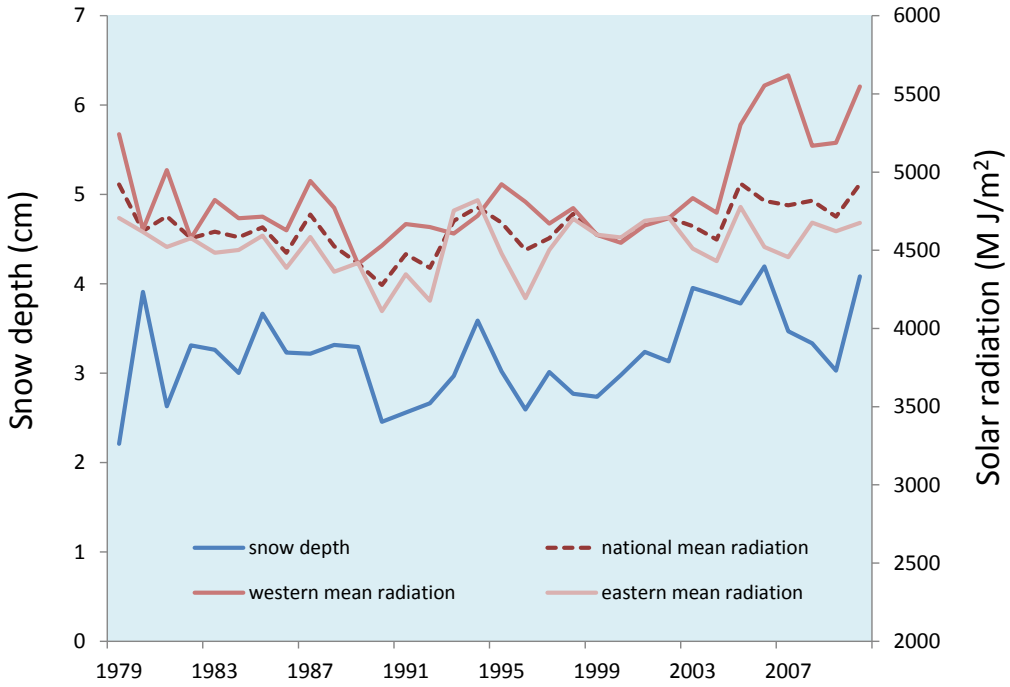

Figure 7.3 Comparison between the variations of mean snow depth of Xinjiang and solar radiation in China.

Table 7.4 The Pearson's correlation (*r*) between snow cover of Xinjiang and solar radiation in China ($p < 0.05$)

	National SR	SR in the West	SR in the East
mean SD	0.37	0.34	0.31
maximum SD	0.18	< 0.05	0.25
SCA	0.09	0.19	< 0.01

Note: SR represents the mean solar radiation in a region.

From the results, snow cover is positively correlated with solar radiation, but their correlations are not so strong ($p < 0.05$). Mean snow depth of Xinjiang is more correlated with solar radiation over China Mainland than the other two snow cover parameters.

7.6 Analysis and discussion

The regional analysis shows that snow cover is relevant to the climatic parameters such as air temperature and humidity. Air temperature is a critical factor for snowfall and snow cover. Higher air temperature causes the melting of snow cover and the ablation of alpine glaciers. Therefore, it is not surprising that a negative correlation has been shown between the snow cover and the temperature. Humidity represents the amount of water contained in the air, which may in turn fall as precipitation. The more snowfall normally means the deeper snow cover so that a positive correlation between the humidity and snow cover is expected.

According to the continental analysis, the relationship between regional snow cover and continental climate represented by solar radiation is not strong. By comparison, mean snow depth is better correlated with the continental climate. Since regional mean snow depth can represent the total amount of snow cover in a region, it implies that the amount of snow cover is more easily affected by the continental climate

It should be pointed out that the Pearson's correlation coefficient (r) describes a linear relation between two variables. Therefore, a low r value

only means that the data sets do not fit into a linear relationship well. This does not exclude the possibility of a non-linear relationship between the snow depth and climatic parameters. In addition, as for some climatic parameters, the relationships with snow depth are valid within a certain range. For example, the impact of temperature on snow cover change is not significant when air temperature is below 0 ℃.

7.7 Summary of this chapter

Snow cover can be affected by climate at various scales. In this chapter, the relationship between snow cover and climate has been analyzed at two spatial scales including the regional and continental scales.

At the regional scale, weather factors such as air temperature and humidity are correlated with snow depth, while precipitation, air pressure and wind speed are not. At the continental scale, a weak relationship is observed between the regional snow cover and solar radiation. To conclude, the impact of regional climate is more likely on the maintenance of snow cover; while the impact of continental climate is more likely on the total amount of snow cover indirectly via the formation of snowfalls.

(Intentionally left blank)

Chapter 8 Discussion

This chapter summarizes and discusses the major findings in the previous chapters and evaluates the whole study. Some key issues of the whole study are also indicated.

8.1 Major findings and comparison with other studies

8.1.1 The reliability of long-term remotely sensed snow cover data for a regional study

Based on passive microwave remote sensing technology, long-term SD/SWE products for global or continental-level studies have been released by different research institutes. To use these products for a regional study, the reliability and applicability of the data need to be examined. Two readily available long-term remote sensing SD/SWE products were compared and evaluated, namely the GlobSnow and WestDC products. Since the two products were produced from the same data source but with different algorithms, the consistency of the two products was first evaluated. Multi-year ground observation data from local weather stations were collected for assessing their accuracies.

Consistency test and accuracy assessment results (refer to Table 4.3) show that the two selected products do not agree well for the western

aridzone of China, and their accuracies are rather low compared to ground measurement data. The WestDC product shows a relatively better accuracy in the study area. The author believes that it is because the snow depth retrieval algorithm of the WestDC product was modified to fit the snow cover condition in China. From the point of view of temporal resolution, data consistency and accuracy could be improved through data generation at coarser time intervals, but maximum snow depth is an exception.

Considering the seasonal effect, the two products get a higher consistency in winters but a lower consistency in springs. It is believed that the inconsistency comes from the loss of data accuracies for both the two products in springs, since the snow depth retrieval algorithms are designed for dry snow rather than wet snow. Geographical effect causes the variation of data accuracy at different places. Latitude is a statistically significant factor that affects the data accuracies. Data quality is appeared better at lower latitude than at higher latitude regions.

Accuracy assessment is normally focused on the absolute errors rather than the relative errors. In this study, the relative accuracy was examined by comparing the estimated snow depth with the actual value. Result implies that the data accuracy depends on the depth of snow cover, excluding the measurements of thin snow (refer to Figures 4.3 and 4.4).

8.1.2 Spatio-temporal pattern of snow cover change in Xinjiang

The WestDC product was employed for snow cover change analysis since it shows a better accuracy of snow depth estimation in the western aridzone of China. Snow cover change was analyzed at two spatial scales, including the regional-level and pixel-based analyses. The long-term trend and spatio-temporal patterns of snow cover change in Xinjiang has been illustrated in Figures 6.5 and 6.6.

According to remote sensing snow observation, the total amount of snow cover in Xinjiang during the studying period is generally stable from the view of a regional-level analysis. However, there still exists a variation or difference no matter in time or space. From the spatial perspective, the increase of snow cover is mainly located in the fringes of the deserts and mountain pass, while the decrease concentrates in high mountainous areas like the Altai and the Tianshan Mountains.

From the temporal perspective, both inter-annual and inner-annual snow distributions were focused. For inter-annual distribution, there is an abrupt change in the hydrological year of 1986/1987 (Figure 8.1) in terms of snow depth (SD) and snow-covered area (SCA). Since then, maximum snow depth has become less; and maximum snow-covered area has expanded. In the meantime, inner-annual distribution shows that snow cover tends to become larger in area in snow accumulation seasons and thinner with the area shrank in snow ablation seasons.

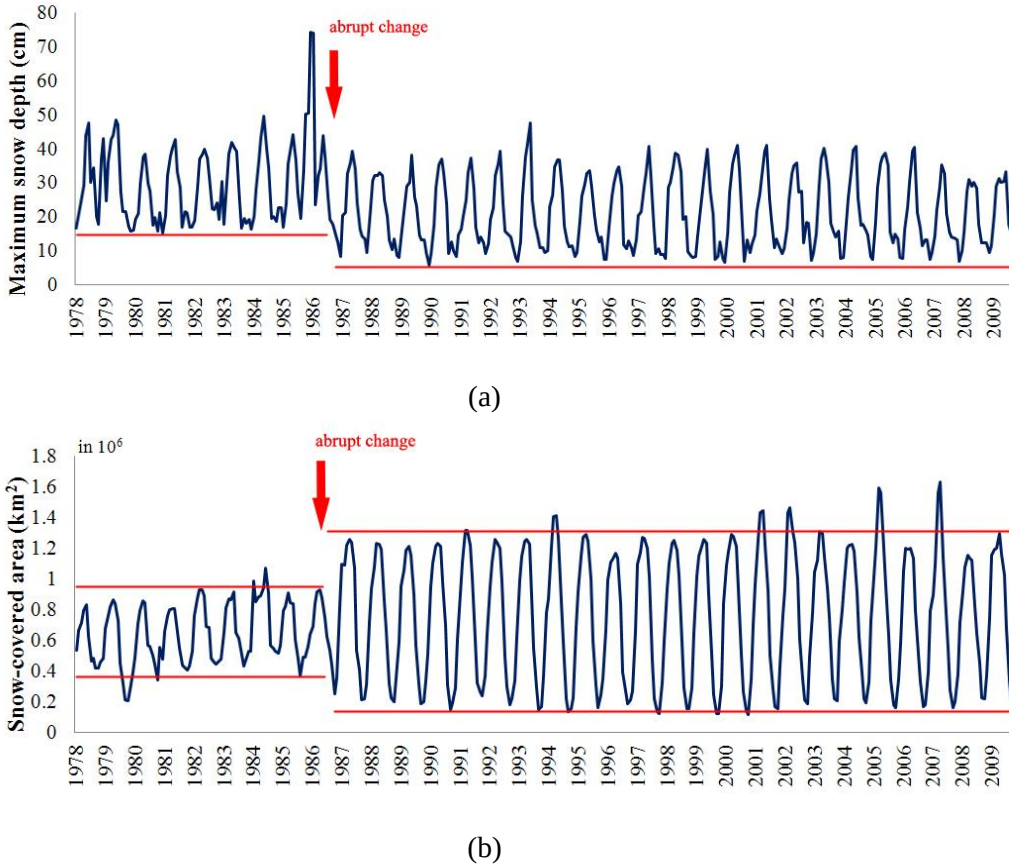

(a)

(b)

Figure 8.1 Abrupt change of snow cover in the hydrological year of 1986/1987, (a) for monthly maximum snow depth, (b) for monthly maximum snow-covered area.

8.1.3 The response of snow cover to climatic change events

Climatic change plays an important role in regional snow cover change. In the study, both regional and continental climates were involved in the correlation analyses. According to the statistical results, snow cover in Xinjiang highly correlates with the climate shift. An abrupt change of snow cover occurred in the hydrological year of 1986/1987. This finding is in keeping with other climatic studies that the regional climate in northwestern China suffered a shift and has mutated from warm-dry to warm-wet since 1987.

The impacts of climatic change on regional snow cover can be discussed from both the spatial and temporal perspectives. From the temporal perspective, the warming climate has resulted in the decrease of snow cover in spring and summer seasons. On the contrary, snow cover has increased in winter seasons due to the increase of water vapor to Xinjiang under the wet climate condition.

From the spatial perspective, alpine snow cover has decreased in the Altai and the Tianshan Mountains due to temperature rising in spring or summer seasons. However, the temperature effect on snow cover change is not so significant in winters, because winter mean temperature of Xinjiang is far below the freezing temperature (zero degree Celsius). Due to high mountain block, water vapor transferred from west into Xinjiang and firstly formed snowfalls in the west. Therefore, the increase of snow cover can be observed in the mountain pass at the western Tianshan Mountains and lower mountainous and plain areas.

8.2 Scale issues

Scale which is relevant to size is a critical issue in geographical studies, particularly the study on snow cover and climatic changes. A geographical phenomenon is commonly defined and expressed at a certain scale, for instance, millennial-scale climatic change and daily-scale temperature variation. In order to represent the change information from local to regional, multi-scale analysis was employed.

Scale issues primarily concern two broad domains, namely spatial and temporal scales. For each domain, scale effect involves two distinct aspects which are commonly called “extent” and “grain”. The former is the overall area or time period encompassed by an investigation, while the latter, also known as the resolution, indicates how large the resolvable unit is (*i.e.*, spatial resolution) or how often the observation is repeated (*i.e.*, temporal resolution).

Regarding the spatial extent, this study aims to link the snow cover change pattern and climatic change at a regional scale. As to the spatial resolution, both regional-level and pixel-based analyses were employed. The former is conducted for a general description of snow cover in the whole study area, while the latter is for illustrating the regional difference of the change. Due to the limitation of the spatial resolution of the data, the pixel-based analysis is under the 25 km-level scale. The spatial resolution of the data can be improved by the proposed data fusion method. However, the problem of lower data accuracy due to the spatial heterogeneity of snow cannot be solved. Although this, the data is still acceptable for large-extent snow cover change like this study.

Because it is not a long history since remote sensing technology being used for snow cover observation, the temporal extent is limited within the past three decades. Correspondingly, the discussion on climatic change based on the snow cover change study is limited to the recent period at decadal level scale. As to the temporal resolution, yearly- and monthly-

scale analyses were adopted for illustrating inter-annual fluctuation of snow cover, and the temporal distribution in different seasons, respectively. In order to analyze the impact of climatic change on snow cover at different scales, climatic data at the corresponding spatial and temporal scales were adopted to match the analyses.

8.3 Uncertainties

The accuracy of change detection relies on the quality of the remote sensing snow cover data. Although low accurate snow depth estimation retrieved from passive microwave data can be improved by fusing with optical snow cover extent product, uncertainties originated from snow cover extent mapping due to the coarse spatial resolution (Yan, 2005; Liang *et al.*, 2008) cannot be solved in this study.

MODIS snow cover extent product is recommended to be utilized in the proposed data fusion method to improve the low spatial resolution and accuracy of passive microwave snow depth data. However, MODIS snow products is available since 2000s, which means the fusion can only be done for about a dozen of years. Other optical snow cover data like NOAA/AVHRR snow cover map could be used in data fusion for those dates without MODIS. It should be pointed out that the fusion work was not carried out for all dates in this study, due to the difficulty of data acquisition.

For better understanding the snow cover change in the WAC region,

snow cover parameters were generated and utilized to describe the change such as SD and SCA. Statistical methods were adopted to generate those parameters such as mean and maximum values. Mean value reflects a general situation of snow cover within a period (temporal mean) or in a region (geographical mean), while maximum value reflects the transient situation of snow cover. The use of statistics in data generation may cause some uncertainties in snow cover change detection. For instance, the application of moving average method can reduce the influence of data outliers, meanwhile, the smoothing of data fluctuation by averaging may also result in the loss of change details in time and space.

Snow cover change as well as its mechanism is a complex issue. Because of the natural relation between snow and climate, the influence of climatic change on regional snow cover has been focused. There is no doubt that human activities also make an impact on snow cover change. Indirect and cumulative impacts like by influencing climate are normally difficult to measure. Given that the study area experienced a low-level urbanization during the past 30 years and most local human activities were limited within cities or small towns, compared with the analytical unit being at a very coarse spatial resolution, the direct impact of human activities that is not obvious was not analyzed in the study.

8.4 Summary of this chapter

The major findings and conclusions of the whole study have been

exhibited and discussed in this chapter. The reliability and application of remote sensing snow cover data for a regional study over the western aridzone of China are discussed. Based on remote sensing snow data, the long-term change trend and spatio-temporal patterns of snow cover in Xinjiang are analyzed and discussed as well as the response to climatic change. Scale issues and uncertainties in the analysis throughout have been discussed and regarded as the restrictions of this study.

(Intentionally left blank)

Chapter 9 Conclusion and Outlook

9.1 Conclusions

Based on passive microwave snow depth data, this study focuses on the modelling of the spatio-temporal pattern of snow cover change and its relationship to the change of climate in Xinjiang from 1978 to 2010. The change analysis is based on different spatial and temporal scales thus the inter-annual fluctuation and seasonal variation at regional-level and pixel-based scales can be investigated.

9.1.1 Contribution to knowledge

The major contributions to the knowledge are listed as follows:

(1) This study has evaluated the reliability and application of long-term remote sensing snow observation data for a regional study over the western aridzone of China. Based on passive microwave technology, the existing long-term snow depth products are known to suffer from a number of issues. Due to the coarse spatial resolution, those products based on a single algorithm are normally utilized for global or continental studies. Given that snow parameters like snow density and snow grain size are not homogenous across the region, the efficiencies of snow depth retrieval algorithms, which are commonly based on a general snow cover

condition, may vary at different places. In this study, the existing long-term remote sensing SD/SWE products were evaluated for the study area based on a large amount of ground observation data (more than 100 thousands of samples). Both data consistency and accuracy are assessed by the ICC and RMSE analyses with different time intervals. This study made a vital first step of calibration before those products can be further used in climatic change studies and hydrological applications.

(2) This study has proposed a methodology of image fusion by combining the passive microwave and optical snow observation data for better snow depth estimations with a higher spatial resolution. The low spatial resolution of passive microwave snow depth data restricts the applications at coarser spatial scales. In addition, the mixed pixel problem due to the coarse spatial resolution also caused the uncertainty in snow depth estimation. The proposed data fusion method attempts to take the advantage of higher spatial resolution offered from optical images to calibrate the low-resolution microwave snow depth estimation. The experiment results have confirmed the improvements in snow depth estimation by this approach.

(3) This study has investigated the spatio-temporal pattern of long-term snow cover change in Xinjiang at different temporal and spatial scales. Traditional snow cover change study is based on ground measurement data from meteorological stations. Since local meteorological stations are mainly distributed in habitat areas (*i.e.*, the

oases), the information on the alpine snow cover change is lacking. Most of the existing remote sensing snow cover studies are focused on the snow cover extent derived from optical images, which is incapable of delivering snow depth measurements. Furthermore, fine-resolution optical snow cover products (*e.g.*, the MODIS product) only date back to the beginning of the new century. The time period is not long enough to exhibit the impact of climatic change on snow cover. In comparison, this study has proposed a new approach that is based on the longest and continuous archive of remote sensing snow observation on both snow cover extent and depth from the late 1970s. Besides a regional level analysis, investigation on snow cover change at pixel level is also conducted so as to illustrate the regional difference of the change.

(4) This study has analyzed the relationship between snow cover and climatic change in terms of local and regional climatic conditions. The impacts of climatic change on snow cover are represented in multiple levels. Global or regional climatic change makes an impact on the change of the amount of snowfall in a certain region, while local climatic change affects the spatial distribution of snow cover. This study is the first for the region that addressed both aspects based on the outcomes of the long-term snow cover change detection.

9.1.2 Summary of research findings

The major findings from this research are summarized as follows.

(1) The long-term snow depth products showed great inconsistency in the western aridzone of China and their accuracies against the corresponding ground measurements are quite low. However, the generalized data with different temporal resolution tend to yield better results in data consistency and accuracy. Being calibrated for the local condition, the WestDC product shows a better accuracy than the GlobSnow. Regarding to the temporal and regional variations, the season and latitude show statistically significant impacts on the data reliability. Data reliability declines with higher latitude and it rapidly falls down to an unacceptable level in snow ablation periods. Therefore, it is suggested that data quality is better at lower latitude except in the cases of thin snow, where the snow depth estimates by remote sensing will become less trustworthy because of the limit of the technology.

(2) The snow depth data can be better calibrated by the image fusion with fine-resolution optical snow cover product. It is confirmed that the outcomes by the proposed data fusion method are generally better in snow depth estimation than the original data.

(3) In general, the snow cover in Xinjiang shows a slight increasing trend during the past three decades, with great inter-annual fluctuation and seasonal variation. According to analyses of maximum snow depth and snow-covered area in the region, an abrupt change in the hydrological year of 1986/1987 was observed. After this time point, maximum snow depth has obviously decreased as well as maximum snow-covered area in

summer seasons. In winter seasons, maximum snow-covered area has an opposite trend that become larger.

The spatial pattern of snow cover change also shows a regional variation. The decrease of snow depth in summer seasons mainly occurred in high mountainous areas. Generally, in winters, the increase of snow depth occurred in mountain pass and piedmont areas, while some of the high mountainous areas had decreased snow depth during the study period.

(4) With the existing theory of regional climatic change at inter-annual temporal scale, the climate shift from warm-dry to warm-wet pattern has made some impacts on the temporal distribution as well as the spatial distribution of snow cover in Xinjiang.

9.2 Further perspectives

According to the present study, some further questions need to be answered. This study can be enriched from the following aspects.

(1) The original optical snow cover extent product may suffer from a lower accuracy due to cloud cover. Some cloud-removal algorithms have been proposed recently. In the future, the microwave-based snow depth product will combined with a cloud-removed snow cover extent product so as to improve the accuracy of snow depth estimation.

(2) In this study, snow cover change has been modeled and its relation to climate has been investigated. However, the reliability of the change or

the accuracy of change detection is not clear. The response to climatic change is also not confirmed since climatic change itself is a complex issue. An appropriate method for evaluating the change detection results is subject to further investigations. For example, the snow cover change can be cross validated by precipitation, soil moisture, surface runoff *etc*.

(3) Air temperature and relative humidity are two observed changing factors that affect the snow cover change. The impact of the other factors like topographical factors on the spatial distribution of snow cover is still needed to be investigated.

(4) Due to the restriction of the length of study period, regional climate was analyzed at decadal level. Apart from the decadal climate pattern, other climate patterns that may affect the temporal distribution of snow cover should be examined.

(5) Simulation of the spatio-temporal pattern of snow cover in the near future by using the above (in aspects (3) and (4)) factors or driving forces is meaningful. By taking a climatic change scenario of global warming as an example, temperature increasing would result in the beginning of snow cover melting at an earlier date. On the other hand, increasing in precipitation or redistribution of water vapor caused by circulation would result in a regional difference of snow cover change in different places. It is vital for snowmelt runoff modelling which are usually conducted in river basins. Thus, simulating the change trends in

the future under climatic change can be conducted as future work. In addition, at which analytical level will the simulation fit best should be studied.

(Intentionally left blank)

References

Armstrong, R. L., & Brodzik, M. J. (2002). Hemispheric-scale comparison and evaluation of passive microwave snow algorithms. *Annals of Glaciology*, 34(1), 38-44.

Bellerby, T., Taberner, M., Wilmshurst, A., Beaumont, M., Barrett, E., Scott, J., & Durbin, C. (1998). Retrieval of land and sea brightness temperatures from mixed coastal pixels in passive microwave data, *IEEE Transactions on Geoscience and Remote Sensing*, 36(6), 1844-1851.

Bengtsson, L. (1999). Numerical modelling of the Earth's climate. In Holland, E.W.R., Joussaume, S., & David, F. (Eds.), *Modelling the Earth's Climate and its Variability*, (pp.139-235). Amsterdam: Elsevier Science Publisher B.V..

Beniston, M., & Diaz, H.F. (2004). The 2003 heat wave as an example of summers in a greenhouse climate? Observations and climate model simulations for Basel, Switzerland. *Global and Planetary Change*, 44, 73-81.

Black, R. (2012, April 15). Some Asian glaciers "putting on mass". *BBC News*. Retrieved from: http://www.bbc.co.uk/news/science-environment-17701677

Bland, J. M., & Altman, D. G. (1990). A note on the use of the intraclass correlation coefficient in the evaluation of agreement between two methods of measurement. *Computers in Biology and Medicine*, 20 (5), 337-340.

Cabanes, C., Cazenave, A., & Le Provost, C. (2001). Sea level rise during past

40 years determined from satellite and in situ observation, *Science*, 294, 840-842.

Cao, M., Li, P., Robinson, D.A., Spies, T.E., & Kukla, G. (1993). Evaluation and primary application of microwave remote sensing SMMR-derived snow cover in western China. *Remote Sensing of Environment China*, 8(4), 260-269. (in Chinese).

Cao, M., & Li, P. (1994). Microwave remote sensing monitoring of snow cover in western China. *Mountain Research*, 12(4), 230-234. (in Chinese).

Chang, A.T.C., Foster, J.L., & Hall, D.K. (1987). Nimbus-7 SMMR derived global snow cover parameters. *Annals of Glaciology*, 9, 39-44.

Chang, A.T.C., Foster, J.L., Hall, D.K., Robinson, D.A., Li, P., & Cao, M. (1992). The use of microwave radiometer data for characterizing snow storage in western China. *Annals of Glaciology*, 16, 215-219.

Chang, A.T.C., Foster, J.L., & Rango, A. (1991). Utilization of surface cover composition to improve the microwave determination of snow water equivalent in a mountain basin. *International Journal of Remote Sensing*, 12(11), 2311-2319.

Chang, A.T.C., Kelly, R.E.J., Josberger, E.G., Armstrong, R.L., Foster, J.L., & Mognard, N.M. (2005). Analysis of ground-measured and passive-microwave-derived snow depth variations in midwinter across the Northern Great Plains. *Journal of Hydrometeorology*, 6, 20-33.

Che, T. (2011). *Introduction of Long-term Snow Depth Dataset of China (1978-*

2010), Cold and Arid Regions Environmental and Engineering Research Institute, Chinese Academy of Sciences, Lanzhou. (in Chinese).

Che, T., & Li, X. (2004). The development and prospect of estimating snow water equivalent using passive microwave remote sensing data. *Advance in Earth Sciences*, 19(2), 204-210. (in Chinese).

Che, T., & Li, X. (2005). Spatial distribution and temporal variation of snow water resources in China during 1993 – 2002. *Journal of Glaciology and Geocryology*, 27(1), 64-67. (in Chinese).

Che, T., Li, X., Jin, R., Armstrong, R., & Zhang, T. (2008). Snow depth derived from passive microwave remote-sensing data in China. *Annals of Glaciology*, 49, 145-154.

Chen, X. (Editor-in-Chief). (2010). *Physical Geography of Arid Land in China*. Beijing: Science Press. (in Chinese).

Chen, X. (Editor-in-Chief). (2012). *Hydrological Model of Inland River Basin in Arid Land*. Beijing: China Environmental Science Press. (in Chinese).

China Meteorological Administration (CMA). (2007). *Regulations of Remote Sensing Snow Monitoring and Assessment (Evaluated version)*. [CMA Document]. Available online on November 30, 2013: www.cma.gov.cn/2011wmhd/.../P020111115369037537082.doc. (in Chinese).

Clifford, D. (2010). Global estimates of snow water equivalent from passive microwave instruments: history, challenges and future developments. *International Journal of Remote Sensing*, 31(14), 3707-3726.

Coppin, P., Jonckheere, I, Nackaerts, K., & Muys, B. (2004). Digital change detection methods in ecosystem monitoring: a review. *International Journal of Remote Sensing*, 25(9), 1565-1596.

Cryer, J.D., & Chan, K. (2008). *Time Series Analysis with Applications in R* (2nd Edition). New York: Springer.

Dai, S., Zhang, B., Cheng, F., Wang, H., & Wang, P. (2010). The spatio-temporal variations of snow cover in China from the snow depth time series dataset based on passive microwave remote sensing. *Journal of Glaciology and Geocryology*, 32(6), 1066-1073. (in Chinese).

DeWalle, D.R., & Rango, A. (2008). *Principles of Snow Hydrology*. New York: Cambridge University Press.

Dong, J. R., Walker, J. P., & Houser, P. R. (2005). Factors affecting remotely sensed snow water equivalent uncertainty. *Remote Sensing of Environment*, 97(1), 69-82.

Dou, Y., Chen, X., Bao, A., & Li, L. (2010). Study of the Temporal and Spatial Distribute of the Snow Cover in the Tianshan Mountains, China. *Journal of Glaciology and Geocryology*, 32(1), 28-34. (in Chinese).

Douglas, B.C. (1991). Global sea level rise. *Journal of Geophysical Research*, 96 (C4), 6981-6992.

Durand, Y., Gérald, G., Laternser, M., Etchevers, P., Mérindol, L., & Lesaffre, B. (2009). Reanalysis of 47 years of climate in the French Alps (1958-2005): Climatology and trends for snow cover, *Journal of Applied Meteorology and*

Climatology, 48, 2487-2512.

Farr, T. G., Rosen, P. A., Caro, E., Crippen, R., Duren, R., Hensley, S., Kobrick, M., Paller, M., Rodriguez, E., Roth, L., Seal, D., Shaffer, S., Shimada, J., Umland, J., Werner, M., Oskin, M., Burbank, D., & Alsdorf. D. (2007). The Shuttle Radar Topography Mission. *Reviews of Geophysics*, 45, RG2004, doi:10.1029/2005RG000183.

Fu, H., Li, S., Huang, Z., Sha, Y., Li, C., & Ji, L. (2007). Verification and analysis of mathematical model for retrieved snow depth based on MODIS data. *Arid Land Geography*, 30(6), 907-914.

Gao, W., Wei, W., & Zhang, L. (2005). Climate changes and seasonal snow cover variability in the western Tianshan Mountains, Xinjiang in 1967-2000. *Journal of Glaciology and Geocryology*, 27(1), 68-73. (in Chinese).

Gao, X., Ye, B., Zhang, S., Qiao, C., & Zhang, X. (2010a). Glacier runoff variation and its influence on river runoff during 1961-2006 in the Tarim River Basin, China. *Science China Earth Sciences*, 40(5), 654-665.

Gao, Y., Xie, H., Lu, N., Yao, T., & Liang, T. (2010b). Toward advanced daily cloud-free snow cover and snow water equivalent products from Terra-Aqua MODIS and Aqua AMSR-E measurements, *Journal of Hydrology*, 385, 23-35.

Gong, J., Sui, H., Ma, G., & Zhou, Q. (2008). A Review of Multi-Temporal Remote Sensing Data Change Detection Algorithms. *The International Archives of the Photogrammetry, Remote Sensing and Spatial Information Sciences*, 37(B7), 757-762.

Hall, D. K., Riggs, G. A. (2007). Accuracy assessment of the MODIS snow-cover products, *Hydrological Processes*, 21, 1534-1547.

Hall, D.K., Riggs, G.A., & Salomonson, V.V. (1995). Development of methods for mapping global snow cover using Moderate Resolution Imaging Spectroradiometer (MODIS) data. *Remote Sensing of Environment*, 54, 127-140.

Hall, D.K., Riggs, G.A., & Salomonson, V.V. (2006). MODIS/Terra Snow Cover 8-Day L3 Global 0.05deg CMG V005 [Digital media], Boulder, Colorado USA: National Snow and Ice Data Center.

Hall, D.K., Riggs, G.A., Salomonson, V.V., DiGirolamo, N.E., & Bayr, K.J. (2002). MODIS snow-cover products. *Remote Sensing of Environment*, 83, 181-194.

Hancock, S., Baxter, R., Evans, J., & Huntley, B. (2013). Evaluating global snow water equivalent products for testing land surface models. *Remote Sensing of Environment*, 28, 107-117.

Hansen, J., Ruedy, R., Sato, M., & Lo, K. (2010). Global surface temperature change. *Reviews of Geophysics*, 48, RG4004, doi:10.1029/2010RG000345.

Hantel, M., Maurer, C., & Mayer, D. (2012). The snowline climate of the Alps 1961 – 2010. *Theoretical and Applied Climatology*, 110 (4), 517-537.

Nemmour, H., & Chibani, Y. (2006). Multiple support vector machines for land cover change detection: An application for mapping urban extension. *ISPRS Journal of Photogrammetry and Remote Sensing*, 61, 125-133.

Ichoku, C., & Karnieli, A. (1996). A review of mixture modeling techniques for sub-pixel land cover estimation. *Remote Sensing Review*, 13, 161-186.

IPCC. (1995). *Climate Change 1995: A Report of the Intergovernmental Panel on Climate Change*. [IPCC Report]. Available online on November 30, 2013: http://www.ipcc.ch/pdf/climate-changes-1995/ipcc-2nd-assessment/2nd-assessment-en.pdf

IPCC. (2001). *Climate Change 2001: Synthesis Report*. A contribution of Working Groups I, II and III to the Third Assessment Report of the Intergovernmental Panel on Climate Change [Watson, R.T. and the Core Writing Team (eds.)]. Cambridge University Press, Cambridge, United Kingdom, and New York, NY, USA, 398 pp.

IPCC. (2007). *Climate Change 2007: Synthesis Report*. Contribution of Working Groups I, II and III to the Fourth Assessment Report of the Intergovernmental Panel on Climate Change [Core Writing Team, Pachauri, R.K and Reisinger, A. (eds.)]. IPCC, Geneva, Switzerland, 104 pp.

IPCC. (2013). *Climate Change 2013: The Physical Science Basis – Summary for Policymakers*. Working Groups I Contribution to the Fifth Assessment Report of the Intergovernmental Panel on Climate Change. IPCC, Switzerland. Available online on November 30, 2013: http://www.climatechange2013.org/images/uploads/WGI_AR5_SPM_brochure.pdf

Jiang, Y., & Dou, Y. (Editors-in-chief). (2001). *The Provincial Atlas of China*, pp. 189-190. Beijing: Star Map Press. (in Chinese).

Jonas, T., Marty, C., & Magnusson, J. (2009). Estimating the snow water equivalent from snow depth measurements in the Swiss Alps, *Journal of Hydrology*, 378, 161-167.

Kasetkasem, T., & Varshney, P.K. (2002). An image change detection algorithm based on Markov random field models. *IEEE Transactions on Geoscience and Remote Sensing*, 40(8), 1815-1823.

Ke, C., & Li, P. (1998). Spatial and temporal characteristics of snow cover over the Qinghai-Xizang Plateau. *Acta Geographica Sinica*, 3, 209-215. (in Chinese).

Knowles, K. W., Savoie, M. H., Armstrong, R. L., & Brodzik, M. J. (2006). AMSR-E/Aqua Daily EASE-Grid Brightness Temperatures [Digital media], Boulder, Colorado USA: National Snow and Ice Data Center.

Lan, Y., Shen, Y., Wu, S., Zhong, Y., Wen, J., Ma, X., & Hu, Z. (2007). Changes of the glaciers and the glacier water resources in the typical river basins on the north and south slopes of the Tianshan Mountains since 1960s. *Journal of Arid Land Resources and Environment*, 21(11), 1-8. (in Chinese).

Landis, J. R., & Koch, G. G. (1977). The measurement of observer agreement for categorical data. *Biometrics*, 33, 159-174.

Li, B., Zhang, Y., & Zhou, C. (2004). Remote sensing detection of glacier changes in Tianshan Mountains for the past 40 years. *Journal of Geographical Sciences*, 14(3), 296-302.

Li, J. (Editor-in-chief). (1991). *A Series of Climate for China: Climate of Xinjiang*. Beijing: China Meteorological Press. (in Chinese).

Li, P. (1988). Preliminary evaluation of seasonal snow resources in China. *Acta Geographica Sinica*, 43(2), 108-119. (in Chinese).

Li, P. (1989). Recent trends and regional differentiation of snow variation in China. In the proceedings of the Baltimore Symposium: *Snow Cover and Glacier Variations*. IAHS Publications, 183, 3-9.

Li, P. (1993). Dynamic characteristic of snow cover in western China. *Acta Geographica Sinica*, 48(6), 505-515. (in Chinese).

Li, P. (1999). Variation of snow water resources in northwestern China, 1951-1997. *Science in China Series D: Earth Sciences*, 42, 72-79.

Li, P. (2001). Response of Xinjiang snow cover to climate change. *Acta Meteorologica Sinica*, 59(4), 491-501. (in Chinese).

Li, X., & Che, T. (2007). A review on passive microwave remote sensing of snow cover. *Journal of Glaciology and Geocryology*, 29(3), 487-496. (in Chinese).

Li, X., Cheng, G., Jin, H., Kang, E., Che, T., Jin, R., Wu, L., Nan, Z., Wang, J., & Shen, Y. (2008). Cryospheric change in China. *Global and Planetary Change*, 62, 210-218.

Li, Y., Gu, J., Zhang, P., Liu, Y., & Ma, L. (2010). Snow cover storage retrieval by remote sensing technology and variation analysis on the Junggar Basin. *Arid Land Geography*, 33(4), 623-629. (in Chinese).

Li, Z., Huffman, T., McConkey, B., Townley-Smith, L. (2013). Monitoring and

modeling spatial and temporal patterns of grassland dynamics using time-series MODIS NDVI with climate and stocking data. *Remote Sensing of Environment*, 138, 232-244.

Li, Z., Shen, Y., Wang, F., Li, H., Dong, Z., Wang, W., & Wang, L. (2007). Response of melting ice to climate change in the Glacier No.1 at the headwaters of Ürümqi River, Tianshan Mountain. *Advances in Climate Change Research*, 3(3), 132-137. (in Chinese).

Liang, S. (2004). *Quantitative Remote Sensing of Land Surfaces*, New Jersey: John Wiley & Sons, Inc.

Liang, T., Wu, C., Chen, Q., & Xu, Z. (2004). Snow classification and monitoring models in the pastoral areas of the northern Xinjiang. *Journal of Glaciology and Geocryology*, 26(2), 160-165. (in Chinese).

Liang, T., Huang, X., Wu, C., Liu, X., Li, W., Guo, Z., & Ren, J. (2008a). An application of MODIS data to snow cover monitoring in a pastoral area: A case study in Northern Xinjiang, China. *Remote Sensing of Environment*, 112, 1514-1526.

Liang, T., Zhang, X., Xie, H., Wu., C., Feng, Q., Huang, X., & Chen, Q. (2008b). Toward improved daily snow cover mapping with advanced combination of MODIS and AMSR-E measurements. *Remote Sensing of Environment*, 112, 3750-3761.

Lillesand, T.M., Kiefer, R.W., & Chipman, J. W. (2008). *Remote Sensing and Image Interpretation* (the 6th edition). New Jersey: John Wiley & Sons.

Liu, Y., Zheng, Z., & Wang, L. (2003). Remote sensing on snow cover and variation analyzing in west of China. *Climatic and Environmental Research*, 8(1), 114-123. (in Chinese).

Liu, Y., Zhang, P., Zhang, M., & Li, H. (2006). Inversion of snow depth based on MODIS data in the North Slope Economic Zone of the Tianshan Mountains. *Science of Surveying and Mapping*, 31(3), 15-17. (in Chinese).

Liu, S., Ding, Y., Zhang, Y., Shangguan, D., Li, J., Han, H., Wang, J., & Xie, C. (2006). Impact of the glacial change on water resources in the Tarim River basin. *Acta Geographica Sinica*, 61(5), 483-490. (in Chinese).

Lu, D., Moran, E., & Batistella, M. (2003). Linear mixture model applied to Amazonian vegetation classification, *Remote Sensing & Environment*, 87, 456-469.

Luber, G., & McGeehin, M. (2008). Climate change and extreme heat events. *American Journal of Preventive Medicine*, 35(5), 429-435.

Luojus, K., Pulliainen, J., Takala, M., Lemmetyinen, J., Derksen, C., & Wang, L. (2010). *Global Snow Monitoring for Climate Research: Snow Water Equivalent (SWE) product guide*. European Space Agency Study Contract Report, ESRIN Contract 21703/08/I-EC. Available online on May 22, 2013: http://www.globsnow.info/swe/GlobSnow_SWE_ product_readme_v1.0a.pdf

Ma, L., Zhao, J., Zhang, H., Fan, J., & Guo, X. (2010). Impacts of glacier and snow melting on Bosten Lake under climate change. *Arid Land Geography*, 33(2), 210-216. (in Chinese).

McGraw, K.O., & Wong, S.P. (1996). Forming inferences about some intraclass correlations coefficients. *Psychological Methods*, 1(1), 30-46.

McIntyre, S., & McKitrick, R. (2005). Hockey sticks, principal components and spurious significance. *Geophysical Research Letters*, 32, L03710, doi:10.1029/2004GL021750.

McIntyre, S., & McKitrick, R. (2011). Discussion of: A statistical analysis of multiple temperature proxies: Are reconstructions of surface temperatures over the last 1000 years reliable? *Annals of Applied Statistics*, 5(1), 56-60.

Miller. L., & Douglas, B.C. (2004). Mass and volume contributions to twentieth-century global sea level rise, *Nature*, 428, 406-409.

Morisette, J.T., Khorram, S., & Mace, T. (1999). Land cover change detection enhanced with generalized linear models. *International Journal of Remote Sensing*, 20(14), 2703-2721.

Mu, Z., Jiang, H., & Liu, F. (2010). Spatial and temporal variations of snow cover area and NDVI in the west of Tianshan Mountains. *Journal of Glaciology and Geocryology*, 32(5), 875-882. (in Chinese).

Nogués-Bravo, D., Araújo, M.B., Errea, M.P., & Martínez-Rica, J.P. (2007). Exposure of global mountain systems to climate warming during the 21st century. *Global Environmental Change*, 17, 420-428.

Norušis, M.J. (2012). *IBM SPSS Statistics 19 Statistical Procedures Companion*. New Jersey: Prentice Hall.

Novotny, E.V., & Stefan, H.G. (2007). Stream flow in Minnesota: Indicator of climate change. *Journal of Hydrology*, 334, 319-333.

Pohl, C. & van Genderen, J. L. (1998). Multisensor image fusion in remote sensing: concepts, methods and applications. *International Journal of Remote Sensing*, 19(5), 823–854.

Prokop, A. (2008). Assessing the applicability of terrestrial laser scanning for spatial snow depth measurements. *Cold Regions Science and Technology*, 54, 155-163.

Pulliainen, J. (2006). Mapping of snow water equivalent and snow depth in boreal and sub-arctic zones by assimilating space-borne microwave radiometer data and ground-based observations. *Remote Sensing of Environment*, 101, 257-269.

Qin, D., Liu, S., & Li, P. (2006). Snow cover distribution variability and response to climate change in western China. *Journal of Climate*, 19, 1820-1833.

Qiu, J., & Sun, X. (1992). Preliminary study on snow cover in the Tianshan Mountains. *Arid Land Geography*, 15(3), 9-21. (in Chinese).

Rees, W.G. (2006). *Remote Sensing of Snow and Ice*. Boca Raton: CRC Press.

Salomonson, V.V., & Appel, I. (2004). Estimating fractional snow cover from MODIS using the normalized difference snow index. *Remote Sensing of Environment*, 89, 351-360.

Schaffhauser, A., Adams, M., Fromm, R., Jörg, P., Luzi, G., Noferini, L., Sailer,

R. (2008). Remote sensing based retrieval of snow cover properties. *Cold Regions Science and Technology*, 54,164-175.

Shi, Y., & Liu, S. (2000). Estimation on the response of glaciers in China to the global warming in the 21st century. *Chinese Science Bulletin*, 45(7), 668-672.

Shi, Y., Shen, Y., Li, D., Zhang, G., Ding, Y., Hu, R., & Kang, E. (2003). Discussion on the present climate change from warm-dry to warm-wet in Northwest China. *Quaternary Sciences*, 23(2), 152-164. (in Chinese).

Shi, Z., Xu, J., Chen, Z., & Li, M. (2009). Analysis on climate changes under global climate change – a case study of Tianshan Snow and Avalanche Research Station. *Journal of Mountain Science*, 27(1), 41-48. (in Chinese).

Shrout, P.E., & Fleiss, J.L. (1979). Intraclass correlations: Uses in assessing rater reliability. *Psychological Bulletin*, 86(2), 420-428.

Singer, R. B., & McCord, T. B. (1979). Mars: Large-scale mixing of bright and dark surface materials and implications for analysis of spectral reflectance, *Proceedings of LPI (Vol. 2, A80-23617 08-91) on Lunar and Planetary Science Conference 10th*, Houston, Tex., March 19-23 (pp.1835-1848). New York: Pergamon Press.

Singh, A. (1989). Digital change detection techniques using remotely sensed data. *International Journal of Remote Sensing*, 10, 989–1003.Statistics Bureau of Xinjiang Uygur Autonomous Region (SBX). (2012). *Xinjiang Statistical Yearbook-2012*. Beijing: China Statistics Press.

State Bureau of Surveying and Mapping (SBSM). (2008). The SBSM

proclamation of the issue of new elevation data for the lowest point in China (Low lying land of Aydingkol Lake, Turpan of Xinjiang). Retrieved from: http://www.sbsm.gov.cn/article//dlxxshgb/201107/20110700086266.shtml

Sun, Z., Shi, J., Jiang, L., Yang, H., & Zhang, L. (2006). Development of snow depth and snow water equivalent algorithm in western China using passive microwave remote sensing data. *Advances in Earth Science*, 21(12), 1363-1369.

Sun, Z., Shi, J., Yang, H., Jiang, L., & Peng, L. (2007). A study on snow depth estimating and snow water equivalent algorithm for FY-3 MWRI. *Remote Sensing Technology and Application*, 22(2), 264-267. (in Chinese).

Tait, A., & Armstrong, R. (1996). Evaluation of SMMR satellite-derived snow depth using ground-based measurements. *International Journal of Remote Sensing*, 17(4), 657- 665.

Takala, M., Luojus, K., Pulliainen, J., Derksen, C., Lemmetyinen, J., Kärnä, J.-P., Koskinen, J., & Bojkov, B. (2011), Estimating northern hemisphere snow water equivalent for climate research through assimilation of space-borne radiometer and ground-based measurements. *Remote Sensing of Environment*, 115, 3517-3529.

Tang, F., Chen, X., Cheng, W., & Zhou, K. (2006). Relief amplitude in Junggar Basin and peripheral Northwest Mountains. *Arid Land Geography*, 29(3), 388-392. (in Chinese).

Veijalainen, N., Lotsari, E., Alho, P., Vehviläinen, B., & Käyhkö, J. (2010). National scale assessment of climate change impacts on flooding in Finland.

Journal of Hydrology, 391, 333-350.

Walker, A. E., & Silis, A. (2002). Snow-cover variations over the Mackenzie River basin, Canada, derived from SSM/I passive-microwave satellite data. *Annuals of Glaciology*, 34, 8-14.

Wang, C., Wang, Z., & Shen, Y. (2010a). A prediction of snow cover depth in the northern Xinjiang in the next 50 years. *Journal of Glaciology and Geocryology*, 32(6), 1059-1065. (in Chinese).

Wang, J., Li, H., & Hao, X. (2010b). Responses of snowmelt runoff to climatic change in an inland river basin, Northwestern China, over the past 50 years. *Hydrology and Earth System Sciences*, 14, 1979-7987.

Wang, J., & Li, S. (2006). Effect of climatic change on snowmelt runoffs in mountainous regions of inland rivers in Northwestern China. *Science in China Series D: Earth Sciences*, 49(8), 881-888.

Wang, L. & L ü, X. (2009). Analysis of the relief amplitude in Xinjiang based on digital elevation model. *Science of Surveying and Mapping*, 34(1), 113-116. (in Chinese).

Wang, X., & Xie, H. (2009). New methods for studying the spatiotemporal variation of snow cover based on combination products of MODIS Terra and Aqua, *Journal of Hydrology*, 371, 192-200.

Wang, X., Xie, H., & Liang, T. (2008a). Evaluation of MODIS snow cover and cloud mask and its application in northern Xinjiang, China, *Remote Sensing of Environment*, 112(4), 1497-1513.

Wang, Y., Hou, S., Lu, A., & Liu, Y. (2008b). Response of glacier variations in the eastern Tianshan Mountains to climate change, during the last 40 years. *Arid Land Geography*, 31(6), 813-821. (in Chinese).

Wang, Z., & Che, T. (2012). Spatiotemporal distributions analysis of snow cover based on combined MODIS and AMSR-E products in the arid land of China, *International Journal of Land Processes and Arid Environment*, 1(1), 19-26.

World Meteorological Organization (WMO). (2014). Climate models. Retrieved from: http://www.wmo.int/pages/themes/climate/climate_models.php

Xu, G., & Wei, W. (2004). Enlightenment of climate change in the middle mountains of western Tianshan – a case of the Tianshan Snow-cover and Avalanche Research Station. *Journal of Arid Land Resources and Environment*, 18(4), 19-22. (in Chinese).

Xu, G. (1997). *Climate Change in China's arid and semi-arid lands*. Beijing: China Metrological Press. (in Chinese).

Yan, H. (2005). A comparison of MODIS and Passive Microwave Snow Mappings. *Journal of Glaciology and Geocryology*, 27(4), 515-519. (in Chinese).

Yang, Q., Cui, C., Sun, C., & Ren, Y. (2007). Snow cover variation during 1959-2003 in Tianshan Mountains, China. *Advances in Climatic change Research*, 3(2), 80-84. (in Chinese).

Zhang, J. (2010). Multi-source remote sensing data fusion: status and trends. *International Journal of Image and Data Fusion*, 1(1), 5-24.

Zhang, J., Wu, Y., Yao, F., & Wei, W. (2008). Analyses of recent Xinjiang snow cover feature utilizing satellite remote sensing and surface observation data. *Plateau Meteorology*, 27(3), 551-557. (in Chinese).

Zhang, L., & Wei, W. (2001). Variation trends of snowcover in the middle mountains of western Tianshan and their relations to temperature and precipitation – Take the valley of Gongnaisi River as example. *Journal of Mountain Science*, 19(5), 403-407. (in Chinese).

Zhang, Y., Liu, S., & Ding, Y. (2007). Glacier meltwater and runoff modelling, Keqicar Baqi glacier, southwestern Tien Shan, China. *Journal of Glaciology*, 53(180), 91-98.

Zhao, H., Li, Y., Yang, J., & Lv, H. (2009). Geomorphic characteristics of Northern Tianshan. *Scientia Geographica Sinica*, 29(3), 445-449. (in Chinese).

Zhou, Q., Sui, H., & Ma, G. (2007). Change detection based on multi-temporal remote sensing imagery. In Gong, J. (Editor-in-chief), *Advances in Earth Observation Data Processing and Analysis*, pp.240-265. Wuhan: Wuhan University Press. (in Chinese).

Appendix I – List of ground weather stations in Xinjiang and data availability periods

No.	Station ID	Name	Name in Chinese	Altitude (m)	Data availability period
1	N/A*	Tianshan Station	天山积雪雪崩站	1776	2003-2011
2	51053	Haba River	哈巴河	534	1980-1996, 2003-2011
3	51059	Jeminay	吉木乃	984	1980-1996, 2003-2011
4	51060	Burqin	布尔津	476	2003-2011
5	51068	Fuhai	福海	502	1980-1996, 2003-2011
6	51076	Altay	阿勒泰	737	1980-1996, 2003-2011
7	51087	Fuyun	富蕴	827	1980-1996, 2003-2011
8	51133	Tacheng	塔城	537	1980-1996, 2003-2011
9	51137	Yumin	裕民	716	2003-2011
10	51145	Emin	额敏	523	2003-2011
11	51156	Hoboksar	和布克赛尔	1294	1981-1996, 2003-2011
12	51186	Qinghe	青河	1220	1980-1996, 2003-2011
13	51232	Alataw Pass	阿拉山口	286	1980-1996, 2003-2011
14	51238	Bole	博乐	533	2003-2011
15	51241	Toli	托里	1078	1980-1996, 2003-2011
16	51243	Keramay	克拉玛依	446	1981-1996, 2003-2011
17	51288	Baytik Mount	北塔山	1655	1980-1996, 2003-2011
18	51329	Huocheng	霍城	641	2003-2011
19	51330	Wenquan	温泉	1354	1980-1996, 2003-2011
20	51334	Jinghe	精河	321	1980-1996, 2003-2011
21	51346	Usu	乌苏	478	1983-1996, 2003-2011

22	51352	Paotai	炮台	338	2003-2011
23	51353	Mosuowan	莫索湾	347	2003-2011
24	51356	Shihezi	石河子	444	1983-1996, 2003-2011
25	51357	Shawan	沙湾	523	2003-2011
26	51358	Ulan Usu	乌兰乌苏	469	2003-2011
27	51359	Manas	玛纳斯	472	2003-2011
28	51365	Caijiahu	蔡家湖	441	1980-1996, 2003-2011
29	51367	Hutubi	呼图壁	524	2003-2011
30	51368	Changji	昌吉	579	2003-2011
31	51378	Jimsar	吉木萨尔	735	2003-2011
32	51379	Qitai	奇台	794	1980-1996, 2003-2011
33	51431	Yining	伊宁	664	1980-1996, 2003-2011
34	51433	Nilka	尼勒克	1106	2003-2011
35	51436	Xinyuan	新源	929	2003-2011
36	51437	Zhaosu	昭苏	1855	1980-1996, 2003-2011
37	51463	Urumqi	乌鲁木齐	919	1980-1996, 2003-2011
38	51469	Mushizhan	牧试站	2356	2003-2011
39	51470	Tianchi	天池	1935	2003-2011
40	51477	Dabancheng	达板城	1104	1980-1996, 2003-2011
41	51467	Balguntay	巴伦台	1752	1980-1996
42	51495	Qijiaojing	七角井	875	1980-1996
43	51526	Kumux	库米什	924	1980-1996
44	51542	Bayinbuluke	巴音布鲁克	2459	1980-1996
45	51567	Yanqi	焉耆	1057	1983-1996
46	51573	Turpan	吐鲁番	35	1980-1996
47	51628	Aksu	阿克苏	1105	1983-1996
48	51633	Baicheng	拜城	1230	1980-1996

49	51642	Luntai	轮台	978	1980-1996
50	51644	Kuqa	库车	103	1980-1996
51	51656	Korla	库尔勒	933	1980-1996
52	51720	Kalpin	柯坪	1163	1980-1996
53	51730	Alaer	阿拉尔	1013	1980-1996
54	52101	Barkol	巴里坤	1639	1980-1996
55	52118	Yiwu	伊吾	1730	1980-1996
56	52203	Hami	哈密	739	1980-1996

* Tianshan station is not a standard weather station but a snow observation station, which is established by Chinese Academy of Sciences (CAS). Therefore, no station ID is assigned.

Appendix II – Program codes of sampling and data processing

Note: the following codes can be executed in MATLAB® software.

Data reading from HDF file (the GlobSnow product format)

```
%% Initiation information %%
clear; clc;                                          % clear screen and release the workspace
filePath = 'C:\SnowData\GlobSnow_HDF\';   % path of the HDF files
files = dir([filePath, '*.hdf']);                 % find all HDF files, save the names
num_files = length(files);                        % count the number of files
c = 0;                                                % mark for the loop
title{1,1} = 'Date';                  % title of the first column in the read-in file (MS Excel)

%% Identify the locations of samples in HDF file %%
num_sta = 37;                                  % set the number of weather stations
staNo = xlsread('C:\sta_info.xls', 'selected_sites_37', 'A2:A38');          % No. of station
staCoord = xlsread('C:\sta_info.xls', 'selected_sites_37', 'D2:E38');      % coordinates
for k = 1:num_sta
   p_str = ['[p', num2str(k), '_row, p', num2str(k), '_col] = PositionXY2(', num2str(staCoord(k, 1)), ', ', num2str(staCoord(k, 2)), ');'];
   eval(p_str);                                % execute the “p_str”
   title{1, k + 1} = num2str(staNo(k));          % take station ID as titles
end
xlsPath = 'D:\SnowData\sampling_GlobSnow.xls';     % path of read-in file (Excel)
xlswrite(xlsPath, title);                                % write station ID as titles into Excel

%% Main program %%
for s = 1:num_files                                  % loop
      fileName = files(s).name;                      % obtain the HDF file name
      fullName = [filePath, fileName];               % include the full path
      CdateStr = fileName(18:25);          % read date information from file name
```

```
%% for GlobSnow SWE L3A daily data %%
PDATA = hdfread(fullName, 'swe', 'Index', {[1.0 1.0], [1.0 1.0], [721.0 721.0]});
%% for GlobSnow SWE L3B weekly data %%
  %% PDATA = hdfread(fullName, 'swe_average', 'Index', {[1.0 1.0], [1.0 1.0],
[721.0 721.0]});
data_array{1, 1} = CdateStr;
for n = 1:num_sta                                   % loop for writing data
    swe = eval(['PDATA(p', num2str(n), '_row, p', num2str(n), '_col);']);    %
writing sample values to the variable “swe”;
    data_array {1, n + 1} = swe;                    % swe values in the same date
end
c = c + 1;                                          % count the records
cellNum = c + 1;
xlswrite(xlsPath, data_array, 'Sheet1', ['A', num2str(cellNum)]);  % write data
clear PDATA;                                                       % clear
workspace
end          % end of main program
```

Data reading from ASCII file (the WestDC product format)

```
%% Initiation information %%
clear; clc;                                          % clear screen and release the workspace
filePath = 'C:\SnowData\WestDC_TXT\';          % path of the TXT files
files = dir([filePath, '*.txt']);                  %  find all TXT files and save the names
num_files = length(files);                         % count the number of files
c = 0;                                               % mark for the loop
title{1,1} = 'Date';                          % title of the first column in the read-in file (MS Excel)

%% Identify the locations of samples in TXT file %%
%% Part I. All stations %%
num_sta = 56;                                    % number of the stations
staNo = xlsread('D:\SnowData\sta_info.xls', 'all_sites_55+1', 'A2:A57');        % station ID
staCoord = xlsread('D:\SnowData\sta_info.xls', 'all_sites_55+1', 'D2:E57');        % coordinates

%% Part II.  Selected stations for matching GlobSnow data %%
num_sta = 37;                                    % number of the stations
staNo = xlsread('D:\SnowData\sta_info.xls', 'selected_sites_37', 'A2:A38');     % station ID
staCoord = xlsread('D:\SnowData\sta_info.xls', 'selected_sites_37', 'D2:E38');% coordinates

for k = 1:num_sta
   p_str = ['p', num2str(k), ' = PositionXY(', num2str(staCoord(k, 1)), ', ', num2str(staCoord(k, 2)), ');'];
   eval(p_str);                                  % execute the string “p(k) = PositionXY((E),(N))”;
   title{1, k + 1} = num2str(staNo(k));     % take station ID as titles
end
xlsPath = 'D:\SnowData\sampling_WestDC.xls';        % path of read-in file (Excel)
xlswrite(xlsPath, title);                            % write station ID as titles into Excel
```

```
%% Main program %%
for s = 1:num_files                                    % loop
    fileName = files(s).name;                          % obtain the TXT file name
    fullName = [filePath, fileName];                   % include the full path

  %% Julian date to Calendar date %%
  yyyy = fileName(1:4);                                % year of Julian date (yyyy)
  ddd = fileName(5:7);                                 % day of Julian date (ddd)
  if isLeap(str2num(yyyy)) == 1                        % if a leap year, isLeap() function
    CdateStr = [yyyy, Julian2Calender(str2num(ddd), 1)];   % Julian to Calendar
  else
    CdateStr = [yyyy, Julian2Calender(str2num(ddd), 0)];   % Julian to Calendar
  end

  %% Read TXT files %%
  fid_in = fopen(fullName, 'r');                       % open ASCII file (read only)
  fid_out = fopen('PureDATA.txt', 'w');                % create PureDATA.txt
  while ~feof(fid_in)
    tline = fgetl(fid_in);                             % read a line
    if ~isempty(tline);                                % if an empty line
      if double(tline(1)) >= 48 && double(tline(1)) <= 57    % if the first character is
 a figure
        fprintf(fid_out, '%s\n\n', tline);                   % if figure, write data to
PureDATA.txt
        continue
      end
    end
  end
  fclose(fid_in);                                      % close file
  fclose(fid_out);                                     % close file
  PDATA = importdata('PureDATA.txt');                  % import file to workspace PDATA

  %% Read the locations of the stations %%
  data_array{1, 1} = CdateStr;                % Initiation the data
   for n = 1:num_sta                                   % loop, give numbers in p(n) to variable
depth(n)
     depth = eval(['PDATA(1, p', num2str(n), ');']);       % execute the string “depth =
PDATA(1, p(n))”;
```

```
        data_array {1, n + 1} = depth;          % depth values in the same date
    end
    c = c + 1;                                  % count the records

   cellNum = c + 1;                             % data start from the second row (the first is the
title)
   xlswrite(xlsPath, data_array, 'Sheet1', ['A', num2str(cellNum)]);   % write data
   clear PDATA;                                                        % clear workspace
end          % end the main program
```

Appendix III – Program codes of time series analysis

Note: the following codes can be executed in MATLAB® software.

Periodicity analysis

```
%% Initiation information %%
clear; clc;                                  % clear screen and release the workspace
data = [];                                   % define data space
n = length(data);                            % length of the data set
N = 2^10;                                    % length of extended data for FFT
f = linspace(0, 0.5, N/2 + 1);

%% Data preprocessing %%
data_var = data – mean(data);                % data standardization
y = [data_var, zeros(1, N - n)];             % extend data length to N, filled with
"0"

%% Fast Fourier Transform (FFT) %%
FFT_y = fft(y);                              % FFT of original data set
density = FFT_y. * conj(FFT_y)/N;            % calculate power spectral density
density;

%% Find the periodicity %%
mirror_d = density(1:N/2 + 1);               % select the half mirror data
d_max = max(mirror_d);                       % find the maximum density
p = find(mirror_d == d_max);                 % the position of the maximum value
f = f(p);                                    % frequency
T = 1/f;                                     % calculate the periodicity
T;
```

Curriculum Vitae

Academic qualifications of the thesis author, Mr. SUN Bo:

- Received the degree of Bachelor of Engineering (Honours) from Wuhan University, June 2006.
- Received the degree of Master of Science from the Hong Kong Polytechnic University, October 2008.
- Received the degree of Master of Philosophy from Hong Kong Baptist University, November 2010.

June 2014

Primary Publications

(# as the corresponding author)

Journal publication:

Zhou, Q. and **Sun, B.#** (2013). Reliability of long-term snow depth data sets from remote sensing over the western aridzone of China. *Remote Sensing Letters*, 4(11), 1039-1048. DOI: 10.1080/2150704X.2013.832841. **(SCI)**

Zhou, Q., & **Sun, B.** (2010). Analysis of spatio-temporal pattern and driving force of land cover change using multi-temporal remote sensing images, *Science China Technological Sciences*, 53(Supplement I), 111-119. DOI: 10.1007/s11431-010-3196-0. **(SCI)**

Peer-reviewed book chapter:

Zhou, Q. & **Sun, B.** (2010). Spatial pattern analysis of water-driven land cover change in aridzone, Northwest of China, in Chuvieco, E., Li, J. and Yang, X. (eds). *Advances in Earth Observation of Global Change*, Dordrecht: Springer. DOI: 10.1007/978-90-481-9085-0_2.

Conference paper:

Zhou, Q. & **Sun, B.#** (2011). Integration of multi-source images for improving spatial resolution of snow depth detection in western China, *Proceedings of International Symposium on Image and Data Fusion*, Proceedings of ISPRS, Tengchong, Yunnan, China, 9-12 August, 2011. DOI:10.1109/ISIDF.2011.6024269. **(EI)**

Zhou, Q. & **Sun, B.** (2008). Spatial pattern of farmland change trajectories in arid zone of China, in Li, D., Gong, J. and Wu, H. (eds.), *Proceedings of International Conference on Earth Observation Data Processing and Analysis*, Proceedings of SPIE, Wuhan, Hubei, China, 28-30 December, 2008, SPIE 7285, 72854J. DOI:10.1117/12.814910. **(EI)**

Zhou, Q. & **Sun, B.** (2008). Analysing spatio-temporal pattern of changing farmland in China's arid zone, in Neale, C.M.U., Owe, M. and D'Urso, G. (eds.), *Remote Sensing for Agriculture, Ecosystems, and Hydrology X*, Proceedings of SPIE, Cardiff, Wales, United Kingdom, 16-18 September, 2008, SPIE 7104, 71040U. DOI: 10.1117/12.801063. **(EI)**